

# Complete Characterization of Incorrect Orthology Assignments in Best Match Graphs

David Schaller<sup>1,2,\*</sup>, Manuela Geiß<sup>3</sup>, Peter F. Stadler<sup>1,2,4-7</sup>, and Marc Hellmuth<sup>8,\*</sup>

<sup>1</sup>Max Planck Institute for Mathematics in the Sciences, Inselstraße 22, D-04103 Leipzig, Germany

<sup>2</sup>Bioinformatics Group, Department of Computer Science & Interdisciplinary Center for Bioinformatics, Universität Leipzig, Härtelstraße 16–18, D-04107 Leipzig, Germany.

<sup>3</sup>Software Competence Center Hagenberg GmbH, Softwarepark 21, A-4232 Hagenberg, Austria

<sup>4</sup>German Centre for Integrative Biodiversity Research (iDiv) Halle-Jena-Leipzig, Competence Center for Scalable Data Services and Solutions Dresden-Leipzig, Leipzig Research Center for Civilization Diseases, and Centre for Biotechnology and Biomedicine at Leipzig University at Universität Leipzig

<sup>5</sup>Institute for Theoretical Chemistry, University of Vienna, Währingerstrasse 17, A-1090 Wien, Austria

<sup>6</sup>Facultad de Ciencias, Universidad Nacional de Colombia, Sede Bogotá, Colombia

<sup>7</sup>Santa Fe Insitute, 1399 Hyde Park Rd., Santa Fe NM 87501, USA

<sup>8</sup>School of Computing, University of Leeds, EC Stoner Building, Leeds LS2 9JT, UK

*mhellmuth@mailbox.org*

\*corresponding author

## Abstract

Genome-scale orthology assignments are usually based on reciprocal best matches. In the absence of horizontal gene transfer (HGT), every pair of orthologs forms a reciprocal best match. Incorrect orthology assignments therefore are always false positives in the Reciprocal Best Match Graph. We consider duplication/loss scenarios and characterize unambiguous false-positive (*u-fp*) orthology assignments, that is, edges in the Best Match Graphs (BMGs) that cannot correspond to orthologs for any gene tree that explains the BMG. We characterize *u-fp* edges in terms of subgraphs of the BMG and show that, given a BMG, there is a unique “augmented tree” that explains the BMG and identifies all *u-fp* edges in terms of overlapping sets of species in certain subtrees. The augmented tree can be constructed as a refinement of the unique least resolved tree of the BMG in polynomial time. Removal of the *u-fp* edges from the reciprocal best matches results in a unique orthology assignment.

**Keywords:** orthology detection; best matches; unambiguous orthologs; colored graphs; cograph; tree reconciliation; polynomial-time algorithm

## 1 Introduction

Orthology is one of the key concepts in evolutionary biology: Two genes are orthologs if their last common ancestor was a speciation event [8]. Distinguishing orthologs from paralogs (originating from gene duplications) or xenologs (i.e., genes that have undergone horizontal gene transfer) is of considerable practical importance for functional genome annotation and thus for a wide array of methods in bioinformatics and computational biology that rely on gene annotation data. Orthologous genes in different species are expected to have essentially the same biological and molecular functions. Paralogs and xenologs, in contrast, tend to have similar, but clearly distinct functions [9, 45, 51]. Most of the commonly used tools for large-scale orthology identification compute reciprocal best hits as a first step followed by some filtering and refinement steps to improve the results, see [10, 35, 44] for reviews and [1] for benchmarking results.

Orthology identification has also received increasing attention from a mathematical perspective starting from the concept of an *evolutionary scenario* comprising a gene tree  $T$  and a species tree  $S$  together with a *reconciliation map*  $\mu$  from  $T$  to  $S$ . The map  $\mu$  identifies the locations in the species tree at which evolutionary events, represented by the vertices of the gene tree, took place. *In this contribution, we consider exclusively duplication/loss scenarios, i.e., we explicitly exclude horizontal gene transfer.* Characterizations of reconciliation maps are given e.g. in [7, 15, 40, 50]. While every gene tree can be reconciled with any species tree [16, 37], this is no longer true if event-labels are prescribed in the gene tree  $T$  [19, 24, 30].

The orthology relation itself has been characterized as a cograph (i.e., graphs that do not contain induced paths  $P_4$  on four vertices) by Hellmuth et al. [22] based on earlier work by Böcker and Dress [2]. This line of research has led to the idea of editing reciprocal best hit data to conform the require cograph structure [23]. Maybe surprisingly, the combinatorial structure of best matches has become a focus only very recently. We consider best matches as an evolutionary concept: A gene  $y$  in species  $s$  is a best match of a gene  $x$  from species  $r \neq s$  if  $s$  contains no gene  $y'$  that is more closely related to  $x$ . In practice, best matches are approximated by sequence similarity. We refer to [46] and the references therein for a detailed account on how best matches can be extracted from sequence similarity data. Best Match Graphs (BMGs) have several appealing properties: They have several alternative characterizations providing polynomial-time recognition algorithms and they are “explained” by a unique least resolved tree [12]. These properties will be introduced formally in the next section and play an important role in our discussion. The Reciprocal Best Match Graphs (RBMGs) are the symmetric parts of BMGs and conceptually correspond to the reciprocal best hits used in orthology detection. In contrast to BMGs, RBMGs are much more difficult to handle and are not associated with unique trees [14].

RBMGs in general are not cographs and thus contain incorrect orthology assignments associated with  $P_4$ s. Importantly, such incorrect assignments are always false positives and thus, correspond to edges in RBMGs that must be deleted [13]. A  $P_4$  in an RBMG arises in particular as a consequence of complementary gene loss, i.e., the complete loss of different paralogous groups in disjoint lineages. Under certain circumstances, such false-positive orthology assignments can be identified, in particular when there are also species in which both paralogs have survived [6]. A subset of false-positive orthology assignments, the “good quartets”, can be identified unambiguously by considering BMGs instead of RBMGs [14]. Their removal already leads to a substantial improvement in simulated data [13]. Here, we consider the false-positive orthology assignments in more detail, using BMGs and their explaining trees as the formal framework. Section 3.2 introduces the notion of *unambiguous false-positive edges*, that is, reciprocal best matches that cannot be orthologs w.r.t. to *any* gene tree explaining the BMG. For BMGs that can be explained by fully resolved, i.e., binary gene trees, Thm. 3.9 shows that unambiguous false-positive are already determined by this particular gene tree. Furthermore, we will see in Prop. 3.15 that these false positives are the middle edges of a good quartet or one of the outer edges of an ugly quartet [13, 14]. This leaves unambiguous false-positive edges in BMGs that have no explanation by a binary tree, i.e., that require hard polytomies in the evolutionary scenario. In Section 3.5 we show that these false-positives are associated with another class of induced subgraphs of the BMG, which we termed *hourglasses*. Thm. 4.5 then provides an additional set of false-positive edges that are embedded in chains of hourglasses in a certain manner.

The gene tree  $T$  “displays” two trees that play a key role for our purposes: the discriminating cotree of the orthology cograph and the least resolved tree of the BMG. While the first can be endowed with an unambiguous event labeling, this not true for the latter [13]. The least resolved tree may contain polytomic vertices arising by the merging of speciation and duplication events. This leads us to the construction of a unique *augmented tree* in Section 4.3, which can be endowed with an unambiguous event labeling and thus, induces a unique cograph. Thm. 4.19 states that a reciprocal best match is an unambiguous false-positive if and only if it is not contained in the cograph induced by augmented tree. Algorithm 1 furthermore computes the augmented tree in polynomial time from the least resolved tree of the BMG, resulting a polynomial-time procedure to identify all unambiguous false-positive edges in a BMG. In simulations, we find that at least three quarters of all false positives fall into this class. The remaining cases are not recognizable from best matches alone and correspond to complementary losses without surviving witnesses.

## 2 Preliminaries

### 2.1 Graphs and Trees

We consider directed graphs  $\vec{G} = (V, E)$ , for brevity just called graphs throughout, with arc set  $E \subseteq V \times V \setminus \{(v, v) \mid v \in V\}$ . We say that  $xy$  is an *edge* in  $\vec{G}$  if and only if both  $(x, y) \in E(\vec{G})$  and  $(y, x) \in E(\vec{G})$ . If all arcs of  $\vec{G}$  in a graph form edges, we call  $\vec{G}$  *undirected*. A graph  $H = (W, F)$  is a *subgraph* of  $G = (V, E)$ , in symbols  $H \subseteq G$ , if  $W \subseteq V$  and  $F \subseteq E$ . The underlying *symmetric part* of a directed graph  $\vec{G} = (V, E)$  is the subgraph  $G = (V, F)$  that contains all edges of  $\vec{G}$ . A subgraph  $H = (W, F)$  (of  $\vec{G}$ ) is called *induced*, denoted by  $\vec{G}[W]$ , if for all  $u, v \in W$  it holds that  $(u, v) \in E$  implies  $(u, v) \in F$ . In addition, we consider *vertex-colored* graphs  $(\vec{G}, \sigma)$  with vertex-coloring  $\sigma: V \rightarrow M$  into some set  $M$  of colors. A vertex-coloring is called *proper* if  $\sigma(x) \neq \sigma(y)$  for every arc  $(x, y)$  in  $\vec{G}$ . We write  $\sigma(W) = \{\sigma(w) \mid w \in W\}$  for subsets  $W \subseteq V$  and  $\sigma|_W$  to denote the restriction of the map  $\sigma$  to  $W \subseteq V$ . In particular,  $(\vec{G}[W], \sigma|_W)$  is an induced vertex-colored subgraph of  $(\vec{G}, \sigma)$ .

A *path* (of length  $\ell$ ) in a directed graph  $\vec{G}$  or an undirected graph  $G$  is a subgraph induced by a nonempty sequence of pairwise distinct vertices  $P(x_0, x_\ell) := (x_0, x_1, \dots, x_\ell)$  such that  $(x_i, x_{i+1}) \in E(\vec{G})$  or  $x_i x_{i+1} \in E(G)$ , resp., for  $0 \leq i \leq \ell - 1$ . We use the notation  $P(x_0, x_\ell)$  both for the sequence of vertices and the subgraph they induce.

All *trees*  $T = (V, E)$  considered here are *undirected*, *planted* and *phylogenetic*, that is, they satisfy (i) the root  $0_T$  has degree 1 and (ii) all inner vertices have degree  $\deg_T(u) \geq 3$ . We write  $L(T)$  for the leaves (not including  $0_T$ ) and  $V^0 = V(T) \setminus (L(T) \cup \{0_T\})$  for the inner vertices (also not including  $0_T$ ). To avoid trivial cases, we will always

assume  $|L(T)| \geq 2$ . An edge  $uv$  in  $T$  is an inner edge if  $u, v \in V^0(T)$  are inner vertices. The *conventional root*  $\rho_T$  of  $T$  is the unique neighbor of  $0_T$ . The main reason for using planted phylogenetic trees instead of modeling phylogenetic trees simply as rooted trees, which is the much more common practice in the field, is that we will often need to refer to the time before the first branching event, i.e., the edge  $0_T\rho_T$ .

We define the *ancestor order* on a given tree  $T$  as follows: if  $y$  is a vertex of the unique path connecting  $x$  with the root  $0_T$ , we write  $x \preceq_T y$ , in which case  $y$  is called an ancestor of  $x$  and  $x$  is called a descendant of  $y$ . We use  $x \prec_T y$  for  $x \preceq_T y$  and  $x \neq y$ . If  $x \preceq_T y$  or  $y \preceq_T x$  the vertices  $x$  and  $y$  are *comparable* and, otherwise, *incomparable*. If  $xy$  is an edge in  $T$ , such that  $y \prec_T x$ , then  $x$  is the *parent* of  $y$  and  $y$  the *child* of  $x$ . We denote by  $\text{child}_T(x)$  the set of all children of  $x$ . It will be convenient for the discussion below to extend the ancestor relation  $\preceq_T$  to the union of the edge and vertex sets of  $T$ . More precisely, for a vertex  $x \in V(T)$  and an edge  $e = uv \in E(T)$  with  $v \prec_T u$  we write  $x \prec_T e$  if and only if  $x \preceq_T v$  and  $e \prec_T x$  if and only if  $u \preceq_T x$ . For edges  $e = uv$  with  $v \prec_T u$  and  $f = ab$  with  $b \prec_T a$  in  $T$  we put  $e \preceq_T f$  if and only if  $v \preceq_T b$ .

For a non-empty subset  $A \subseteq V \cup E$  we define  $\text{lca}_T(A)$ , the *last common ancestor* of  $A$ , to be the unique  $\preceq_T$ -minimal vertex of  $T$  that is an ancestor of every vertex or edge in  $A$ . For simplicity we drop the brackets and write  $\text{lca}_T(x_1, \dots, x_k) := \text{lca}_T(\{x_1, \dots, x_k\})$  whenever we specify a set of vertices or edges explicitly.

A vertex  $v \in V(T)$  is *binary* if  $\deg_T(v) = 3$ , i.e., if  $v$  has exactly two children. A tree is *binary*, if all vertices  $v \in V^0$  are binary. For  $v \in V(T)$  we denote by  $T(v)$  the subtree of  $T$  rooted in  $v$ . The set of *clusters* of a tree  $T$  is  $\mathcal{C}(T) = \{L(T(v)) \mid v \in V(T)\}$ . It is well-known that  $\mathcal{C}(T)$  uniquely determines  $T$  [42]. We say that a tree  $T$  is a *refinement* of some tree  $T'$  if  $\mathcal{C}(T') \subseteq \mathcal{C}(T)$ . A tree  $T'$  is *displayed* by a tree  $T$ , in symbols  $T' \leq T$ , if  $T'$  can be obtained from a subtree of  $T$  by contraction of edges [43], where the contraction of an edge  $e = uv$  in a tree  $T = (V, E)$  refers to the removal of  $e$  and identification of  $u$  and  $v$ . It is easy to verify that every refinement  $T$  of  $T'$  also displays  $T'$ . However, the converse is not always true since  $L(T') \subsetneq L(T)$  and thus,  $\mathcal{C}(T') \not\subseteq \mathcal{C}(T)$  may be possible.

## 2.2 (Reciprocal) Best Matches

We consider a pair  $T = (V, E)$  and  $S = (W, F)$  of planted phylogenetic trees together with a map  $\sigma: L(T) \rightarrow L(S)$ . We interpret  $T$  as a *gene tree* and  $S$  as a *species tree*; the map  $\sigma$  describes, for each gene  $x \in L(T)$ , in the genome of which species  $\sigma(x) \in L(S)$  it resides. W.l.o.g. we assume that the “gene-species-association”  $\sigma$  is a surjective map to avoid trivial cases. Since  $\sigma$  can be viewed as a coloring of the leaves of  $T$ , we call  $(T, \sigma)$  a *leaf-colored tree*. For  $s \in L(S)$  we write  $L[s] := \{x \in L(T) \mid \sigma(x) = s\}$ .

**Definition 2.1.** Let  $(T, \sigma)$  be a leaf-colored tree. A leaf  $y \in L(T)$  is a *best match* of the leaf  $x \in L(T)$  if  $\sigma(x) \neq \sigma(y)$  and  $\text{lca}(x, y) \preceq_T \text{lca}(x, y')$  holds for all leaves  $y'$  from species  $\sigma(y') = \sigma(y)$ . The leaves  $x, y \in L(T)$  are *reciprocal best matches* if  $y$  is a best match for  $x$  and  $x$  is a best match for  $y$ .

The graph  $\vec{G}(T, \sigma) = (V, E)$  with vertex set  $V = L(T)$ , vertex coloring  $\sigma$ , and with arcs  $(x, y) \in E$  if and only if  $y$  is a best match of  $x$  w.r.t.  $(T, \sigma)$  is known as the (colored) *Best Match Graph* of  $(T, \sigma)$  [12]. The symmetric part  $G(T, \sigma)$  of  $\vec{G}(T, \sigma)$  obtained by retaining the edges of  $\vec{G}(T, \sigma)$  is the (colored) *Reciprocal Best Match Graph* [14].

**Definition 2.2.** An arbitrary vertex-colored graph  $(\vec{G}, \sigma)$  is a *Best Match Graph (BMG)* if there exists a leaf-colored tree  $(T, \sigma)$  such that  $(\vec{G}, \sigma) = \vec{G}(T, \sigma)$ . In this case, we say that  $(T, \sigma)$  *explains*  $(\vec{G}, \sigma)$ . An arbitrary undirected vertex-colored graph  $(G, \sigma)$  is a *Reciprocal Best Match Graph (RBMG)* if it is the symmetric part of a BMG  $(\vec{G}, \sigma)$ .

For the symmetric part of the BMG  $(\vec{G}, \sigma)$ , i.e., the RBMG  $(G, \sigma)$ , we have  $xy \in E(G)$  if and only if  $x$  and  $y$  are reciprocal best matches in  $(T, \sigma)$ . In this sense,  $(T, \sigma)$  also explains  $(G, \sigma)$ . We note, furthermore, that RBMGs are not associated with unique least resolved tree [14].

In the following we collect some useful properties of BMGs and RBMGs for later reference.

**Lemma 2.3.** [14, Lemma 10] Let  $(T, \sigma)$  be a leaf-colored tree on  $L$  and let  $v \in V(T)$ . Then, for any two distinct colors  $r, s \in \sigma(L(T(v)))$ , there is an edge  $xy$  in  $\vec{G}(T, \sigma)$  with  $x \in L[r] \cap L(T(v))$  and  $y \in L[s] \cap L(T(v))$ .

**Lemma 2.4.** Let  $(\vec{G}, \sigma)$  be a BMG explained by a tree  $(T, \sigma)$ . Moreover, let  $x, y \in L(T)$  with  $\sigma(x) \neq \sigma(y)$  and  $v_x, v_y \in \text{child}(\text{lca}_T(x, y))$  with  $x \preceq_T v_x$  and  $y \preceq_T v_y$ . Then,  $\sigma(x) \notin \sigma(L(T(v_x)))$  and  $\sigma(y) \notin \sigma(L(T(v_y)))$  if and only if  $xy$  is an edge in  $\vec{G}$ .

*Proof.* By the definition of best matches, it holds that  $xy$  is an edge in  $\vec{G}$  if and only if  $\text{lca}_T(x, y) \preceq_T \text{lca}_T(x, y')$  for all  $y' \in L(T)$  of color  $\sigma(y)$  and  $\text{lca}_T(x, y) \preceq_T \text{lca}_T(x', y)$  for all  $x' \in L(T)$  of color  $\sigma(x)$ . Clearly,  $\text{lca}_T(x, y) \preceq_T \text{lca}_T(x, y')$  for all such  $y'$  if and only if  $\sigma(y) \notin \sigma(L(T(v_x)))$ , and  $\text{lca}_T(x, y) \preceq_T \text{lca}_T(x', y)$  for all such  $x'$  if and only if  $\sigma(x) \notin \sigma(L(T(v_y)))$ . □

**Definition 2.5.** Suppose that  $(T, \sigma)$  explains  $(\vec{G}, \sigma)$ . Then we say that  $(T, \sigma)$  is *least resolved* (w.r.t.  $(\vec{G}, \sigma)$ ) if no tree  $(T', \sigma)$  displayed by  $(T, \sigma)$  explains  $(\vec{G}, \sigma)$ .

Recall all trees in this contribution are planted, and thus least resolved trees (LRTs) are also considered as planted. Strictly speaking, this differs from the construction in [12–14], the additional (non-contractible) edge  $0_T\rho_T$  is a trivial detail that does not affect the properties of LRTs.

**Theorem 2.6.** [12, Thm. 8 and Cor. 4] Every BMG  $(\vec{G}, \sigma)$  is explained by a unique least resolved tree  $(T^*, \sigma)$ . In particular, every other tree  $(T, \sigma)$  explaining  $(\vec{G}, \sigma)$  is a refinement of  $(T^*, \sigma)$ . The least resolved tree  $(T^*, \sigma)$  of a BMG  $(\vec{G}, \sigma)$  can be constructed in polynomial time.

**Definition 2.7.** Let  $(\vec{G}, \sigma)$  be a Best Match Graph. We say that a triple  $ab|b'$  is informative for  $\vec{G}$  if  $a, b$  and  $b'$  are three different vertices with  $\sigma(a) \neq \sigma(b) = \sigma(b')$  in  $\vec{G}$  such that  $(a, b) \in E(\vec{G})$  and  $(a, b') \notin E(\vec{G})$ .

**Lemma 2.8.** Let  $(\vec{G}, \sigma)$  be a BMG and  $ab|b'$  an informative triple for  $\vec{G}$ . Then, every tree  $T$  that explains  $(\vec{G}, \sigma)$  displays the triple  $ab|b'$ , i.e.  $\text{lca}_T(a, b) \prec_T \text{lca}_T(a, b') = \text{lca}_T(b, b')$ .

*Proof.* The definition of informative triples implies that  $(a, b) \in E(\vec{G})$  and  $(a, b') \notin E(\vec{G})$ . Using  $\sigma(b) = \sigma(b')$  and the definition of best matches we immediately conclude  $\text{lca}_T(a, b) \prec_T \text{lca}_T(a, b')$ .  $\square$

**Lemma 2.9.** Let  $ab|b'$  and  $cb'|b$  be informative triples for a BMG  $(\vec{G}, \sigma)$ . Then every tree  $(T, \sigma)$  that explains  $(\vec{G}, \sigma)$  contains two distinct children  $v_1, v_2 \in \text{child}_T(\text{lca}_T(a, c))$  such that  $a, b \prec_T v_1$  and  $b', c \prec_T v_2$ .

*Proof.* Let  $(T, \sigma)$  be an arbitrary tree that explains  $(\vec{G}, \sigma)$ . By Lemma 2.8,  $T$  displays the informative triples  $ab|b'$  and  $cb'|b$ . Thus we have  $\text{lca}_T(a, b) \prec_T \text{lca}_T(a, b') = \text{lca}_T(b, b')$  and  $\text{lca}_T(c, b') \prec_T \text{lca}_T(c, b) = \text{lca}_T(b, b')$ . In particular,  $\text{lca}_T(a, b') = \text{lca}_T(b, b') = \text{lca}_T(c, b) =: u$ . Therefore,  $a \preceq_T v_1$  and  $b' \preceq_T v_2$  for distinct  $v_1, v_2 \in \text{child}_T(u)$ . Since  $\text{lca}_T(a, b) \prec_T u$ , we have  $a, b \prec_T v_1$  and thus  $v_1$  is an inner node. Likewise,  $\text{lca}_T(b', c) \prec_T u$  implies  $b', c \prec_T v_2$ .  $\square$

Given a tree  $T$  and an edge  $e$ , denote by  $T_e$  the tree obtained from  $T$  by contracting the edge  $e$ . An edge  $e \neq 0_T \rho_T$  in  $(T, \sigma)$  is *redundant* (w.r.t.  $(\vec{G}, \sigma)$ ) if  $(T, \sigma)$  explains  $(\vec{G}, \sigma)$  and  $\vec{G}(T_e, \sigma) = \vec{G}(T, \sigma)$ . Redundant edges have already been characterized in [12, Lemma 15, Thm. 8] in terms of equivalence classes using a somewhat complicated notation. Here we give a simpler characterization.

**Lemma 2.10.** Let  $(\vec{G}, \sigma)$  be a BMG explained by a tree  $(T, \sigma)$ . The edge  $e = uv$  with  $v \prec_T u$  in  $(T, \sigma)$  is redundant w.r.t.  $(\vec{G}, \sigma)$  if and only if (i)  $e$  is an inner edge of  $T$  and (ii) there is no arc  $(a, b) \in E(\vec{G}, \sigma)$  such that  $\text{lca}_T(a, b) = v$  and  $\sigma(b) \in \sigma(L(T(u)) \setminus L(T(v)))$ .

*Proof.* Let  $w_e$  be the vertex in  $T_e$  resulting from the contraction  $e = uv$  with  $v \prec_T u$  in  $T$ . By assumption we have  $(\vec{G}, \sigma) = \vec{G}(T, \sigma)$ .

First, assume that  $e$  is redundant and thus,  $\vec{G}(T_e, \sigma) = \vec{G}(T, \sigma)$ . Then  $e$  must be an inner edge, since otherwise  $L(T) \neq L(T_e)$  and, therefore,  $(T_e, \sigma)$  does not explain  $(\vec{G}, \sigma)$ . Now assume, for contradiction, that there is an arc  $(a, b) \in E(\vec{G})$  such that  $\text{lca}_T(a, b) = v$  and  $\sigma(b) \in \sigma(L(T(u)) \setminus L(T(v)))$ . Then there is a leaf  $b' \in L(T(u)) \setminus L(T(v))$  with  $\sigma(b') = \sigma(b)$  and  $\text{lca}_T(a, b) = v \prec_T u = \text{lca}_T(a, b')$ . Thus,  $(a, b') \notin E(\vec{G})$ . After contraction of  $e$ , we have  $\text{lca}_{T_e}(a, b) = \text{lca}_{T_e}(a, b') = w_e$ . Hence, by definition of best matches,  $(a, b)$  is an arc in  $\vec{G}(T_e, \sigma)$  if and only if  $(a, b')$  is an arc in  $\vec{G}(T_e, \sigma)$ ; a contradiction to the assumption that  $(T_e, \sigma)$  explains  $(\vec{G}, \sigma)$ .

Conversely, assume that  $e = uv$  with  $v \prec_T u$  is an inner edge in  $T$  and that there is no arc  $(a, b) \in E(\vec{G})$  such that  $\text{lca}_T(a, b) = v$  and  $\sigma(b) \in \sigma(L(T(u)) \setminus L(T(v)))$ . In order to show that an edge  $e$  is redundant, we need to verify that  $\vec{G}(T, \sigma) = \vec{G}(T_e, \sigma)$ . To this end, consider an arbitrary leaf  $c \in L(T)$ . Then we have either Case (1)  $c \in L(T) \setminus L(T(v))$ , or Case (2)  $c \in L(T(v))$ .

In Case (1) it is easy to verify that  $\text{lca}_T(c, d) = \text{lca}_{T_e}(c, d)$  for every  $d \in L(T)$ . In particular, therefore,  $(c, d) \in E(\vec{G}(T, \sigma))$  if and only if  $(c, d) \in E(\vec{G}(T_e, \sigma))$ .

In Case (2), i.e.  $c \in L(T(v))$ , consider another, arbitrary, leaf  $d \in L(T)$ . Note, if  $\sigma(c) = \sigma(d)$ , then  $c$  and  $d$  never form a best match. Thus, we assume  $\sigma(c) \neq \sigma(d)$ . Now, we consider three mutually exclusive Subcases (a)  $\text{lca}_T(c, d) \preceq_T v$ , (b)  $\text{lca}_T(c, d) = u$  and (c)  $\text{lca}_T(c, d) \succ_T u$ .

*Case (a).* Since no edge below  $v$  is contracted, we have for every  $d'$  with  $\sigma(d') = \sigma(d)$ ,  $\text{lca}_T(c, d') \prec_T \text{lca}_T(c, d) \preceq_T v$  if and only if  $\text{lca}_{T_e}(c, d') \prec_{T_e} \text{lca}_{T_e}(c, d) \preceq_{T_e} w_e$ . In particular, therefore,  $(c, d) \in E(\vec{G}(T, \sigma))$  if and only if  $(c, d) \in E(\vec{G}(T_e, \sigma))$ .

*Case (b).*  $\text{lca}_T(c, d) = u$  and  $c \prec_T v$  implies that  $d \in L(T(u) \setminus L(T(v)))$  and thus,  $\sigma(d) \in \sigma(L(T(u)) \setminus L(T(v)))$ . If  $(c, d) \in E(\vec{G}(T, \sigma))$ , then  $\sigma(d) \notin \sigma(L(T(v)))$  must hold. Therefore,  $(c, d)$  is still an arc after contraction of  $e$ . For the case  $(c, d) \notin E(\vec{G}(T, \sigma))$ , assume for contradiction  $(c, d) \in E(\vec{G}(T_e, \sigma))$ . Then  $(c, d) \notin E(\vec{G}(T, \sigma))$  implies that there must be a vertex  $d'$  with  $\sigma(d') = \sigma(d)$  and  $\text{lca}_T(c, d') \preceq_T v \prec_T u = \text{lca}_T(c, d)$ . In particular,  $d' \in L(T(v))$  can be chosen such that  $\text{lca}_T(c, d')$  is farthest away from  $v$  and thus,  $(c, d') \in E(\vec{G}(T, \sigma))$ . Now,  $\text{lca}_T(c, d') \preceq_T v$  and  $(c, d) \in E(\vec{G}(T_e, \sigma))$  imply that  $\text{lca}_{T_e}(c, d') = w_e = \text{lca}_{T_e}(c, d)$ , which is only possible if  $\text{lca}_T(c, d') = v$ . In summary, we found an arc  $(c, d') \in E(\vec{G}(T, \sigma))$  with  $\text{lca}_T(c, d') = v$  and  $\sigma(d') \in \sigma(L(T(u)) \setminus L(T(v)))$ ; a contradiction to our assumption. Hence, in Case (b) we have  $(c, d) \in E(\vec{G}(T, \sigma))$  if and only if  $(c, d) \in E(\vec{G}(T_e, \sigma))$ .

*Case (c).* Since  $\text{lca}_T(c, d) \succ_T u$ , it is again easy to see that, for every  $d'$  with  $\sigma(d') = \sigma(d)$ ,  $\text{lca}_T(c, d') \prec_T \text{lca}_T(c, d)$  if and only if  $\text{lca}_{T_e}(c, d') \prec_{T_e} \text{lca}_{T_e}(c, d)$  and thus,  $(c, d) \in E(\vec{G}(T, \sigma))$  if and only if  $(c, d) \in E(\vec{G}(T_e, \sigma))$ .

In summary, we have  $(c, d) \in E(\vec{G}(T, \sigma))$  if and only if  $(c, d) \in E(\vec{G}(T_e, \sigma))$  for all  $c, d \in L(T)$ . Thus,  $e$  is redundant.  $\square$

As a consequence of Lemma 2.10, we obtain

**Corollary 2.11.** *Let  $(T, \sigma)$  be a leaf-colored tree explaining  $(G, \sigma)$  and  $uv$  an inner edge inner of  $T$  with  $v \prec_T u$ . If  $\sigma(L(T(v))) \cap \sigma(L(T(v'))) = \emptyset$  for every  $v' \in \text{child}_T(u) \setminus \{v\}$ , then  $uv$  is redundant in  $T$  (w.r.t.  $(G, \sigma)$ ).*

*Proof.* If there is an arc  $e = (a, b) \in E(\vec{G})$  with  $\text{lca}_T(a, b) = v$  we have  $\sigma(b) \notin L(T(u)) \setminus L(T(v)) = \cup_{v' \in \text{child}(u) \setminus \{v\}} L(T(v'))$  because  $\sigma(L(T(v))) \cap \sigma(L(T(v'))) = \emptyset$  for every  $v' \in \text{child}_T(u) \setminus \{v\}$ . By Lemma 2.10, the inner edge  $uv$  is redundant.  $\square$

Finally, we show that redundant edges can be contracted in arbitrary order, similar to [12, Lemma 6 & Cor. 2]. To this end, we first prove a more general statement.

**Lemma 2.12.** *If  $T_A$  is obtained from  $T$  by contracting all edges in  $A \subseteq E(T)$ , then  $\vec{G}(T, \sigma) \subseteq \vec{G}(T_A, \sigma)$ .*

*Proof.* Let  $(x, y)$  be an arc in  $\vec{G}(T, \sigma)$ . This implies that there is no  $y'$  with  $\sigma(y') = \sigma(y)$  such that  $\text{lca}_T(x, y') \prec_T \text{lca}_T(x, y)$ . It is easy to verify that the latter is still true after contraction of an arbitrary edge  $e$ , i.e. there is no  $y'$  with  $\sigma(y') = \sigma(y)$  such that  $\text{lca}_{T_e}(x, y') \prec_{T_e} \text{lca}_{T_e}(x, y)$ . Hence,  $(x, y)$  is an arc in  $\vec{G}(T_e, \sigma)$ . Now consider the subsets  $A_1 \subset A_2 \subset \dots \subset A_{|A|} = A$  where each  $|A_i| = i$ ,  $1 \leq i \leq |A|$ . The argument above implies  $\vec{G}(T, \sigma) \subseteq \vec{G}(T_{A_1}, \sigma) \subseteq \dots \subseteq \vec{G}(T_A, \sigma)$ , which completes the proof.  $\square$

**Lemma 2.13.** *Let  $A$  and  $B$  be disjoint sets of redundant edges in  $(T, \sigma)$  w.r.t.  $(\vec{G}, \sigma)$  and denote by  $T_A$  the tree obtained by contraction of all edges in  $A$  in arbitrary order. Then  $B$  is a set of redundant edges in  $T_A$  w.r.t.  $\vec{G}(T_A, \sigma) = \vec{G}(T, \sigma)$ .*

*Proof.* By Lemma 2.12, contraction of any inner edge  $e = uv \in E(T)$  never leads to a loss of arcs in the BMG  $(\vec{G}, \sigma) = \vec{G}(T, \sigma)$ . Furthermore, the redundant edges in  $T$  w.r.t.  $(G, \sigma)$  are completely characterized by Lemma 2.10. Thm. 8 in [12] states that by contraction of all redundant edges (in an arbitrary order), one obtains the unique least resolved tree  $(T^*, \sigma)$  of  $(\vec{G}, \sigma)$ . As argued above, no arc of  $\vec{G}(T, \sigma)$  can be lost in the stepwise contraction of redundant edges. Together with  $\vec{G}(T, \sigma) = \vec{G}(T^*, \sigma) = (\vec{G}, \sigma)$  this implies  $\vec{G}(T_A, \sigma) = (\vec{G}, \sigma)$ . Since by assumption  $A \cap B = \emptyset$  and  $A \cup B$  is a set of redundant edges w.r.t.  $(\vec{G}, \sigma)$ , we have  $(T_A)_B = T_{A \cup B}$  and  $\vec{G}(T_A, \sigma) = (\vec{G}, \sigma) = \vec{G}(T_{A \cup B}, \sigma) = \vec{G}((T_A)_B, \sigma)$ . Hence,  $B$  is a set of redundant edges in  $T_A$  w.r.t.  $\vec{G}(T_A, \sigma)$ .  $\square$

### 2.3 Reconciliation Maps, Event-Labeling, and Orthology Relations

An *evolutionary scenario* extends the map  $\sigma : L(T) \rightarrow L(S)$  to an embedding of the gene tree into the species tree. It (implicitly) describes different types of evolutionary events: speciations, gene duplications, and gene losses. In this contribution we do not consider other types of events such as horizontal gene transfer. Gene losses do not appear explicitly since  $L(T)$  only contains extant genes. Inner vertices in the gene tree  $T$  that designate speciations have their correspondence in inner vertices of the species tree. In contrast, gene duplications occur independently of speciations and thus belong to edges of the species tree. The embedding of  $T$  into  $S$  is formalized by

**Definition 2.14** (Reconciliation Map). *Let  $S = (W, F)$  and  $T = (V, E)$  be two planted phylogenetic trees and let  $\sigma : L(T) \rightarrow L(S)$  be a surjective map. A reconciliation from  $(T, \sigma)$  to  $S$  is a map  $\mu : V \rightarrow W \cup F$  satisfying*

**(R0)** Root Constraint.  $\mu(x) = 0_S$  if and only if  $x = 0_T$ .

**(R1)** Leaf Constraint. If  $x \in L(T)$ , then  $\mu(x) = \sigma(x)$ .

**(R2)** Ancestor Preservation. If  $x \prec_T y$ , then  $\mu(x) \preceq_S \mu(y)$ .

**(R3)** Speciation Constraints. Suppose  $\mu(x) \in W^0$ .

(i)  $\mu(x) = \text{lca}_S(\mu(v'), \mu(v''))$  for at least two distinct children  $v', v''$  of  $x$  in  $T$ .

(ii)  $\mu(v')$  and  $\mu(v'')$  are incomparable in  $S$  for any two distinct children  $v'$  and  $v''$  of  $x$  in  $T$ .

Several alternative definitions of reconciliation maps for duplication/loss scenarios have been proposed in the literature, many of which have been shown to be equivalent. This type of reconciliation map has been established in [13]. Moreover, it has been shown in [13] that the axiom set used here is equivalent to axioms that are commonly used in the literature, see e.g. [7, 15, 19, 36, 40, 50], and the references therein. Without any further constraints, Def. 2.14 gives rise to a well-known result:

**Lemma 2.15.** [13, Lemma 3] *For every tree  $(T, \sigma)$  there is a reconciliation map  $\mu$  to any species tree  $S$  with leaf set  $L(S) = \sigma(L(T))$ .*

The reconciliation map  $\mu$  from  $(T, \sigma)$  to  $S$  determines the types of evolutionary events in  $T$ . This can be formalized by associating an event labeling with the vertices of  $T$ . We use the notation introduced in [13]:

**Definition 2.16.** *Given a reconciliation map  $\mu$  from  $(T, \sigma)$  to  $S$ , the event labeling on  $T$  (determined by  $\mu$ ) is the map  $t_\mu : V(T) \rightarrow \{\odot, \ominus, \bullet, \square\}$  given by:*

$$t_\mu(u) = \begin{cases} \odot & \text{if } u = 0_T, \text{ i.e., } \mu(u) = 0_S \text{ (root)} \\ \ominus & \text{if } u \in L(T), \text{ i.e., } \mu(u) \in L(S) \text{ (leaf)} \\ \bullet & \text{if } \mu(u) \in V^0(S) \text{ (speciation)} \\ \square & \text{else, i.e., } \mu(u) \in E(S) \text{ (duplication)} \end{cases}$$

The following result is a simple but useful consequence of combining the axioms of the reconciliation map with the event labeling of Def. 2.16.

**Lemma 2.17.** [13, Lemma 2] *Let  $\mu$  be a reconciliation map from  $(T, \sigma)$  to a tree  $S$  and suppose that  $u \in V(T)$  is a vertex with  $\mu(u) \in V^0(S)$  and thus,  $t(\mu(u)) = \bullet$ . Then,  $\sigma(L(T(v_1))) \cap \sigma(L(T(v_2))) = \emptyset$  for any two distinct  $v_1, v_2 \in \text{child}(u)$ .*

We will regularly make use of the observation that, by contraposition of Lemma 2.17,  $\sigma(L(T(v))) \cap \sigma(L(T(v'))) \neq \emptyset$  for two distinct  $v_1, v_2 \in \text{child}(u)$  implies that  $\mu(u) \in E(S)$ , and thus  $t_\mu(u) = \square$ .

Lemma 2.17 suggests to define *event-labeled trees* as trees  $(T, t)$  endowed with a map  $t : V(T) \rightarrow \{\odot, \ominus, \bullet, \square\}$  such that  $t(0_T) = \odot$  and  $t(u) = \ominus$  for all  $u \in L(T)$ . In [13], Lemma 2.17 also served as a motivation for

**Definition 2.18.** *Let  $(T, \sigma)$  be a leaf-colored tree. The extremal event labeling of  $T$  is the map  $\hat{t}_T : V(T) \rightarrow \{\odot, \ominus, \bullet, \square\}$  defined for  $u \in V(T)$  by*

$$\hat{t}_T(u) = \begin{cases} \odot & \text{if } u = 0_T \\ \ominus & \text{if } u \in L(T) \\ \square & \text{if there are two children } v_1, v_2 \in \text{child}(u) \text{ such that} \\ & \sigma(L(T(v_1))) \cap \sigma(L(T(v_2))) \neq \emptyset \\ \bullet & \text{otherwise} \end{cases}$$

The extremal event labeling  $\hat{t}_T$  is completely defined by  $(T, \sigma)$  and, in contrast to the event labeling in Def. 2.16, does not depend on a reconciliation map. However, there is no guarantee that there always exists a reconciliation map  $\mu$  from  $(T, \sigma)$  to any species tree  $S$  such that  $t_\mu = \hat{t}_T$ , cf. [13, Fig. 2] for a counterexample.

The event labeling on  $T$  defines the orthology graph.

**Definition 2.19.** *The orthology graph  $\Theta(T, t)$  of an event-labeled tree  $(T, t)$  has vertex set  $L(T)$  and edges  $uv \in E(\Theta)$  if and only if  $t(\text{lca}(u, v)) = \bullet$ .*

The orthology graph is often referred to as the orthology relation. Orthology graphs coincide with a well-known graph class:

**Theorem 2.20.** [22, Cor. 4] *A graph  $G$  is an orthology graph for some event-labeled tree  $(T, t)$ , i.e.,  $G = \Theta(T, t)$  if and only if  $G$  is a cograph.*

One of many equivalent characterizations of cographs identifies them with the graphs that do not contain an induced path  $P_4$  on four vertices [4].

The orthology graph is a subgraph of the BMG for any given reconciliation map connecting a gene with a species tree.

**Theorem 2.21.** [13, Lemma 4 & 5] *Let  $(T, \sigma)$  be a leaf-colored tree and  $\mu$  a reconciliation map from  $(T, \sigma)$  to some species tree  $S$ . Then  $\Theta(T, t_\mu) \subseteq \Theta(T, \hat{t}_T) \subseteq \bar{G}(T, \sigma)$ .*

In particular,  $t_\mu(v) = \bullet$  implies  $\hat{t}_T(v) = \bullet$  for any reconciliation map. By contraposition, therefore, if  $\hat{t}_T(v) = \square$  then  $t_\mu(v) = \square$  for all possible reconciliation maps  $\mu$  from  $(T, \sigma)$  to any species tree  $S$ . A crucial implication of Thm. 2.21 is that edges in a BMG  $\bar{G}(T, \sigma)$  always correspond to either correct orthologous pairs of genes or false-positive orthology assignments. Hence,  $\bar{G}(T, \sigma)$  does never contain false-negative orthology assignments.

## 3 False-positive orthology assignments

### 3.1 Motivation

Denote by  $(\tilde{T}, \tilde{t}, \sigma)$  the true leaf-colored and event-labeled gene tree and let  $(\bar{G}, \sigma)$  be a BMG estimated for the same data. An edge  $xy$  of  $(\bar{G}, \sigma)$ , or equivalently of the corresponding RBMG  $(G, \sigma)$  is a false-positive orthology assignment if  $xy \in E(G)$  but  $xy \notin E(\Theta(\tilde{T}, \tilde{t}, \sigma))$ ; it is a false negative orthology assignment if  $xy \notin E(G)$  but  $xy \in E(\Theta(\tilde{T}, \tilde{t}, \sigma))$ . There are two distinct sources of error: inaccuracies in the assignment of best matches [46] and limits in the reconstruction of  $(\tilde{T}, \tilde{t}, \sigma)$  from Best Match Graphs [13]. In this contribution, we are only concerned with the latter. Observation 1 of [13], see also Thm. 2.21 above, implies that for evolutionary scenarios that involve only speciations, gene duplications, and gene losses, there are no false-negative orthology assignments. Our task at hand therefore reduces to understanding the false-positive orthology assignments.

We first note that these cannot be avoided altogether. The simplest example, Fig. 1, comprises a gene duplication and a subsequent speciation and complementary gene losses in the descendant lineages such that each paralog survives only in one of them. In this situation  $xy$  is a reciprocal best match. If there are no other descendants that harbor genes witnessing the duplication event, then the framework of best matches provides no information to recognize  $xy$  as a false-positive assignment.

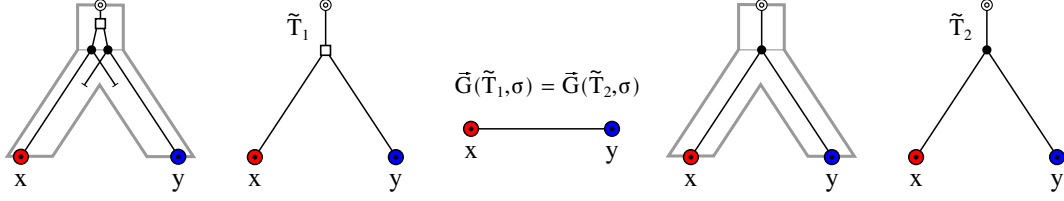


**Figure 1:** Complementary gene loss (left) that is not witnessed by any other species. In particular, two different true histories  $(\tilde{T}_1, \tilde{t}_1, \sigma)$  and  $(\tilde{T}_2, \tilde{t}_2, \sigma)$  produce the same BMG, whereas the only edge  $xy$  is a true false-positive in the first history.

### 3.2 $(T, \sigma)$ - and Unambiguous False-Positive Edges

In order to study false-positive orthology assignments in more detail, we assume that we have a tree  $(T, \sigma)$  that explains the BMG  $(\vec{G}, \sigma)$ . Note that we do not make the assumption that  $(T, \sigma)$  is least resolved.

**Definition 3.1** ( $(T, \sigma)$ -false-positive). *Let  $(T, \sigma)$  be a tree explaining the BMG  $(\vec{G}, \sigma)$ . An edge  $xy$  in  $\vec{G}$  is called  $(T, \sigma)$ -false-positive, or  $(T, \sigma)$ -fp for short, if for every reconciliation map  $\mu$  from  $(T, \sigma)$  to some species tree  $S$  we have  $t_\mu(\text{lca}_T(x, y)) = \square$ , i.e.,  $\mu(\text{lca}_T(x, y)) \in E(S)$ .*

In other words,  $xy$  is called  $(T, \sigma)$ -fp whenever  $x$  and  $y$  cannot be orthologous w.r.t. every possible reconciliation map  $\mu$  from  $(T, \sigma)$  to any species tree. Interestingly,  $(T, \sigma)$ -fps can be identified without considering reconciliation maps explicitly.

**Lemma 3.2.** *Let  $(\vec{G}, \sigma)$  be a BMG,  $xy$  be an edge in  $\vec{G}$  and  $(T, \sigma)$  be a tree that explains  $(\vec{G}, \sigma)$ . Then, the following statements are equivalent:*

1. *The edge  $xy$  is  $(T, \sigma)$ -fp.*
2. *There are two children  $v_1$  and  $v_2$  of  $\text{lca}_T(x, y)$  such that  $\sigma(L(T(v_1))) \cap \sigma(L(T(v_2))) \neq \emptyset$ .*
3. *For the extremal labeling  $\hat{t}_T$  of  $(T, \sigma)$  it holds that  $\hat{t}_T(\text{lca}_T(x, y)) = \square$ .*

*Proof.* (2) implies (1). Suppose that there are two children  $v_1$  and  $v_2$  of  $\text{lca}_T(x, y)$  such that  $\sigma(L(T(v_1))) \cap \sigma(L(T(v_2))) \neq \emptyset$ . By Lemma 2.17,  $\mu(\text{lca}_T(x, y)) \in E(S)$  and thus,  $t_\mu(\text{lca}_T(x, y)) = \square$  for all possible reconciliation maps  $\mu$  from  $(T, \sigma)$  to any species tree  $S$ . Hence,  $xy$  is  $(T, \sigma)$ -fp.

(1) implies (2). By contraposition, let  $v = \text{lca}_T(x, y)$  and suppose that for all distinct children  $v_i, v_j \in \text{child}(v) = \{v_1, \dots, v_k\}$ ,  $k \geq 2$  we have  $\sigma(L(T(v_i))) \cap \sigma(L(T(v_j))) = \emptyset$ . In the following, we show that there is a species tree  $S$  and a reconciliation map  $\mu$  from  $(T, \sigma)$  to  $S$  such that  $t_\mu(\text{lca}_T(x, y)) = \bullet$ , which implies that  $xy$  is not  $(T, \sigma)$ -fp.

We construct the species tree  $S$  as follows:  $S$  has root edge  $0_S \rho_S$ . Now add  $k$  children  $u_1, \dots, u_k$  to  $\rho_S$ . For each of these children  $u_i$  with  $|\sigma(L(T(v_i)))| > 1$ , we add a leaf  $t$  for every color  $t \in \sigma(L(T(v_i)))$  and the edge  $u_i t$ . Any other  $u_i$  is considered to be a leaf in  $S$ , and we identify  $u_i$  with the single element in  $\sigma(L(T(v_i)))$ . Furthermore, add for all  $t \in \sigma(L(T)) \setminus \sigma(L(T(v)))$  a leaf  $t$  that is adjacent to  $\rho_S$ . Since the color sets  $\sigma(L(T)) \setminus \sigma(L(T(v))), \sigma(L(T(v_1))), \dots, \sigma(L(T(v_k)))$  are pairwise distinct,  $S$  is well-defined, and, by construction, a planted phylogenetic tree. To construct a reconciliation map we put (i)  $\mu(0_T) = 0_S$ ; (ii)  $\mu(x) = \sigma(x)$  for all  $x \in L(T)$ ; (iii)  $\mu(v) = \rho_S$ ; (iv)  $\mu(w) = 0_S \rho_S$  for all  $w \in V^0(T \setminus T(v))$ ; and (v)  $\mu(w) = \rho_S u_i$  for all  $w \in V^0(T(v_i))$ . By Condition (i) and (ii), the Axioms (R0) and (R1) are satisfied, respectively. By Condition (v), we have  $\mu(v_i) = \rho_S u_i$  if  $v_i$  is an inner vertex. Otherwise,  $v_i$  is a leaf and  $|\sigma(L(T(v_i)))| = 1$ . Therefore,  $\mu(v_i) = \sigma(v_i) = u_i$  by (ii) and by construction. It is easy to verify that  $\mu$  satisfies (R2). A sketch of construction of the species tree  $S$  and the reconciliation map  $\mu$  is provided in Fig. 2.

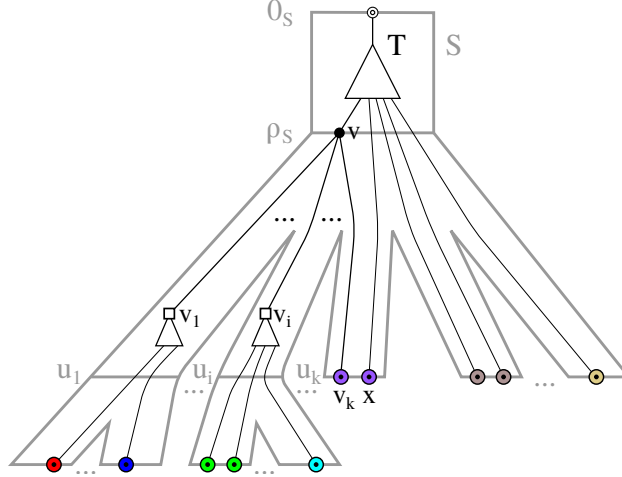


**Figure 2:** Visualization of the construction of a species tree  $S$  and reconciliation map  $\mu$  as described in the proof of Lemma 3.2. Note that, in the example,  $v_k$  is already a leaf in the gene tree  $T$ . Hence, the corresponding  $u_k$  is also a leaf since  $|\sigma(L(T(v_k)))| = 1$ . Moreover, note that for  $x \in L(T) \setminus L(T(v))$ , it is possible that  $\mu(x) = u_j$  or  $\mu(x) = t$  with  $t \in \text{child}_S(u_j)$  for some  $u_j$ .

The only vertex of  $T$  that is mapped to a vertex in  $S$  is  $v$ . Hence, it remains to show that  $\mu(v) = \rho_S \in V^0(S)$  satisfies (R3). Note that for every two distinct children  $v_i, v_j$  of  $v$  we have  $\mu(v_i) \in \{\rho_S u_i, u_i\}$  and  $\mu(v_j) \in \{\rho_S u_j, u_j\}$ . In any case,  $\mu(v_i)$  and  $\mu(v_j)$  are incomparable in  $S$ . Hence, (R3.ii) is satisfied. In particular,  $\mu(v) = \rho_S = \text{lca}_S(\mu(v_i), \mu(v_j))$  for all distinct  $v_i, v_j \in \text{child}(v)$ . Hence, (R3.i) is satisfied. In summary,  $\mu$  is a reconciliation map from  $(T, \sigma)$  to  $S$ . Since  $\mu(v) = \rho_S \in V^0(S)$ , we have  $t_\mu(v) = \bullet$ .

Statements (2) and (3) are equivalent by definition of the extremal event labeling.  $\square$

Lemma 3.2 implies that  $(T, \sigma)$ -fp can be verified in polynomial-time for any given gene tree  $(T, \sigma)$ .

**Definition 3.3** (Unambiguous false-positive). *Let  $(\vec{G}, \sigma)$  be a BMG. An edge  $xy$  in  $\vec{G}$  is called unambiguous false-positive ( $u$ -fp) if for all trees  $(T, \sigma)$  that explain  $(\vec{G}, \sigma)$  the edge  $xy$  is  $(T, \sigma)$ -fp.*

Hence, if an edge  $xy$  in  $\vec{G}$  is  $u$ -fp, then it is in particular  $(T, \sigma)$ -fp in the true history that explains  $\vec{G}$ . Thus,  $u$ -fp edges are always “correct” false-positives.

Clearly, not all “correct” false-positives are covered by this definition, since it may be possible that, for an edge  $xy$  in  $\vec{G}$ , we have  $t_\mu(\text{lca}_T(x, y)) = \square$  for the true gene tree and the true species tree, but  $xy$  is not  $(T', \sigma)$ -fp for some gene tree  $(T', \sigma)$  possibly different from  $(T, \sigma)$ . One of the simplest examples is shown in Fig. 1, assuming that  $(\vec{T}_1, \sigma)$  is the “true” history. Since  $t_\mu(\text{lca}_{\vec{T}_1}(x, y)) = \bullet$  may be possible (Fig. 1, right), the edge  $xy$  is not  $(\vec{T}_1, \sigma)$ -fp and therefore not  $u$ -fp.

### 3.3 The Color-Intersection $\mathcal{S}^\cap$

In this subsection, we introduce the color-intersection  $\mathcal{S}^\cap$ , which can be used to identify false-positive edges, and establish its most salient properties. Given a gene tree  $(T, \sigma)$  and a pair of distinct leaves  $x, y \in L(T)$  we denote by  $v_x, v_y \in \text{child}_T(\text{lca}_T(x, y))$  the unique children of the last common ancestor of  $x$  and  $y$  for which  $x \preceq_T v_x$  and  $y \preceq_T v_y$ . That is,  $T(v_x)$  and  $T(v_y)$  are the subtrees of  $T$  rooted in the children of  $\text{lca}_T(x, y)$  with  $x \in L(T(v_x))$  and  $y \in L(T(v_y))$ . The set

$$\mathcal{S}_T^\cap(x, y) := \sigma(L(T(v_x))) \cap \sigma(L(T(v_y))) \quad (1)$$

contains the colors, i.e. species, that are common to both subtrees. Lemma 2.4 immediately implies

**Corollary 3.4.** *Let  $xy$  be an edge in a BMG  $(\vec{G}, \sigma)$ . Then  $\sigma(\{x, y\}) \cap \mathcal{S}_T^\cap(x, y) = \emptyset$  for all trees  $(T, \sigma)$  that explain  $(\vec{G}, \sigma)$ .*

The following result shows that the color-intersection of a given edge in a BMG  $(\vec{G}, \sigma)$  in fact does not depend on the tree representation of  $(\vec{G}, \sigma)$ .

**Lemma 3.5.** *Let  $(\vec{G}, \sigma)$  be a BMG and  $(T^*, \sigma)$  the corresponding unique least resolved tree explaining  $(\vec{G}, \sigma)$ . Then, for each tree  $(T, \sigma)$  that explains  $(\vec{G}, \sigma)$ , every edge  $xy$  in  $(\vec{G}, \sigma)$  satisfies  $\mathcal{S}_{T^*}^\cap(x, y) = \mathcal{S}_T^\cap(x, y)$ . Thus, in particular,  $\mathcal{S}_{T^*}^\cap(x, y) \neq \emptyset$  if and only if  $\mathcal{S}_T^\cap(x, y) \neq \emptyset$ .*



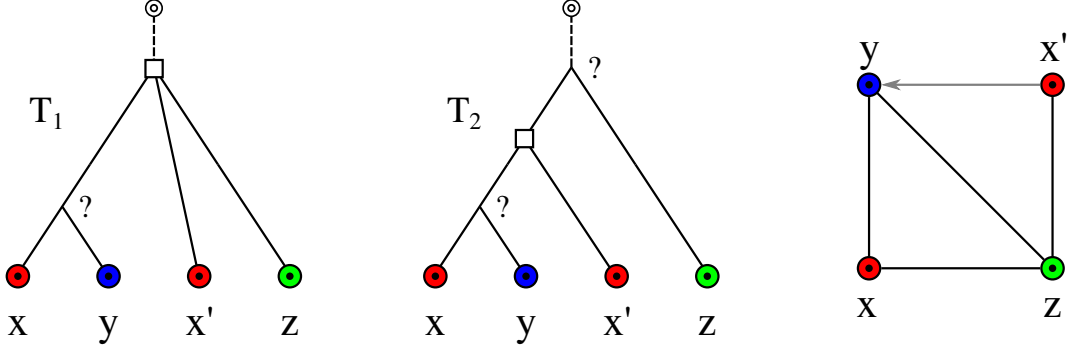


**Figure 3:** The BMG  $(\vec{G}, \sigma)$  shown on the right is explained by both  $(T_1, \sigma)$ , which is the unique least resolved tree for  $(\vec{G}, \sigma)$ , and  $(T_2, \sigma)$ . The vertices labeled  $\square$  must be duplications due to Lemma 2.17, while the vertices labeled “?” could be both duplications or speciations. The edges  $xz$ ,  $x'z$  and  $yz$  are  $(T_1, \sigma)$ -*fp* but not  $(T_2, \sigma)$ -*fp* (cf. Lemma 3.2). Thus, neither of the edges  $xz$ ,  $x'z$  and  $yz$  is *u-fp*.

*Proof.* Let  $(T, \sigma)$  be an arbitrary tree that explains  $(\vec{G}, \sigma)$ . Moreover, let  $xy$  be an edge in  $\vec{G}$  and denote by  $v_x$  and  $v_y$  be the unique children  $v_x, v_y \in \text{child}_T(\text{lca}_T(x, y))$  with  $x \preceq_T v_x$  and  $y \preceq_T v_y$ . Analogously,  $v_x^*$  and  $v_y^*$  are the unique children  $v_x^*, v_y^* \in \text{child}_{T^*}(\text{lca}_{T^*}(x, y))$  with  $x \preceq_{T^*} v_x^*$  and  $y \preceq_{T^*} v_y^*$ .

First, we show that  $t \in \mathcal{S}_{T^*}^\cap(x, y)$  implies  $t \in \mathcal{S}_T^\cap(x, y)$ . Since  $(T, \sigma)$  explains  $(\vec{G}, \sigma)$ , we apply Thm. 2.6 to conclude that  $T$  is a refinement of  $T^*$  and thus,  $\mathcal{C}(T^*) \subseteq \mathcal{C}(T)$ . Therefore,  $L(T^*(\text{lca}_{T^*}(x, y)))$ ,  $L(T^*(v_x^*))$  and  $L(T^*(v_y^*))$  are contained in  $\mathcal{C}(T)$ . This implies that there must be vertices  $u$ ,  $w_x$ , and  $w_y$  in  $T$  with  $L(T(u)) = L(T^*(\text{lca}_{T^*}(x, y)))$ ,  $L(T(w_x)) = L(T^*(v_x^*))$  and  $L(T(w_y)) = L(T^*(v_y^*))$ . Note that  $L(T^*(v_x^*)) \cap L(T^*(v_y^*)) = \emptyset$ , and thus  $L(T(w_x)) \cap L(T(w_y)) = \emptyset$ . In particular,  $w_x$  and  $w_y$  are incomparable in  $T$ . Moreover,  $u = \text{lca}_T(x, y) = \text{lca}_T(w_x, w_y)$ , thus we have  $w_x \preceq_T v_x$  and  $w_y \preceq_T v_y$ . Therefore,  $L(T^*(v_x^*)) \subseteq L(T(v_x))$  and  $L(T^*(v_y^*)) \subseteq L(T(v_y))$ . Therefore,  $t \in \mathcal{S}_{T^*}^\cap(x, y)$  implies  $t \in \mathcal{S}_T^\cap(x, y)$ .

Now, we show that  $t \in \mathcal{S}_T^\cap(x, y)$  implies  $t \in \mathcal{S}_{T^*}^\cap(x, y)$ . Let  $t \in \mathcal{S}_T^\cap(x, y) \neq \emptyset$ . In this case,  $t \in \sigma(L(T(v_x)))$  and we can choose a vertex  $z_1 \in L(T(v_x))$  such that  $\sigma(z_1) = t$  and  $\text{lca}_T(x, z_1)$  is as far away as possible from  $v_x$  compared to all  $\text{lca}_T(x, z)$  with  $z \in L[t]$ , i.e.,  $\text{lca}_T(x, z_1) \preceq_T \text{lca}_T(x, z)$  for all  $z \in L[t]$ . Thus,  $(x, z_1) \in E(\vec{G})$ . An analogous argument ensures that there is a vertex  $z_2 \in L(T(v_y))$  such that  $\sigma(z_2) = t$  and  $(y, z_2) \in E(\vec{G})$ . Clearly,  $\text{lca}_T(x, z_2) = \text{lca}_T(x, y) = \text{lca}_T(y, z_1)$  and thus  $\text{lca}_T(x, z_1) \preceq_T v_x \prec_T \text{lca}_T(x, z_2)$ , which in turn implies that  $(x, z_2) \notin E(\vec{G})$ . Since  $(x, z_1) \in E(\vec{G})$  and  $(x, z_2) \notin E(\vec{G})$ , we obtain the informative triple  $xz_1|z_2$  for  $\vec{G}$ . Analogously,  $yz_2|z_1$  is an informative triple for  $\vec{G}$ . Lemma 2.9 and the fact that  $T^*$  explains  $(\vec{G}, \sigma)$  implies that there are distinct vertices  $v_1, v_2 \in \text{child}_{T^*}(\text{lca}_{T^*}(x, y))$  such that  $x, z_1 \preceq_{T^*} v_1$  and  $y, z_2 \preceq_{T^*} v_2$ . Since  $t = \sigma(z_1) = \sigma(z_2)$ , we have  $t \in \mathcal{S}_{T^*}^\cap(x, y)$ .

Finally,  $t \in \mathcal{S}_{T^*}^\cap(x, y)$  if and only if  $t \in \mathcal{S}_T^\cap(x, y)$  implies both  $\mathcal{S}_{T^*}^\cap(x, y) = \mathcal{S}_T^\cap(x, y)$  and  $\mathcal{S}_{T^*}^\cap(x, y) \neq \emptyset$  if and only if  $\mathcal{S}_T^\cap(x, y) \neq \emptyset$ . □

**Remark 1.** By Lemma 3.5, we have  $\mathcal{S}_T^\cap(x, y) = \mathcal{S}_{T^*}^\cap(x, y)$  for every tree  $(T, \sigma)$  explaining a BMG  $(\vec{G}, \sigma)$  with corresponding least resolved tree  $(T^*, \sigma)$ . Therefore, it is sufficient to consider  $\mathcal{S}_{T^*}^\cap(x, y)$ . We will therefore drop the explicit reference to the tree and simply write  $\mathcal{S}^\cap(x, y)$ . We can verify in polynomial time whether or not  $\mathcal{S}^\cap(x, y) = \emptyset$  because the least resolved tree  $(T^*, \sigma)$  explaining  $(\vec{G}, \sigma)$  can be computed in polynomial time.

**Proposition 3.6.** Every edge  $xy$  in a BMG  $(\vec{G}, \sigma)$  with  $\mathcal{S}^\cap(x, y) \neq \emptyset$  is *u-fp*.

*Proof.* By Lemma 3.5 and Remark 1,  $\mathcal{S}^\cap(x, y) \neq \emptyset$  if and only if  $\mathcal{S}_T^\cap(x, y) \neq \emptyset$  for all trees  $(T, \sigma)$  that explain  $(\vec{G}, \sigma)$ . By Lemma 2.17,  $\mu(\text{lca}_T(x, y)) \in E(S)$  and thus,  $t_\mu(\text{lca}_T(x, y)) = \square$  for all trees  $(T, \sigma)$  that explain  $(\vec{G}, \sigma)$ . Hence,  $xy$  is *u-fp*. □

As we shall see later, the converse of Prop. 3.6 is not always satisfied (cf. also Fig. 5). An immediate consequence of Prop. 3.6 is the following:

**Corollary 3.7.** An edge  $xy$  in a BMG  $\vec{G}(T, \sigma)$  with  $\mathcal{S}^\cap(x, y) \neq \emptyset$  is  $(T, \sigma)$ -*fp*.

The converse, however, is not true in general. For an example consider the unique least resolved tree  $(T_1, \sigma)$  that explains the BMG  $(\vec{G}, \sigma)$  in Fig. 3. Here, the edge  $xz$  is  $(T_1, \sigma)$ -*fp* (cf. Lemma 3.2) but  $\mathcal{S}^\cap(x, z) = \emptyset$ . Although not necessarily true in general, the converse of Prop. 3.6 and Cor. 3.7 does hold for the special case of binary trees.

**Lemma 3.8.** Let  $xy$  be an edge in  $\vec{G}(T, \sigma)$  and suppose  $\text{lca}_T(x, y)$  is a binary vertex. Then, the following three statements are equivalent:

1. The edge  $xy$  is  $(T, \sigma)$ -fp.
2.  $\mathcal{S}^\cap(x, y) \neq \emptyset$ .
3. The edge  $xy$  is u-fp.

*Proof.* (1) implies (2). Suppose  $xy$  is  $(T, \sigma)$ -fp. Since  $v$  is binary, it has precisely two children  $v_1$  and  $v_2$ . In particular,  $v = \text{lca}_T(x, y)$  implies that  $x \preceq_T v_i$  and  $y \preceq_T v_j$  for  $i, j \in \{1, 2\}$  being distinct. By Lemma 3.2, the two children  $v_1$  and  $v_2$  of  $v$  satisfy  $\sigma(L(T(v_1))) \cap \sigma(L(T(v_2))) \neq \emptyset$ . By Lemma 3.5 and Remark 3.5, we have  $\mathcal{S}^\cap(x, y) \neq \emptyset$ .

(2) implies (3). If  $\mathcal{S}^\cap(x, y) \neq \emptyset$ , we can apply Prop. 3.6 to conclude that  $xy$  is u-fp.

(3) implies (1). By definition, if  $xy$  is u-fp, then it is in particular also  $(T, \sigma)$ -fp. □

**Theorem 3.9.** Let  $(\vec{G}, \sigma)$  be a BMG that is explained by a binary tree  $(T, \sigma)$ . Then  $xy$  is  $(T, \sigma)$ -fp if and only if  $xy$  is u-fp.

*Proof.* For every edge  $xy$  in  $\vec{G}$  the last common ancestor  $\text{lca}_T(x, y)$  is binary. Now apply Lemma 3.8. □

Thm. 3.9 implies that all u-fp edges can be detected in a BMG that is explained by a known binary gene tree. However, not all BMGs  $(\vec{G}, \sigma)$  can be explained by a binary tree, as e.g. the BMG in Fig. 6(A). Thm. 3.9 does not generalize to the non-binary case, and  $\mathcal{S}^\cap(x, y)$  is not sufficient to identify all u-fp edges. Furthermore, it is not difficult to find non-binary trees in which  $(T, \sigma)$ -fp and u-fp edges are not the same: As show in Fig. 3, the edge  $xz$  in is  $(T_1, \sigma)$ -fp but not  $(T_2, \sigma)$ -fp according to Lemma 3.2. Since both trees explain the same BMG, the edge  $xy$  is not u-fp.

### 3.4 The Case $\mathcal{S}^\cap(x, y) \neq \emptyset$ and Quartets

Since every orthology graph is a cograph (Thm. 2.20) and thus free of induced  $P_4$ s, every induced  $P_4$  in the RBMG necessarily contains a false-positive orthology assignments. The subgraphs of the BMG spanned by a  $P_4$  in its symmetric part (i.e., the RBMG) are known as quartets. The quartets on three colors of a BMG  $(\vec{G}, \sigma)$  fall into three distinct classes depending on the coloring and the additional, non-symmetric edges (cf. [14, Lemma 32]). We write  $\langle abcd \rangle$  or, equivalently,  $\langle dcba \rangle$  for an induced  $P_4$  with edges  $ab$ ,  $bc$ , and  $cd$ .

**Definition 3.10** (Good, bad, and ugly quartets). Let  $(\vec{G}, \sigma)$  be a BMG with symmetric part  $(G, \sigma)$  and vertex set  $L$ , and let  $Q := \{x, y, z, z'\} \subseteq L$  with  $x \in L[r]$ ,  $y \in L[s]$ , and  $z, z' \in L[t]$ . The set  $Q$ , resp., the induced subgraph  $(\vec{G}[Q], \sigma|_Q)$  is

a good quartet if (i)  $\langle zxyz' \rangle$  is an induced  $P_4$  in  $(G, \sigma)$  and (ii)  $(z, y), (z', x) \in E(\vec{G})$  and  $(y, z), (x, z') \notin E(\vec{G})$ ,

a bad quartet if (i)  $\langle zxyz' \rangle$  is an induced  $P_4$  in  $(G, \sigma)$  and (ii)  $(y, z), (x, z') \in E(\vec{G})$  and  $(z, y), (z', x) \notin E(\vec{G})$ ,

an ugly quartet if  $\langle zxz'y \rangle$  is an induced  $P_4$  in  $(G, \sigma)$ .

The edge  $xy$  in a good quartet  $\langle zxyz' \rangle$  is its middle edge. The edge  $zx$  of an ugly quartet  $\langle zxz'y \rangle$  or a bad quartet  $\langle zxyz' \rangle$  is called its first edge. First edges in ugly quartets are uniquely determined due to the colors. In bad quartets, this is not the case and therefore, the edge  $yz'$  in  $\langle zxyz' \rangle$  is a first edge as well.

An RBMG never contains induced  $P_4$ s on two colors [14, Observation 5]. This, in particular, implies that for the induced  $P_4$ s in Def. 3.10 the colors  $r, s, t$  must be pairwise distinct. Note that BMGs can also contain induced  $P_4$ s on four colors. However, these are of no further interest for our purpose.

Good quartets are the characteristic subgraphs that appear in a BMG whenever a complementary gene loss (as shown in Fig. 1) is “witnessed” by a third species ( $\sigma(z) = \sigma(z')$ ), in which both child branches of the problematic duplication event survive. We remark that previous work also noted that complementary gene loss can be resolved successfully under certain circumstances [6] such as this one. The key property of good quartets for our purpose is a consequence of [13, Cor. 5]:

**Proposition 3.11.** If  $\langle zxyz' \rangle$  is a good quartet in the BMG  $(\vec{G}, \sigma)$ , then  $\mathcal{S}^\cap(x, y) \neq \emptyset$  and thus,  $xy$  is u-fp.

*Proof.* Let  $\langle zxyz' \rangle$  in  $(\vec{G}, \sigma)$  be a good quartet in  $(\vec{G}, \sigma)$  and let  $(T, \sigma)$  be an arbitrary tree explaining  $(\vec{G}, \sigma)$ . Then [14, Lemma 36] implies that  $v := \text{lca}_T(x, y, z, z')$  has two distinct children  $v_1, v_2 \in \text{child}(v)$  such that  $x, z \preceq_T v_1$  and  $y, z' \preceq_T v_2$ . Hence,  $v = \text{lca}_T(x, y)$ . Since  $\sigma(z) \in \sigma(L(T(v_1))) \cap \sigma(L(T(v_2)))$ , we have  $\mathcal{S}^\cap(x, y) \neq \emptyset$  and, by Prop. 3.6, the edge  $xy$  is u-fp. □

Prop. 3.11 thus provides a convenient way to identify unambiguous false-positive edges in the BMG.

**Lemma 3.12.** If  $xy$  is an edge in a BMG  $\vec{G}(T, \sigma)$  and  $t \in \mathcal{S}^\cap(x, y)$ , then there is a good quartet  $\langle z_1x^*y^*z_2 \rangle$  such that

- (a)  $\sigma(x^*) = \sigma(x)$ ,  $\sigma(y^*) = \sigma(y)$ , and  $\sigma(z_1) = \sigma(z_2) = t$ ;
- (b)  $x^*, z_1 \in L(T(v_x))$  and  $y^*, z_2 \in L(T(v_y))$  with  $v_x$  and  $v_y$  being the unique children in  $\text{child}_T(\text{lca}_T(x, y))$  such that with  $x \preceq_T v_x$  and  $y \preceq_T v_y$ .

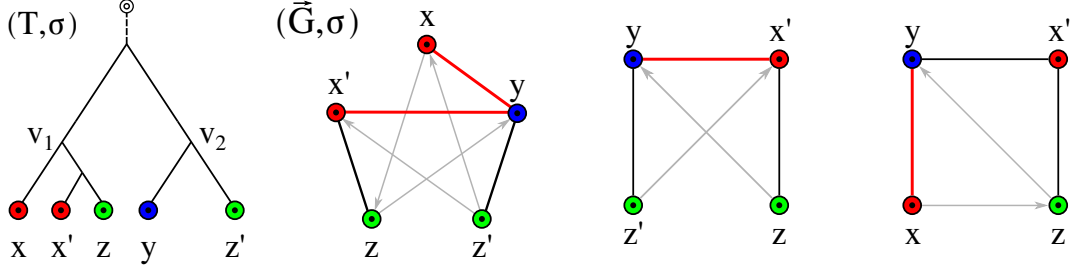


**Figure 4:** Example for a  $(T, \sigma)$ -fp edge  $xy$  in  $(\vec{G}, \sigma)$  which is not the middle edge of a good quartet, but the first edge in an ugly quartet (right). Note,  $(\vec{G}, \sigma)$  does not contain bad quartets.

*Proof.* Consider an edge  $xy$  of  $\vec{G}(T, \sigma)$  and a color  $t \in \mathcal{S}^\cap(x, y)$ . By Cor. 3.4,  $t \neq \sigma(x), \sigma(y)$ . Lemma 2.3 ensures the existence of an edge  $x^*z_1$  in  $\vec{G}$  for some leaves  $x^* \in L(T(v_x)) \cap L[\sigma(x)]$  and  $z_1 \in L(T(v_x)) \cap L[t]$ . By the same arguments as in the proof of Cor. 3.4, we can conclude that  $z_1y'$  is not an edge in  $\vec{G}$  for all  $y' \in L(T(v_y)) \cap L[\sigma(y)]$ . However,  $(z_1, y') \in E(\vec{G})$  since the color of  $y'$  is not present in  $T(v_x)$ . Likewise, there are leaves  $y^* \in L(T(v_y)) \cap L[\sigma(y)]$  and  $z_2 \in L(T(v_y)) \cap L[t]$  such that  $y^*z_2$  forms an edge in  $\vec{G}$ . Reusing the arguments from  $L(T(v_x))$ , we find that  $x'z_2$  is not an edge in  $\vec{G}$  and  $(z_2, x') \in E(\vec{G})$  for any  $x' \in L(T(v_x)) \cap L[\sigma(x)]$ . Finally,  $\sigma(x) \notin \sigma(L(T(v_y)))$  and  $\sigma(y) \notin \sigma(L(T(v_x)))$  implies that  $x^*y^*$  forms an edge in  $\vec{G}$ . Hence,  $\langle z_1x^*y^*z_2 \rangle$  is a good quartet.  $\square$

Note that the edge  $x^*y^*$  in Lemma 3.12 is the middle edge of a good quartet. For completeness, we provide a result for the identification of  $u$ -fp edges using bad quartets

**Proposition 3.13.** *Let  $\langle zxy'z' \rangle$  be a bad quartet in a BMG  $(\vec{G}, \sigma)$ . Then, the edges  $xz$  and  $yz'$  are  $u$ -fp and every tree that explains  $(\vec{G}, \sigma)$  is non-binary.*

*Proof.* Let  $(T, \sigma)$  be an arbitrary tree that explains  $(\vec{G}, \sigma)$ , set  $u := \text{lca}_T(x, z)$  and let  $v_x, v_z \in \text{child}_T(u)$  be the two distinct children of  $u$  such that  $x \preceq_T v_x$  and  $z \preceq_T v_z$ . By symmetry, it suffices to show that  $xz$  is  $u$ -fp. Since  $\langle zxy'z' \rangle$  is a bad quartet, we have  $(x, z), (x, z') \in E(\vec{G})$  and thus  $\text{lca}_T(x, z') = \text{lca}_T(x, z) = u$ . Let  $v_{z'} \in \text{child}_T(u)$  be the child of  $u$  such that  $z' \preceq_T v_{z'}$ . Since  $\text{lca}_T(x, z') = u$  we have  $v_x \neq v_{z'}$ . Now, assume for contradiction that  $v_z = v_{z'}$ , and thus  $z' \in L(T(v_z))$ . Since  $\langle zxy'z' \rangle$  is a bad quartet, we have  $(z', x) \notin E(\vec{G})$ , which implies the existence of a vertex  $x'$  with  $\sigma(x) = \sigma(x')$  and  $\text{lca}_T(x', z') \prec_T \text{lca}_T(x, z') = u$  and therefore,  $x' \in L(T(v_z))$ . However, this implies that  $\text{lca}_T(x', z) \preceq_T v_z \prec_T u = \text{lca}_T(x, z)$ , which together with  $\sigma(x) = \sigma(x')$  contradicts the fact that  $xz$  is an edge in  $\vec{G}$ . Hence,  $v_z \neq v_{z'}$ . Therefore,  $\sigma(z) = \sigma(z') \in \sigma(L(T(v_z))) \cap \sigma(L(T(v_{z'}))) \neq \emptyset$  for distinct children  $v_z, v_{z'} \in \text{child}_T(u)$ . By Lemma 3.2, the edge  $xz$  is  $(T, \sigma)$ -fp and since  $(T, \sigma)$  was chosen arbitrarily, the edge  $xz$  is  $u$ -fp. Moreover, we have shown that  $v_x, v_z$  and  $v_{z'}$  must be pairwise distinct and thus,  $(T, \sigma)$  is non-binary.  $\square$

Edges of good and bad quartets can be used to identify  $u$ -fp edges. The example in Fig. 4 shows, however, that not all false-positive edges  $xy$  with  $\mathcal{S}^\cap(x, y) \neq \emptyset$  are middle edges of good quartets or first edges of bad quartets. The top vertex in the tree in Fig. 4 must be a duplication event since  $\mathcal{S}^\cap(x, y) = \sigma(L(T(v_x))) \cap \sigma(L(T(v_y))) \neq \emptyset$  (cf. Prop. 3.6). The only good quartet is  $\langle z'x'y'z' \rangle$  identifying  $x'y$  as false-positive. Moreover,  $(\vec{G}, \sigma)$  does not contain a bad quartet. The edge  $xy$ , on the other hand, is the first edge in the ugly quartet  $\langle xyx'z \rangle$ . Thus, in this example, there is no evidence provided by good or bad quartets to identify the edge  $xy$  as  $u$ -fp. Therefore, we focus on ugly quartets as additional source of information to identify  $u$ -fp's. In particular, as it will turn out,  $u$ -fp edges in bad quartets are entirely covered by  $u$ -fp edges in good quartets, ugly quartets and a more general subgraph construction that is introduced in Section 3.5.

**Proposition 3.14.** *If  $\langle xyx'z \rangle$  is an ugly quartet in a BMG  $(\vec{G}, \sigma)$ , then the edges  $xy$  and  $yx'$  are  $u$ -fp.*

*Proof.* Consider an ugly quartet  $\langle xyx'z \rangle$ . Let  $(T, \sigma)$  be an arbitrary tree explaining  $(\vec{G}, \sigma)$ , put  $u := \text{lca}_T(x, y)$  and let  $v_x, v_y \in \text{child}_T(u)$  be the two distinct children of  $u$  such that  $x \preceq_T v_x$  and  $y \preceq_T v_y$ .

Since  $x'y$  and  $xy$  are edges in  $\vec{G}$  we have  $\text{lca}_T(x', y) \preceq_T u$ . Moreover, Cor. 3.4 implies  $\sigma(x') = \sigma(x) \notin \sigma(L(T(v_y)))$  and thus  $x' \notin L(T(v_y))$ . Therefore,  $\text{lca}_T(x', y) = \text{lca}_T(x, y) = u$ .

Now consider an arbitrary reconciliation map  $\mu$  from  $(T, \sigma)$  to some species tree  $S$ . The existence of  $\mu$  is guaranteed by Lemma 2.15. If  $x' \notin L(T(v_x))$ , then there is a vertex  $v_3 \in \text{child}_T(u)$ ,  $v_3 \neq v_x, v_y$  such that  $x' \preceq_T v_3$  and  $\sigma(x) = \sigma(x') \in \sigma(L(T(v_x))) \cap \sigma(L(T(v_3))) \neq \emptyset$ , which by Lemma 2.17 implies  $t_\mu(u) = \square$ .

Now suppose  $x' \in L(T(v_x))$  and recall that  $x'z$  is an edge in  $\vec{G}$  by assumption. Since  $\text{lca}_T(x', z)$  and  $\text{lca}_T(x, x')$  are both ancestors of  $x'$  they are comparable. If  $\text{lca}_T(x', z) \succ_T \text{lca}_T(x, x')$ , then  $\text{lca}_T(x, z) = \text{lca}_T(x', z)$ . Together with the fact that  $x'z$  is an edge in  $\vec{G}$  but not  $xz$ , this implies that there is a  $z' \in L[\sigma(z)]$  such that  $\text{lca}_T(x, z') \prec_T \text{lca}_T(x, z)$ . This in turn implies  $\text{lca}_T(x', z') \prec_T \text{lca}_T(x', z)$ , which contradicts that  $x'z$  is an edge in  $\vec{G}$ . Therefore,  $x' \in L(T(v_x))$  implies

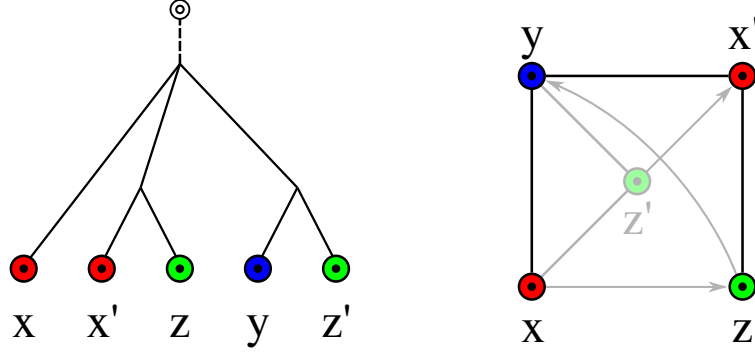


**Figure 5:** The edge  $xy$  is  $u$ - $fp$  since it is the first edge of an ugly quartet. However,  $\mathcal{S}^\cap(x, y) = \emptyset$  and thus, the converse of Prop. 3.15 is not satisfied.

$\text{lca}_T(x', z) \preceq_T \text{lca}_T(x, x')$  and  $x, x', z \in L(T(v_x))$ . Since  $yz$  is not an edge in  $\vec{G}$  by assumption and Cor. 3.4 implies  $\sigma(y) \notin \sigma(L(T(v_x)))$ , there is a leaf  $z'$  with color  $\sigma(z') = \sigma(z)$  such that  $\text{lca}_T(y, z') \prec_T \text{lca}_T(y, z)$ . This is only possible if  $z' \in L(T(v_y)) \cap L[\sigma(z)]$ . Therefore,  $\sigma(z) \in \sigma(L(T(v_x))) \cap \sigma(L(T(v_y)))$  and Lemma 2.17 implies that  $t_\mu(u) = \square$ .

In summary,  $\text{lca}_T(x', y) = \text{lca}_T(x, y) = u$  and  $t_\mu(u) = \square$  for every tree explaining  $(\vec{G}, \sigma)$  and every possible reconciliation map  $\mu$  from  $(T, \sigma)$  to any species tree. Thus both  $xy$  and  $x'y$  are  $u$ - $fp$ .  $\square$

**Proposition 3.15.** *Let  $(\vec{G}, \sigma)$  be a BMG and  $xy$  an edge in  $\vec{G}$  with  $\mathcal{S}^\cap(x, y) \neq \emptyset$ . Then  $xy$  is either the middle edge of some good quartet  $\langle zxy'z' \rangle$  or the first edge in some ugly quartet  $\langle xyx'z \rangle$  or  $\langle yxy'z \rangle$ .*

*Proof.* Let  $(T, \sigma)$  be a leaf-colored tree explaining the BMG  $(\vec{G}, \sigma)$  with symmetric part  $(G, \sigma)$ . Let  $v_x, v_y \in \text{child}_T(\text{lca}_T(x, y))$  such that  $x \preceq_T v_x$  and  $y \preceq_T v_y$ . Since  $\mathcal{S}^\cap(x, y) \neq \emptyset$ , Lemma 3.12 implies that there is a good quartet  $\langle z_1x^*y^*z_2 \rangle$  with  $\sigma(x^*) = \sigma(x)$ ,  $\sigma(y^*) = \sigma(y)$ ,  $\sigma(z_1) = \sigma(z_2) = t \in \mathcal{S}^\cap(x, y)$ ,  $x^*, z_1 \in L(T(v_x))$  and  $y^*, z_2 \in L(T(v_y))$ .

If  $x = x^*$  and  $y = y^*$  we are done. By symmetry it suffices to consider the case  $x \neq x^*$ . Before we proceed, we consider the (non-)existence of certain edges in the RBMG  $G(T, \sigma)$  and the BMG  $\vec{G}(T, \sigma)$ . By definition of good quartets, we have  $x^*z_1, x^*y^*, y^*z_2 \in E(G)$  and Cor. 3.4 implies  $\sigma(x), \sigma(y) \notin \mathcal{S}^\cap(x, y)$ . Hence,  $\sigma(x^*) = \sigma(x) \notin \sigma(L(T(v_y)))$  and  $\sigma(y^*) = \sigma(y) \notin \sigma(L(T(v_x)))$ , and thus  $x^*y \in E(G)$  and  $xy^* \in E(G)$ . Moreover, since  $\text{lca}_T(y, z_2) \prec_T \text{lca}_T(y, z_1)$ , we have  $yz_1 \notin E(G)$ . Similarly,  $xz_2 \notin E(G)$ . However,  $\sigma(x) \notin \sigma(L(T(v_y)))$  implies that  $\text{lca}_T(z_2, x) = \text{lca}_T(x, y) \preceq \text{lca}_T(z_2, x')$  for all  $x' \in L[\sigma(x)]$  and thus,  $(z_2, x) \in E(\vec{G})$ . Similarly,  $(z_1, y) \in E(\vec{G})$ . Furthermore, we note that neither  $x$  and  $x^*$  nor  $y$  and  $y^*$  can be adjacent in  $G$  or  $\vec{G}$  since  $\sigma(x) = \sigma(x^*)$  and  $\sigma(y) = \sigma(y^*)$ .

If  $xz_1 \notin E(G)$ , then  $\langle xyx^*z_1 \rangle$  forms an ugly quartet. Now suppose that  $xz_1 \in E(G)$ . Assume that there is an edge  $yz' \in E(G)$  with  $z' \in L(T(v_y)) \cap L[t]$ . Then,  $\text{lca}(x, z_1) \prec_T \text{lca}(x, z')$  implies  $xz' \notin E(G)$ . Moreover, since  $\sigma(x) \notin \sigma(L(T(v_y)))$  we have, by similar arguments as above, that  $(z', x) \in E(\vec{G})$ . Thus,  $\langle z'yxz_1 \rangle$  forms a good quartet. Finally, if there is no such edge  $yz' \in E(G)$  then, in particular,  $yz_2 \notin E(G)$  and  $y \neq y^*$ . In this case,  $\langle yxy^*z_2 \rangle$  forms an ugly quartet.  $\square$

The example Fig. 5 shows that the converse of Prop. 3.15 is not true in general. We summarize the results of Prop. 3.6, 3.11 and 3.15 and Prop. 3.14 in the following

**Observation 3.16.** *Let  $(\vec{G}, \sigma)$  be a BMG that contains the edge  $xy$ . Then,  $\mathcal{S}^\cap(x, y) \neq \emptyset$  implies that  $xy$  is either the middle edge of some good quartet or the first edge of some ugly quartet, which in turn implies that  $xy$  is  $u$ - $fp$ .*

All  $u$ - $fp$  edges  $xy$  with  $\mathcal{S}^\cap(x, y) \neq \emptyset$  in  $(\vec{G}, \sigma)$  are therefore completely determined by the middle edges of good quartets and the first edges of ugly quartets. Furthermore, if  $xy$  is the middle edge of a good quartet, then  $\mathcal{S}^\cap(x, y) \neq \emptyset$ . Therefore, only ugly quartets provide more information about  $u$ - $fp$  edges than  $\mathcal{S}^\cap(x, y) \neq \emptyset$  as shown in Fig. 5. On the other hand, ugly quartets do not convey complete information either. The edge  $xy$  in the BMG illustrated in Fig. 6(A) is  $u$ - $fp$ , but it is not contained in a good, bad or an ugly quartet.

### 3.5 The Case $\mathcal{S}^\cap(x, y) = \emptyset$ and Hourglasses

In this section we turn to the case  $\mathcal{S}^\cap(x, y) = \emptyset$  and ask how unambiguous false-positive edges that are associated with a possibly non-binary duplication node of  $(T, \sigma)$  can be identified. To this end, we consider a motive in  $\vec{G}(T, \sigma)$  that is not necessarily part of an induced  $P_4$ .

**Definition 3.17** (Hourglass). An hourglass in a proper vertex-colored graph  $(\vec{G}, \sigma)$ , denoted by  $[xy \bowtie x'y']$ , is a subgraph  $(\vec{G}[Q], \sigma|_Q)$  induced by a set of four pairwise distinct vertices  $Q = \{x, x', y, y'\} \subseteq V(\vec{G})$  such that (i)  $\sigma(x) = \sigma(x') \neq \sigma(y) = \sigma(y')$ , (ii)  $xy$  and  $x'y'$  are edges in  $\vec{G}$ , (iii)  $(x, y'), (y, x') \in E(\vec{G})$ , and (iv)  $(y', x), (x', y) \notin E(\vec{G})$ .

Note that Condition (i) rules out arcs between  $x, x'$  and  $y, y'$ , respectively, i.e., the only arcs in an hourglass are the ones specified by Conditions (ii) and (iii). An example is shown in Fig. 6(A).

**Observation 3.18.** Every hourglass is a BMG since it can be explained by a tree as shown in Fig. 6(B).

First, we note that hourglasses cannot appear in a BMG that can be explained by a binary tree.

**Lemma 3.19.** If  $(\vec{G}, \sigma)$  is a BMG containing the hourglass  $[xy \bowtie x'y']$ , then every tree  $(T, \sigma)$  that explains  $(\vec{G}, \sigma)$  contains a vertex  $u \in V^0(T)$  with three distinct children  $v_1, v_2$ , and  $v_3$  such that  $x \preceq_T v_1$ ,  $\text{lca}_T(x', y') \preceq_T v_2$  and  $y \preceq_T v_3$ .

*Proof.* By assumption,  $xy$  and  $x'y'$  are edges in  $\vec{G}$ ,  $(x, y'), (y, x') \in E(\vec{G})$ , and  $(y', x), (x', y) \notin E(\vec{G})$ . By Lemma 2.8, the informative triples  $x'y'|x$  and  $x'y'|y$  thus must be displayed by every tree  $(T, \sigma)$  that explains  $(\vec{G}, \sigma)$ . Thus  $u_{x'y'} := \text{lca}_T(x', y') \prec_T u_x := \text{lca}_T(x, u_{x'y'})$  and  $u_{x'y'} \prec_T u_y := \text{lca}_T(y, u_{x'y'})$ . Furthermore,  $u_x$  and  $u_y$  are both ancestors of  $u_{x'y'}$  and thus comparable w.r.t.  $\preceq_T$ . If  $u_x \prec_T u_y$ , then  $\text{lca}_T(x, y') \prec_T \text{lca}_T(x, y)$  which implies that  $xy$  cannot form an edge in  $\vec{G}$ ; a contradiction. By similar arguments,  $u_y \prec_T u_x$  is not possible and therefore,  $u_x = u_y =: u$ .

Since  $u_{x'y'} \prec_T u$ , there are two distinct children  $v_1, v_2 \in \text{child}_T(u)$  of  $u$  such that  $x \preceq_T v_1$  and  $u_{x'y'} \preceq_T v_2$ . Clearly,  $y \notin L(T(v_2))$  since  $\text{lca}_T(y, u_{x'y'}) = u \succ_T v_2$ . We also have  $y \notin L(T(v_1))$  since  $y \in L(T(v_1))$  would imply  $\text{lca}_T(x, y) \preceq_T v_1 \prec_T u = \text{lca}_T(x, u_{x'y'}) = \text{lca}_T(x, y')$ , contradicting  $(x, y') \in E(\vec{G})$ . Together with  $y \in L(T(u))$ , this implies the existence of a vertex  $v_3 \in \text{child}(u)$  such that  $v_3 \notin \{v_1, v_2\}$  and  $y \preceq_T v_3$ .  $\square$

The result shows that hourglasses  $[xy \bowtie x'y']$  can be used to identify false-positive edges  $xy$  with  $\mathcal{S}^\cap(x, y) = \emptyset$ .

**Proposition 3.20.** If a BMG  $(\vec{G}, \sigma)$  contains an hourglass  $[xy \bowtie x'y']$ , then the edge  $xy$  is  $u$ -fp.

*Proof.* According to Lemma 3.19, every tree  $(T, \sigma)$  that explains  $(\vec{G}, \sigma)$  contains a vertex  $u \in V^0(T)$  with three distinct children  $v_1, v_2$ , and  $v_3$  such that  $x \preceq_T v_1$ ,  $\text{lca}_T(x', y') \preceq_T v_2$  and  $y \preceq_T v_3$ . Thus,  $u = \text{lca}_T(x, y)$  and  $\sigma(x) \in \sigma(L(T(v_1))) \cap \sigma(L(T(v_2)))$ . Hence, we can apply Lemma 3.2 to conclude that  $xy$  is  $(T, \sigma)$ -fp for every tree that explains  $(\vec{G}, \sigma)$ . Therefore, the edge  $xy$  is  $u$ -fp.  $\square$

Prop. 3.20 implies that there are  $u$ -fp edges that are not contained in a quartet, since an hourglass (see Fig. 6(A)) does not contain a  $P_4$ . We next generalize the concept of hourglasses.

**Definition 3.21** (Hourglass chain). An hourglass chain  $\mathfrak{H}$  in a graph  $(\vec{G}, \sigma)$  is a sequence of  $k \geq 1$  hourglasses  $[x_1y_1 \bowtie x'_1y'_1], \dots, [x_ky_k \bowtie x'_ky'_k]$  such that the following two conditions are satisfied for all  $i \in \{1, \dots, k-1\}$ :

(H1)  $y_i = x'_{i+1}$  and  $y'_i = x'_{i+1}$ , and

(H2)  $x_iy'_j$  is an edge in  $\vec{G}$  for all  $j \in \{i+1, \dots, k\}$

A vertex  $z$  is called a left (resp., right) tail of the hourglass chain  $\mathfrak{H}$  if it holds that  $(z, x_1) \in E(\vec{G})$  and  $(z, x'_1) \notin E(\vec{G})$  (resp.,  $(z, y_k) \in E(\vec{G})$  and  $(z, y'_k) \notin E(\vec{G})$ ). We call  $\mathfrak{H}$  tailed if it has a left or right tail.

Note that in contrast to the quartets and the hourglass, an hourglass chain in  $(\vec{G}, \sigma)$  is not necessarily an induced subgraph.

**Observation 3.22.** If  $\mathfrak{H} = [x_1y_1 \bowtie x'_1y'_1], \dots, [x_ky_k \bowtie x'_ky'_k]$  be an hourglass chain in  $(\vec{G}, \sigma)$ , then  $[x_iy_i \bowtie x'_iy'_i], \dots, [x_jy_j \bowtie x'_jy'_j]$  is an hourglass chain in  $(\vec{G}, \sigma)$  for every  $1 \leq i < j \leq k$ .

Hourglass chains are ‘‘overlapping’’ hourglasses. The additional condition that  $x_iy'_j \in E(G)$  for all  $1 \leq i < j \leq k$  ensures that the two pairs  $x'_k, y'_k$  and  $x'_l, y'_l$  with  $k \neq l$  cannot lie in the same subtree below the last common ancestor  $u$  which is common to all hourglasses in the chain.

**Lemma 3.23.** Let  $\mathfrak{H} = [x_1y_1 \bowtie x'_1y'_1], \dots, [x_ky_k \bowtie x'_ky'_k]$  be an hourglass chain in a BMG  $(\vec{G}, \sigma)$ . Then, for every tree  $(T, \sigma)$  that explains  $(\vec{G}, \sigma)$  there is a vertex  $u \in V^0(T)$  with pairwise distinct children  $v_0, v_1, \dots, v_k, v_{k+1}$  such that it holds  $x_1 \in L(T(v_0))$ ,  $y_k \in L(T(v_{k+1}))$ , and, for all  $1 \leq i \leq k$ , we have  $x'_i, y'_i \in L(T(v_i))$ .

*Proof.* We prove the statement by induction on  $k$ . For the base case  $k = 1$ , observe that the hourglass  $[x_1y_1 \bowtie x'_1y'_1]$  together with Lemma 3.19 implies that there is a vertex  $u \in V^0(T)$  with pairwise distinct children  $v_0, v_1$  and  $v_2$  such that  $x_1 \preceq_T v_0$ ,  $\text{lca}_T(x'_1, y'_1) \preceq_T v_1$  (thus  $x'_1, y'_1 \preceq_T v_1$ ) and  $y_1 \preceq_T v_2$ .

Now let  $k > 1$  and assume that the statement is true for all hourglass chains containing less than  $k$  hourglasses. Let  $\mathfrak{H} = [x_1y_1 \bowtie x'_1y'_1], \dots, [x_ky_k \bowtie x'_ky'_k]$  be an hourglass chain. By induction hypothesis, for every subsequence  $\mathfrak{H}_{[i]} := [x_1y_1 \bowtie x'_1y'_1], \dots, [x_iy_i \bowtie x'_iy'_i]$  of  $\mathfrak{H}$  with  $1 \leq i < k$ , which by Observation 3.22 is again an hourglass chain, the statement is true.

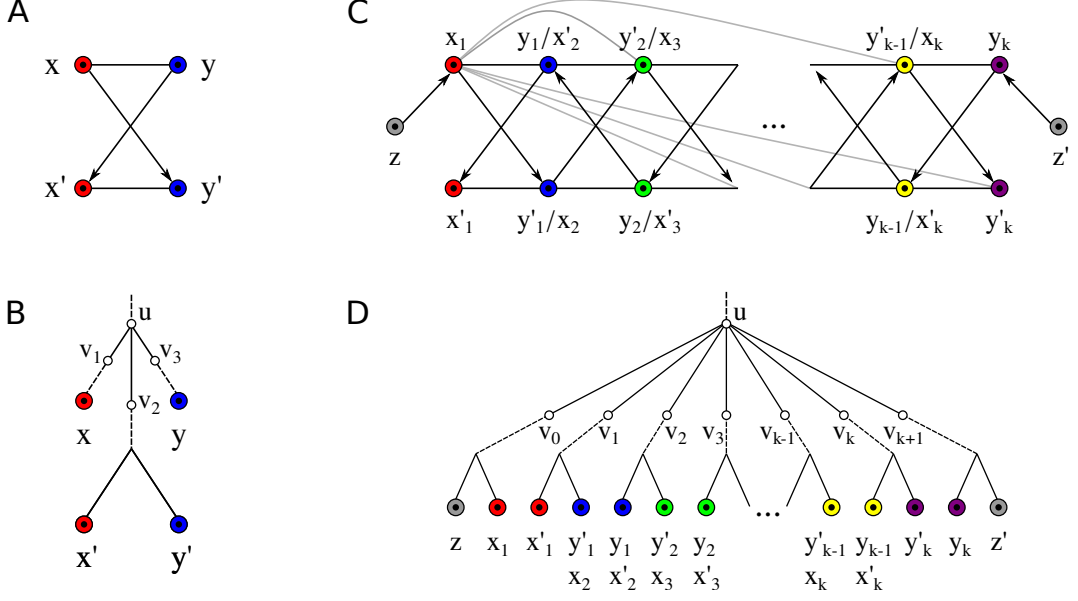


**Figure 6:** A: Hourglass. B: Visualization of Lemma 3.19. C: Hourglass chain with left tail  $z$  and right tail  $z'$  for an odd number of hourglasses in the chain. Edges of the form  $x_i y'_j \in E(G)$  are only shown for  $x_1$ , the others are omitted. An hourglass chain  $\mathfrak{H}$  is a subgraph but not necessarily induced and thus additional arcs may exist. In particular, the elements  $e \in \{x_1 y_k, z y_k, x_1 z', z z'\}$  are not necessarily edges in an hourglass chain. However, whenever they exist, they are  $u$ - $fp$  (cf. Lemma 3.25). Moreover, each single hourglass in  $\mathfrak{H}$  is an induced subgraph of the BMG; by definition, therefore, there are no arcs  $(z, x'_1)$  or  $(z', y'_k)$ . Note,  $\sigma(z) \neq \sigma(z')$  is possible. D: Visualization of Lemmas 3.23 and 3.24.

Consider the subsequence  $\mathfrak{H}_{|i}$  with  $i = k - 1$ . By assumption, there is a vertex  $u \in V^0(T)$  with pairwise distinct children  $v_0, v_1, \dots, v_i, v_{i+1}$  such that it holds  $x_1 \in L(T(v_0))$ ,  $y_i \in L(T(v_{i+1}))$ , and, for all  $1 \leq j \leq i$ , we have  $x'_j, y'_j \in L(T(v_j))$ . The hourglass  $[x_{i+1} y_{i+1} \bowtie x'_{i+1} y'_{i+1}]$  and Lemma 3.19 imply the existence of a vertex  $u' \in V^0(T)$  with pairwise distinct children  $v'_i, v'_{i+1}$  and  $v'_{i+2}$  such that  $x_{i+1} \preceq_T v'_i$ ,  $\text{lca}_T(x'_{i+1}, y'_{i+1}) \preceq_T v'_{i+1}$  and  $y_{i+1} \preceq_T v'_{i+2}$ . By the definition of hourglass chains, we have  $y_i = x'_{i+1}$  and  $y'_i = x_{i+1}$ . Therefore,  $u' = \text{lca}_T(x'_{i+1}, x_{i+1}) = \text{lca}_T(y_i, y'_i) = u$ . Since  $v_i$  and  $v'_i$  are both children of  $u$ ,  $y'_i = x_{i+1}$  and it holds both that  $y'_i \preceq_T v_i$  and  $x_{i+1} \preceq_T v'_i$ , we conclude that  $v_i = v'_i$ . Similarly, it holds  $v_{i+1} = v'_{i+1}$  since  $v_{i+1}, v'_{i+1} \in \text{child}(u)$  and  $y_i = x'_{i+1}$ . In particular, we have  $v'_{i+2} \neq v'_{i+1} = v_{i+1}$  and  $v'_{i+2} \neq v'_i = v_i$ . It remains to show that  $v'_{i+2} \neq v_j$  for  $0 \leq j < i$ . Assume, for contradiction, that  $v'_{i+2} = v_j$  for some fixed  $j$  with  $0 \leq j < i$ . By assumption,  $x_1 \preceq_T v_j$  if  $j = 0$ , and otherwise,  $x_{j+1} = y'_j \preceq_T v_j$ . Moreover, since  $v'_{i+2} = v_j$ , we have  $y_{i+1} \preceq_T v_j$ . Hence,  $\text{lca}_T(x_{j+1}, y_{i+1}) \preceq_T v_j$ . Furthermore, since  $y'_{i+1} \preceq_T v_{i+1} \neq v_j$ , it holds  $\text{lca}_T(x_{j+1}, y'_{i+1}) = u \succ_T v_j$ . Since  $\sigma(y_{i+1}) = \sigma(y'_{i+1})$  by the definition of hourglasses, the latter two arguments contradict  $x_{j+1} y'_{i+1} \in E(G)$ , which must hold by the definition of hourglass chains. Hence, we can conclude that  $v'_{i+2} \neq v_j$  for and  $0 \leq j < i$  and we set  $v_{i+2} := v'_{i+2}$ . In summary, the statement holds for the hourglass chain  $\mathfrak{H}_{|i+1} = \mathfrak{H}$ .  $\square$

It is straightforward to generalize the latter statement to tailed hourglass chains.

**Lemma 3.24.** *Let  $\mathfrak{H} = [x_1 y_1 \bowtie x'_1 y'_1], \dots, [x_k y_k \bowtie x'_k y'_k]$  be an hourglass chain with left (resp. right) tail  $z$  in a BMG  $(\vec{G}, \sigma)$ . Then, every tree  $(T, \sigma)$  that explains  $(\vec{G}, \sigma)$  contains a vertex  $u \in V^0(T)$  with pairwise distinct children  $v_0, v_1, \dots, v_k, v_{k+1}$  such that it holds  $x_1 \in L(T(v_0))$ ,  $y_k \in L(T(v_{k+1}))$ , and, for all  $1 \leq i \leq k$ , we have  $x'_i, y'_i \in L(T(v_i))$ . Furthermore, we have  $z \preceq_T v_0$  (resp.  $z \preceq_T v_{k+1}$ ).*

*Proof.* By Lemma 3.23, there is a vertex  $u \in V^0(T)$  with pairwise distinct children  $v_0, v_1, \dots, v_k, v_{k+1}$  such that it holds  $x_1 \in L(T(v_0))$ ,  $y_k \in L(T(v_{k+1}))$ , and, for all  $1 \leq i \leq k$ , we have  $x'_i, y'_i \in L(T(v_i))$ .

Suppose that  $z$  is a left tail of  $\mathfrak{H}$ . We need to show that  $z \preceq_T v_0$ . By definition,  $(z, x_1) \in E(\vec{G})$ ,  $(z, x'_1) \notin E(\vec{G})$ , and  $\sigma(x_1) = \sigma(x'_1)$ . Therefore,  $z x_1 | x'_1$  is an informative triple for  $T$ , and hence  $\text{lca}_T(z, x_1) \prec_T \text{lca}_T(z, x'_1) = \text{lca}_T(x_1, x'_1) = u$ . Since  $v_0$  is the unique child of  $u$  with  $x_1 \prec_T v_0$ , we can conclude that  $\text{lca}_T(z, x_1) \preceq_T v_0$  and thus,  $z \preceq_T v_0$ .

If  $z$  is a right tail of  $\mathfrak{H}$ , a similar argument using the informative triple  $z' y_k | y'_k$ , which must be displayed by  $T$  because  $(z, y_k) \in E(\vec{G})$  and  $(z, y'_k) \notin E(\vec{G})$ , implies  $z \preceq_T v_{k+1}$ .  $\square$

We are now in the position to show that hourglass chains identify additional  $u$ - $fp$  edges that are not contained in a single hourglass.

**Lemma 3.25.** *Let  $\mathfrak{H} = [x_1y_1 \times x'_1y'_1], \dots, [x_ky_k \times x'_ky'_k]$  be an hourglass chain in  $(\vec{G}, \sigma)$ , possibly with a left tail  $z$  or a right tail  $z'$ . Then every edge  $e \in \{x_1y_k, zy_k, x_1z', zz'\} \cap E(G)$  is  $u$ - $fp$ , where  $G$  denotes the symmetric part of  $\vec{G}$ .*

*Proof.* Let  $(T, \sigma)$  be an arbitrary tree that explains  $(\vec{G}, \sigma)$ . By the definition of hourglass chains, we have  $k \geq 1$ . Hence, the sequence contains at least the hourglass  $[x_1y_1 \times x'_1y'_1]$ . Since  $\mathfrak{H} = [x_1y_1 \times x'_1y'_1], \dots, [x_ky_k \times x'_ky'_k]$  in  $\vec{G}(T, \sigma)$ , Lemma 3.24 implies the existence of a vertex  $u \in V^0(T)$  with pairwise distinct children  $v_0, v_1, \dots, v_k, v_{k+1}$  such that it holds  $x_1 \in L(T(v_0))$ ,  $y_k \in L(T(v_{k+1}))$ , and, for all  $1 \leq i \leq k$ , we have  $x'_i, y'_i \in L(T(v_i))$ . Furthermore, this lemma also implies  $z \preceq_T v_0$  if  $z$  is a left tail of  $\mathfrak{H}$ , and  $z' \preceq_T v_{k+1}$  if  $z'$  is a right tail of  $\mathfrak{H}$ . Note that  $\text{lca}_T(x_1, x'_1) = u$ , and  $x_1$  and  $x'_1$  lie below distinct children of  $u$ . More precisely  $x_1 \preceq_T v_0$  and  $x'_1 \preceq_T v_1$ . Since  $\sigma(x_1) = \sigma(x'_1)$ , we have  $\sigma(L(T(v_0))) \cap \sigma(L(T(v_1))) \neq \emptyset$ . Moreover,  $\text{lca}_T(a, b) = u$  for every edge  $e = ab$  in  $\vec{G}$  that coincides with one of  $x_1y_k, zy_k, x_1z',$  and  $zz'$ . The latter two arguments together with Lemma 3.2 imply that every such edge is  $(T, \sigma)$ - $fp$ . Since  $(T, \sigma)$  was chosen arbitrarily, every such edge is also  $u$ - $fp$ .  $\square$

It is important to note that the construction of hourglass chains does not imply that an edge  $e \in \{x_1y_k, zy_k, x_1z', zz'\}$  must exist in  $(\vec{G}, \sigma)$ . Nevertheless, whenever such an edge occurs, it is  $u$ - $fp$ . We will take a closer look at the properties of hourglass chains in Section 5. Finding hourglass chains in  $(\vec{G}, \sigma)$  is closely related to the NP-complete SUBGRAPH ISOMORPHISM problem [11], and hence a difficult endeavor in practice. In the following section we shall see, however, the identification of  $u$ - $fp$  edges does not require the explicit enumeration of hourglass chains.

## 4 Characterization of Unambiguous False-Positive Edges

### 4.1 Color-Set Intersection Graphs

So far we focused on the set  $\mathcal{S}^\cap(x, y)$  for individual edges  $xy$  and induced subgraphs of BMGs to identify  $u$ - $fp$  edges. This has led to several sufficient conditions. We now shift our point of view and consider the color allocation to the subtrees below each vertex of a tree explaining a given BMG. This leads us to the idea of a color intersection graph.

**Definition 4.1.** *The color-set intersection graph  $\mathfrak{C}_T(u)$  of an inner vertex  $u$  of a leaf-colored gene tree  $(T, \sigma)$  is the undirected graph with vertex set  $V := \text{child}_T(u)$  and edge set*

$$E := \{v_1v_2 \mid v_1, v_2 \in V, v_1 \neq v_2 \text{ and } \sigma(L(T(v_1))) \cap \sigma(L(T(v_2))) \neq \emptyset\}.$$

This construction is similar to the definition of intersection graphs e.g. used in [34].  $\mathfrak{C}_T(u)$  can be viewed as a natural generalization of  $\mathcal{S}^\cap(x, y)$  in the following sense: if  $u = \text{lca}_T(x, y)$  is a binary vertex, then  $\mathfrak{C}_T(u) = K_2$  iff  $\mathcal{S}^\cap(x, y) \neq \emptyset$  and therefore,  $\mathfrak{C}_T(u) = K_1 \cup K_1$  iff  $\mathcal{S}^\cap(x, y) = \emptyset$ . In the non-binary case, there is an edge  $v_1v_2$  iff  $\mathcal{S}^\cap(x, y) \neq \emptyset$  for some  $x \in L(T(v_1))$  and  $y \in L(T(v_2))$ . Shortest paths in the color-set intersection graphs will play an important role in identifying many  $u$ - $fp$  edges.

**Lemma 4.2.** *Let  $v_1$  and  $v_k$  be two distinct vertices in the same connected component of the color-set intersection graph  $\mathfrak{C}_T(u)$  of a leaf-colored gene tree  $(T, \sigma)$ , and let  $P(v_1, v_k) = (v_1, \dots, v_k)$  be a shortest path in  $\mathfrak{C}_T(u)$  connecting  $v_1$  and  $v_k$ . Then  $\sigma(L(T(v_i))) \cap \sigma(L(T(v_j))) = \emptyset$  for all  $i$  and  $j$  satisfying  $1 \leq i < i+2 \leq j \leq k$ .*

*Proof.* Assume, for contradiction, that  $\sigma(L(T(v_i))) \cap \sigma(L(T(v_j))) \neq \emptyset$  for some  $i, j$  with  $1 \leq i < i+2 \leq j \leq k$ . Then the edge  $v_iv_j$  must be contained in  $\mathfrak{C}_T(u)$ , contradicting the fact that  $P(v_1, v_k)$  is a shortest path.  $\square$

**Lemma 4.3.** *Let  $(\vec{G}, \sigma)$  be a BMG that is explained by  $(T, \sigma)$  and suppose that  $x, y \in L(T)$  are two distinct leaves with  $u := \text{lca}_T(x, y)$  and  $v_x, v_y \in \text{child}_T(u)$  such that (i)  $x \preceq_T v_x$  and  $y \preceq_T v_y$ , and (ii) there is a shortest path  $(v_x = v_0, v_1, \dots, v_k, v_{k+1} = v_y)$  of length at least two in  $\mathfrak{C}_T(u)$ . Then there is an hourglass chain  $\mathfrak{H} = [x_1y_1 \times x'_1y'_1], \dots, [x_ky_k \times x'_ky'_k]$  in  $(\vec{G}, \sigma)$ . In particular, precisely one of the following conditions is satisfied:*

1.  $x_1 = x$  and  $y_k = y$ ;
2.  $y_k = y$  and  $z := x$  is a left tail of  $\mathfrak{H}$ ;
3.  $x_1 = x$  and  $z' := y$  is a right tail of  $\mathfrak{H}$ ; or
4.  $z := x$  is a left tail and  $z' := y$  is a right tail of  $\mathfrak{H}$ .

*Proof.* Lemma 4.2 implies  $\mathcal{S}^\cap(x, y) = \sigma(L(T(v_x))) \cap \sigma(L(T(v_y))) = \sigma(L(T(v_0))) \cap \sigma(L(T(v_{k+1}))) = \emptyset$ . We proceed by showing that the BMG  $\vec{G}(T, \sigma)$  contains an hourglass chain  $\mathfrak{H} = [x_1y_1 \times x'_1y'_1], \dots, [x_ky_k \times x'_ky'_k]$  possibly with left tail  $z$  and right tail  $z'$  such that one of the Conditions 1–4 is satisfied.

We first consider the two cases: either (A)  $\sigma(x) \in \sigma(L(T(v_1)))$  or (B)  $\sigma(x) \notin \sigma(L(T(v_1)))$ . In Case (A), we set  $x_1 := x$  and  $c_0 := \sigma(x)$ . In Case (B), we set  $z := x$ , choose  $c_0 \in \sigma(L(T(v_0))) \cap \sigma(L(T(v_1)))$  arbitrarily (note  $v_0v_1$  forms

an edge in  $\mathcal{C}_T(u)$  and thus, the latter intersection is non-empty) and we set  $x_1 = v$  for some  $v \in L(T(v_0)) \cap L[c_0]$  such that  $\text{lca}(v, x) \preceq_T \text{lca}_T(v', x) \preceq_T v_0$  for all  $v' \in L(T(v_0)) \cap L[c_0]$ . Clearly, such a vertex  $v$  exists. Moreover,  $c_0 \neq \sigma(x)$  and we obtain  $(x, v) = (z, x_1) \in E(\vec{G})$  as necessary requirement for left tails. In summary, we have in Case (A)  $x_1 = x$  and in Case (B)  $x$  plays the role of the left tail  $z$  and  $x_1$  is some other vertex. Moreover, in both Cases (A) and (B), we have  $\sigma(x_1) = c_0 \in \sigma(L(T(v_0))) \cap \sigma(L(T(v_1)))$ .

We now consider the ‘‘other end’’ of the hourglass chain, that is, vertex  $y_k$  and the possible right tail. Again, we have two cases: either (A')  $\sigma(y) \in \sigma(L(T(v_{k+1})))$  or (B')  $\sigma(y) \notin \sigma(L(T(v_{k+1})))$ . In Case (A'), we set  $y_k := y$  and  $c_k := \sigma(y)$ . In Case (B'), we set  $z' := y$ , and, by similar arguments as in Case (A) and (B), we can choose  $c_k \in \sigma(L(T(v_k))) \cap \sigma(L(T(v_{k+1})))$  arbitrarily and set  $y_k = w$  for some vertex  $w \in L(T(v_{k+1})) \cap L[c_k]$  such that  $(y, w) = (z', y_k) \in E(\vec{G})$  as a necessary requirement for right tails. Again, for both cases (A') and (B') we have  $\sigma(y_k) = c_k \in \sigma(L(T(v_k))) \cap \sigma(L(T(v_{k+1})))$ .

We continue by picking an arbitrary color  $c_i$  from  $\sigma(L(T(v_i))) \cap \sigma(L(T(v_{i+1})))$  for each  $1 \leq i < k$ . This is possible because  $v_i v_{i+1} \in E(\mathcal{C}_T(u))$ , and thus  $\sigma(L(T(v_i))) \cap \sigma(L(T(v_{i+1}))) \neq \emptyset$ . Note that now  $c_i \in \sigma(L(T(v_i))) \cap \sigma(L(T(v_{i+1})))$  holds for all  $0 \leq i \leq k$ . In particular, the colors  $c_0, c_1, \dots, c_k$  are pairwise distinct. To see this, assume, for contradiction, that  $c_i = c_j$  for some  $i, j$  with  $i < j$ . Then  $c_i \in \sigma(L(T(v_i)))$  and  $c_i = c_j \in \sigma(L(T(v_{j+1})))$  which implies  $c_i \in \sigma(L(T(v_i))) \cap \sigma(L(T(v_{j+1})))$ . This contradicts Lemma 4.2 for  $j+1 \geq i+2$ .

For each  $1 \leq i \leq k$ , we have  $c_{i-1}, c_i \in \sigma(L(T(v_i)))$ . Thus Lemma 2.3 ensures the existence of vertices  $x'_i \in L(T(v_i)) \cap L[c_{i-1}]$  and  $y'_i \in L(T(v_i)) \cap L[c_i]$  that form an edge  $x'_i y'_i$  in  $\vec{G}$ . By assumption we have  $x'_i y'_i \in E(G)$  for all  $1 \leq i \leq k$  since  $[x_i y_i \times x'_i y'_i]$  is an hourglass. We already set  $x_1$  and  $y_k$ . We furthermore set  $x_i := y'_{i-1}$  for all  $1 < i \leq k$ , and  $y_i := x'_{i+1}$  for all  $1 \leq i < k$ . This ensures that (H1) in Def. 3.21 is satisfied. Moreover, since  $\sigma(x_1) = c_0 = \sigma(x'_1)$  and  $\sigma(x_i) = \sigma(y'_{i-1}) = c_{i-1}$  for all  $1 < i \leq k$ , we have  $\sigma(x_i) = c_{i-1} = \sigma(x'_i)$  for all  $1 \leq i \leq k$ . Similar arguments imply  $\sigma(y_i) = c_i = \sigma(y'_i)$  for all  $1 \leq i \leq k$ .

We next show that the induced subgraph  $\vec{G}[x_i, x'_i, y_i, y'_i]$  is an hourglass for  $1 \leq i \leq k$  and thus  $x_i y'_i$  is an edge in  $\vec{G}$  for all  $i < j \leq k$ . We also know, by construction, that  $x'_i y'_i$  is an edge in  $\vec{G}$ .

Independent of whether  $x_1$  was constructed based on the cases (A) or (B), we have  $x_i \preceq_T v_0$  if  $i = 1$  and  $x_i = y'_{i-1} \preceq_T v_{i-1}$  otherwise. Thus  $x_i \preceq_T v_{i-1}$ . Likewise, independent of whether  $y_k$  was constructed based on the cases (A') or (B'), we have  $y_i \preceq_T v_{k+1}$  if  $i = k$  and  $y_i = x'_{i+1} \preceq_T v_{i+1}$  otherwise. Thus  $y_i \preceq_T v_{i+1}$ . In summary, we have  $x_i \preceq_T v_{i-1}$ ;  $x'_i, y'_i \preceq_T v_i$ ; and  $y_i \preceq_T v_{i+1}$  for all  $i \in \{1, \dots, k\}$ . This implies  $\text{lca}_T(x_i, y'_i) = \text{lca}_T(x_i, y_i) = \text{lca}_T(x'_i, y_i) = u$ . Since  $i+1 \geq (i-1)+2$  and  $P(v_0, v_{k+1})$  is a shortest path, Lemma 4.2 implies  $\sigma(L(T(v_{i-1}))) \cap \sigma(L(T(v_{i+1}))) = \emptyset$ .

From  $\sigma(x_i) \in \sigma(L(T(v_{i-1})))$  and  $\sigma(y_i) \in \sigma(L(T(v_{i+1})))$  we obtain  $\sigma(x_i) \notin \sigma(L(T(v_{i+1})))$  and  $\sigma(y_i) \notin \sigma(L(T(v_{i-1})))$ . Thus, there is no  $\tilde{y}$  such that  $\sigma(\tilde{y}) = \sigma(y'_i) = \sigma(y_i)$  and  $\text{lca}_T(x_i, \tilde{y}) \prec_T u = \text{lca}_T(x_i, y'_i) = \text{lca}_T(x_i, y_i)$ , and no  $\tilde{x}$  such that  $\sigma(\tilde{x}) = \sigma(x'_i) = \sigma(x_i)$  and  $\text{lca}_T(y_i, \tilde{x}) \prec_T u = \text{lca}_T(y_i, x'_i) = \text{lca}_T(y_i, x_i)$ . Hence,  $\vec{G}$  contains the arcs  $(x_i, y'_i)$ ,  $(x_i, y_i)$ ,  $(y_i, x_i)$  and  $(y_i, x'_i)$ . Moreover,  $x_i y_i$  is an edge in  $\vec{G}$ . However, since  $\sigma(x'_i) = \sigma(x_i)$  and  $\text{lca}_T(x'_i, y'_i) \preceq_T v_i \prec_T u = \text{lca}_T(x_i, y'_i)$  we conclude  $(y'_i, x_i) \notin E(\vec{G})$ . Likewise,  $\sigma(y'_i) = \sigma(y_i)$  and  $\text{lca}_T(x'_i, y'_i) \preceq_T v_i \prec_T u = \text{lca}_T(x'_i, y_i)$  imply that  $(x'_i, y_i) \notin E(\vec{G})$ . In summary,  $\vec{G}[x_i, x'_i, y_i, y'_i] = [x_i y_i \times x'_i y'_i]$  is an hourglass, for all  $i \in \{1, \dots, k\}$ , and  $x_i \preceq_T v_{i-1}$  and  $y'_j \preceq_T v_j$  for all  $1 \leq i < j \leq k$ .

Since  $j \geq (i-1)+2$  and  $P(v_0, v_{k+1})$  is a shortest path, Lemma 4.2 implies that  $\sigma(L(T(v_{i-1}))) \cap \sigma(L(T(v_j))) = \emptyset$ . Thus, there is no  $\tilde{y}$  such that  $\sigma(\tilde{y}) = \sigma(y'_j)$  and  $\text{lca}_T(x_i, \tilde{y}) \prec_T u = \text{lca}_T(x_i, y'_j)$ , and no  $\tilde{x}$  such that  $\sigma(\tilde{x}) = \sigma(x_i)$  and  $\text{lca}_T(y'_j, \tilde{x}) \prec_T u = \text{lca}_T(y'_j, x_i)$ . This implies that  $(x_i, y'_j) \in E(\vec{G})$  and  $(y'_j, x_i) \in E(\vec{G})$ , respectively. Therefore  $x_i y'_j$  is an edge in  $\vec{G}$  for  $1 \leq i < j \leq k$ . In summary, (H2) of in Def. 3.21 is always satisfied.

Hence, if  $x_1$  and  $y_1$  are constructed based on Case (A) and (A'), respectively, we are done.

It remains to show that  $z$  and  $z'$  are a left and a right tail, resp., of the hourglass chain in Case (B) or (B'). First assume Case (B), and thus  $z = x$ . We have  $z, x_1 \preceq_T v_0$  by construction and  $(z, x_1) \in E(\vec{G})$  as shown above. Together with  $x'_1 \preceq_T v_1$ , this implies that  $\text{lca}_T(z, x_1) \preceq_T v_0 \prec_T u = \text{lca}_T(z, x'_1)$ . Using  $\sigma(x_1) = \sigma(x'_1)$  we therefore obtain  $(z, x'_1) \notin E(\vec{G})$ . and hence  $z$  is a left tail of the constructed hourglass chain. Now assume Case (B'), and thus,  $z' = y$ . We have  $z', y_k \preceq_T v_{k+1}$  and  $(z', y_k) \in E(\vec{G})$  by construction. Together with  $y'_k \preceq_T v_k$  this implies  $\text{lca}_T(z', y_k) \preceq_T v_{k+1} \prec_T u = \text{lca}_T(z', y'_k)$ . Using  $\sigma(y_k) = \sigma(y'_k)$ , we obtain  $(z', y'_k) \notin E(\vec{G})$  and hence  $z'$  is a right tail of the constructed hourglass chain.

In summary,  $\mathfrak{H} = [x_1 y_1 \times x'_1 y'_1], \dots, [x_k y_k \times x'_k y'_k]$  is an hourglass chain, possibly with left tail  $z$  and right tail  $z'$ . Furthermore, precisely one of the Conditions 1–4 in the statement holds by construction.  $\square$

Lemma 4.3 establishes a close connection between color-set intersection graphs and hourglass chains, which we will use below to simplify the identification of the corresponding  $u$ -fp edges. To this end, we first consider properties in relation of a tree  $T$  explaining  $(\vec{G}, \sigma)$  that are common to the three types of  $u$ -fp edges we have encountered so far.

## 4.2 Hug-edges and no-hug graphs

**Definition 4.4.** *An edge  $xy$  in a vertex-colored graph  $(\vec{G}, \sigma)$  is a hug-edge if it satisfies at least one of the following conditions:*



- (C1)  $xy$  is the middle edge of a good quartet in  $(\vec{G}, \sigma)$ ;  
(C2)  $xy$  is the first edge of an ugly quartet in  $(\vec{G}, \sigma)$ ; or  
(C3) there is an hourglass chain  $\mathfrak{H} = [x_1y_1 \times x'_1y'_1], \dots, [x_ky_k \times x'_ky'_k]$  in  $(\vec{G}, \sigma)$ , and one of the following cases holds:
1.  $x_1 = x$  and  $y_k = y$ ;
  2.  $y_k = y$  and  $z := x$  is a left tail of  $\mathfrak{H}$ ;
  3.  $x_1 = x$  and  $z' := y$  is a right tail of  $\mathfrak{H}$ ; or
  4.  $z := x$  is a left tail and  $z' := y$  is a right tail of  $\mathfrak{H}$ .

The term **hug-edge** refers to the fact  $xy$  is a particular edge of an hourglass-chain, an ugly quartet, or a good quartet.

**Theorem 4.5.** *An edge  $xy$  in  $\vec{G}(T, \sigma)$  with  $u := \text{lca}_T(x, y)$ ,  $v_x, v_y \in \text{child}_T(u)$ ,  $x \preceq_T v_x$ , and  $y \preceq_T v_y$  is a hug-edge if  $v_x$  and  $v_y$  belong to the same connected component of  $\mathcal{C}_T(u)$ . Moreover, every hug-edge is  $u$ -fp.*

*Proof.* We show first that  $xy$  satisfies one of the Conditions (C1), (C2), or (C3), and hence is hug-edge. First, note that  $v_x \neq v_y$ . Moreover, Lemma 2.4 implies  $\sigma(x) \notin \sigma(L(T(v_y)))$  and  $\sigma(y) \notin \sigma(L(T(v_x)))$ . Since by assumption  $v_x, v_y$  belong to the same connected component, there is a shortest path  $P := (v_x = v_0, \dots, v_{k+1} = v_y)$  in  $\mathcal{C}_T(u)$ . For  $k = 0$ ,  $v_x v_y \in E(\mathcal{C}_T(u))$ . This implies  $\mathcal{S}^\cap(x, y) = \sigma(L(T(v_x))) \cap \sigma(L(T(v_y))) \neq \emptyset$ . By Prop. 3.15, the edge  $xy$  is either the middle edge of a good quartet or the first edge of an ugly quartets in  $(\vec{G}, \sigma)$ . Hence, Condition (C1) or (C2) is satisfied. If  $k > 0$ , Lemma 4.3 implies Condition (C3).

For each of the three cases we have already shown that  $xy$  is  $u$ -fp: For (C1) Prop. 3.11 applies, for (C2) Prop. 3.14 provides the desired result, and for (C3) we use Lemma 3.25. □

**Lemma 4.6.** *If the BMG  $\vec{G}(T, \sigma)$  contains a hug-edge  $xy$  in a BMG  $\vec{G}(T, \sigma)$ , then there are distinct vertices  $v_1, v_2 \in \text{child}_T(\text{lca}_T(x, y))$  such that  $\sigma(L(T(v_1))) \cap \sigma(L(T(v_2))) \neq \emptyset$ .*

*Proof.* Let  $xy$  be a hug-edge in the BMG  $(\vec{G}, \sigma) = \vec{G}(T, \sigma)$ , i.e. one of (C1), (C2), or (C3) applies.

If  $e = xy$  satisfies (C1), then  $xy$  is the middle edge of a good quartet  $(zxyz')$  in  $(\vec{G}, \sigma)$ . By [14, Lemma 36], there is a vertex  $u := \text{lca}_T(x, y, z, z')$  such that  $x, z \preceq_T v_1$  and  $y, z' \preceq_T v_2$  for some distinct  $v_1, v_2 \in \text{child}_T(u)$ . Thus,  $u = \text{lca}_T(x, y)$ . Moreover, since  $\sigma(z) = \sigma(z')$ , we have  $\sigma(L(T(v_1))) \cap \sigma(L(T(v_2))) \neq \emptyset$  for two distinct vertices  $v_1, v_2 \in \text{child}_T(u)$ .

If  $e = xy$  satisfies (C2), then it is the first edge of some ugly quartet, which w.l.o.g. has the form  $(xyx'z)$ . Re-using the arguments in the proof of Prop. 3.14 shows that there must be two distinct children  $v_1$  and  $v_2$  of vertex  $u = \text{lca}_T(x, y)$  such that  $\sigma(L(T(v_1))) \cap \sigma(L(T(v_2))) \neq \emptyset$ .

If  $e = xy$  satisfies (C3), then there is a (tailed) hourglass chain  $\mathfrak{H} = [x_1y_1 \times x'_1y'_1], \dots, [x_ky_k \times x'_ky'_k]$ ,  $k \geq 1$ , in  $\vec{G}(T, \sigma)$ , such that either  $x = x_1$  or  $z := x$  is a left tail of  $\mathfrak{H}$ , and either  $y = y_k$  or  $z' := y$  is a right tail of  $\mathfrak{H}$ . In either case, Lemma 3.24 implies  $x \preceq_T v_0$  and  $y \preceq_T v_{k+1}$ . Since  $x_1$  and  $x'_1$  lie below distinct children  $v_0$  and  $v_1$  of vertex  $\text{lca}_T(x, y)$  and  $\sigma(x_1) = \sigma(x'_1)$  by the definition of hourglasses, it holds that  $\sigma(L(T(v_0))) \cap \sigma(L(T(v_1))) \neq \emptyset$ .

In each case, therefore, there are distinct vertices  $v_1, v_2 \in \text{child}_T(\text{lca}_T(x, y))$  such that  $\sigma(L(T(v_1))) \cap \sigma(L(T(v_2))) \neq \emptyset$ . □

The fact that all hug-edges are  $u$ -fp by Thm. 4.5 suggests to consider the subgraph of a BMG that is left after removing all these unambiguously recognizable false-positive orthology assignments.

**Definition 4.7.** *Let  $(\vec{G}, \sigma)$  be a BMG with symmetric part  $G$  and let  $F$  be the set of its hug-edges. The no-hug<sup>1</sup> graph  $\text{NH}(\vec{G}, \sigma)$  is the subgraph of  $G$  with vertex set  $V(\vec{G})$ , coloring  $\sigma$  and edge set  $E(G) \setminus F$ .*

The  $\text{NH}(\vec{G}, \sigma)$  is therefore the subgraph of the underlying RBMG of  $\vec{G}$  that contains all edges that cannot be identified as  $u$ -fp by using only good quartets, ugly quartets and (tailed) hourglass chains as outlined in Thm. 4.5.

**Corollary 4.8.** *Let  $(T, \sigma)$  be a leaf-colored tree and  $\mu$  a reconciliation map from  $(T, \sigma)$  to some species tree  $S$ . Then,*

$$\Theta(T, t_\mu) \subseteq \Theta(T, \hat{t}_T) \subseteq \text{NH}(\vec{G}(T, \sigma)) \subseteq \vec{G}(T, \sigma).$$

*Proof.* By Thm. 2.21,  $\Theta(T, t_\mu) \subseteq \Theta(T, \hat{t}_T) \subseteq \vec{G}(T, \sigma)$ ; and by definition, we have  $\text{NH}(\vec{G}(T, \sigma)) \subseteq \vec{G}(T, \sigma)$ . Now, let  $xy$  be an edge in  $\Theta(T, \hat{t}_T)$  and thus,  $\hat{t}_T(\text{lca}_T(x, y)) = \bullet$ . By definition of  $\hat{t}_T$ , we have  $\sigma(L(T(v_1))) \cap \sigma(L(T(v_2))) = \emptyset$  for any two distinct  $v_1, v_2 \in \text{child}_T(\text{lca}_T(x, y))$ . The contraposition of Lemma 4.6 implies that  $xy$  is not a hug-edge and thus an edge of  $\text{NH}(\vec{G}(T, \sigma))$ , which completes the proof. □

The no-hug graph still may contain false positive orthology assignments, i.e.,  $\text{NH}(\vec{G}(T, \sigma)) = \Theta(T, \hat{t}_T)$  does not hold in general. As an example, consider the BMG  $\vec{G}(T_1, \sigma)$  in Fig. 3. Here, none of the edges  $xz, x'z$  and  $yz$  are  $u$ -fp and thus, by Thm. 4.5 also not hug-edges. Hence, they still remain in  $\text{NH}(\vec{G}(T_1, \sigma))$ . However, these edges are not contained in  $\Theta(T_1, \hat{t}_T)$ , since  $\hat{t}_T(\text{lca}_{T_1}(x, x', y, z)) = \square$  and thus,  $\Theta(T_1, \hat{t}_T) \subsetneq \text{NH}(\vec{G}(T_1, \sigma))$ . In the following section we shall see that there are, however, no  $u$ -fp edges left in the no-hug graph.

<sup>1</sup>a good advice in the time of SARS-CoV-2

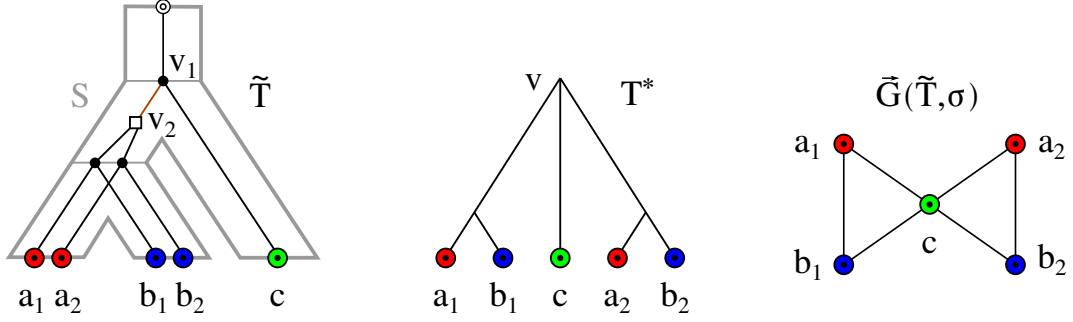


**Figure 7:** A “true” scenario, that is, an event-labeled gene tree  $(\tilde{T}, \tilde{i}, \sigma)$  embedded into a species tree (left). To obtain the least resolved tree  $(T^*, \sigma)$  of  $\vec{G}(\tilde{T}, \sigma)$ , the edge  $v_1v_2$  has been contracted into vertex  $v$ . The BMG  $\vec{G}(\tilde{T}, \sigma)$  does not contain any  $u$ - $fp$  edge. See text for further explanations.

### 4.3 Resolving Least Resolved Trees

Every BMG  $(\vec{G}, \sigma)$  contains all information necessary to determine the trees  $(T, \sigma)$  by which it is explained. Since  $u$ - $fp$  edges are defined in terms of the explaining trees, every BMG  $(\vec{G}, \sigma)$  also contains – at least implicitly – all information needed to identify its  $u$ - $fp$  edges. Since  $(\vec{G}, \sigma)$  is determined by its unique least resolved tree  $(T^*, \sigma)$ , the  $u$ - $fp$  edges must also be determined by  $(T^*, \sigma)$ . It is not sufficient for this purpose, however, to find an event labeling  $t$  of the vertices of  $T^*$ .

To see this, consider for example the “true” history  $(\tilde{T}, \tilde{i}, \sigma)$  of the BMG  $\vec{G}(\tilde{T}, \sigma)$  as shown in Fig. 7. The unique least resolved tree  $(T^*, \sigma)$  for  $\vec{G}(\tilde{T}, \sigma)$  is obtained by merging the two vertices  $v_1$  and  $v_2$  of  $\tilde{T}$  resulting in the vertex  $v$  of  $T^*$ . We have  $\tilde{i}(v_1) = \bullet \neq \square = \tilde{i}(v_2)$ . For vertex  $v$  and every reconciliation map  $\mu$  from  $(T^*, \sigma)$  to any species tree  $S$  it must hold  $\mu(v) \in E(S)$  and thus  $t_\mu^*(v) = \square$ , since  $v$  has two children with overlapping color sets and by Lemma 2.17. Thus, the edges  $cx$  with  $x \in \{a_1, a_2, b_1, b_2\}$  are  $(T^*, \sigma)$ - $fp$  although they are not false positives at all. Since speciation and duplication vertices may be merged into the same vertex  $v$  of  $T^*$ , the least resolved tree  $T^*$  in general cannot simply inherit the event labeling from the true gene history, and thus there may not be a “correct” labeling  $t^*$  of  $T^*$  that provides evidence for all  $u$ - $fp$  edges.

The example in Fig. 7 shows that the least resolved tree  $T^*$  simply may not be “resolved enough”. In the following, we therefore describe how the unique least resolved tree can be resolved further to provide more evidence about  $u$ - $fp$  edges. Eventually, this will lead us to a characterization of the  $u$ - $fp$  edges. To this end, we need to gain more insights into the structure of redundant edges, i.e., those edges  $e$  in  $T$  for which  $(T_e, \sigma)$  still explains  $\vec{G}(T, \sigma)$ .

Since the color sets of distinct subtrees below a speciation vertex cannot overlap by Lemma 2.17, Cor. 2.11 implies that all edges below a speciation vertex are redundant and thus can be contracted. More precisely, we have

**Observation 4.9.** *Let  $\mu$  be a reconciliation map from  $(T, \sigma)$  to  $S$  and assume that there is a vertex  $u \in V^0(T)$  such that  $\mu(u) \in V^0(S)$  and thus,  $t_\mu(u) = \bullet$ . Then every inner edge  $uv$  with  $v \in \text{child}_T(u)$  is redundant w.r.t.  $\vec{G}(T, \sigma)$ . Moreover, if an inner edge  $uv$  with  $v \in \text{child}_T(u)$  is non-redundant, then  $u$  must have two children with overlapping color sets, and hence,  $t_\mu(u) = \square$ .*

Our goal is to identify those vertices in  $(T^*, \sigma)$  that can be expanded to yield a tree that still explains  $\vec{G}(T^*, \sigma)$ . To this end, we need to introduce a particular way of “augmenting” a leaf-colored tree.

**Definition 4.10.** *Let  $(T, \sigma)$  be a leaf-colored tree,  $u$  be an inner vertex of  $T$ ,  $\mathfrak{C}_T(u)$  the corresponding color-set intersection graph, and  $\mathcal{C}$  the set of connected components of  $\mathfrak{C}_T(u)$ . Then the tree  $T_u$  augmented at vertex  $u$  is obtained by applying the following editing steps to  $T$ :*

- If  $\mathfrak{C}_T(u)$  is connected, do nothing.
- Otherwise, for each  $C \in \mathcal{C}$  with  $|C| > 1$ 
  - introduce a vertex  $w$  and attach it as a child of  $u$ , i.e., add the edge  $uw$ ,
  - for every element  $v_i \in C$ , substitute the edge  $uv_i$  by the edge  $wv_i$ .

The augmentation step is trivial if  $T_u = T$ , in which case we say that no edit step was performed.

An example of an augmentation is shown in Fig. 8. It is easy to see that the tree  $T_u$  obtained by an augmentation of a phylogenetic tree  $T$  is again a phylogenetic tree. The augmentation step at vertex  $u$  of  $T$  is trivial if and only if either  $\mathfrak{C}_T(u)$  is connected or all connected components  $C \in \mathcal{C}$  are singletons, i.e.,  $|C| = 1$ . If  $(T_u, \sigma)$  is obtained by augmenting  $(T, \sigma)$  at node  $u$ , we denote the set of newly introduced vertices by  $V_{-T} := V(T_u) \setminus V(T)$ . Note that  $V_{-T} = \emptyset$  whenever no edit step was performed.

Since augmentation only inserts vertices between  $u$  and its children, it affects neither  $L(T(u))$  nor  $L(T(v))$  for  $v \in \text{child}(u)$ . As an immediate consequence we find

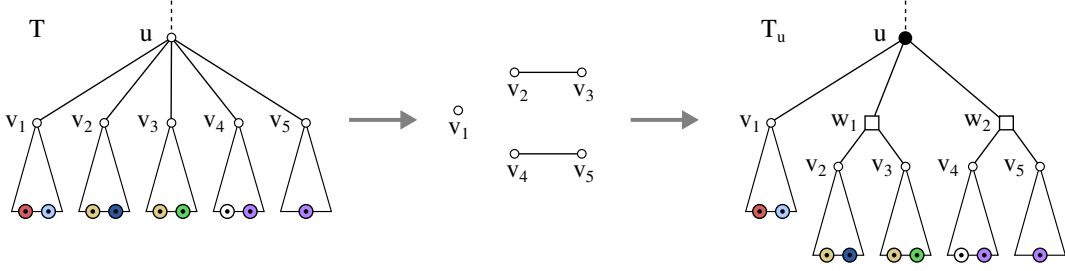


**Figure 8:** Left, a (part of a) leaf-colored tree  $(T, \sigma)$ . The tree  $(T_u, \sigma)$  on the right is obtained from  $(T, \sigma)$  by augmenting  $T$  at vertex  $u$ . The color-set intersection graph  $\mathcal{C}_T(u)$  (shown in the middle) has more than one connected component and there are connected components consisting of more than two vertices  $v_i \in \text{child}_T(u)$ . According to Lemma 4.12,  $\sigma(L(T_u(v))) \cap \sigma(L(T_u(v'))) = \emptyset$  for any two distinct vertices  $v, v' \in \text{child}_{T_u}(u) = \{v_1, w_1, w_2\}$ . By Cor. 2.11, the edges  $uw_1$  and  $uw_2$  are redundant w.r.t.  $\tilde{G}(T_u, \sigma)$  and thus, both trees explain the same BMG.

**Observation 4.11.** Let  $(T, \sigma)$  be a leaf-colored tree,  $u \neq v$  two inner vertices of  $T$ ,  $\mathcal{C}_T(u)$  the corresponding color-set intersection graph, and  $(T_u, \sigma)$  the tree obtained by augmenting  $T$  at  $u$ . Then  $\mathcal{C}_{T_u}(v) = \mathcal{C}_T(v)$ .

**Lemma 4.12.** Let  $(T, \sigma)$  be a leaf-colored tree. Let  $u \in V^0(T)$  and  $T_u$  be the tree after augmenting  $T$  at vertex  $u$ . If  $\mathcal{C}_T(u)$  is unconnected, then  $\sigma(L(T_u(w_1))) \cap \sigma(L(T_u(w_2))) = \emptyset$  for any two distinct vertices  $w_1, w_2 \in \text{child}_{T_u}(u)$ .

*Proof.* By construction, the vertex  $w_i$  in  $T_u$ ,  $i = 1, 2$ , is either a child of  $u$  in  $T$  or was inserted in the augmentation step. Therefore, the two connected components  $C_1$  and  $C_2$  of  $\mathcal{C}_T(u)$  to which  $w_1$  and  $w_2$  belong are disjoint. Thus  $\sigma(L(T(v_i))) \cap \sigma(L(T(v_j))) = \emptyset$  for all  $v_i, v_j \in \text{child}_T(u)$  with  $v_i \in C_1$  and  $v_j \in C_2$  because otherwise there would be an edge  $v_i v_j$  in  $\mathcal{C}_T(u)$  and thus,  $C_1 = C_2$ . Since  $w_i$  is either the single vertex in  $C_i$  or  $w_i$  has as children the vertices of  $C_i$  in  $T_u$ ,  $i \in \{1, 2\}$ , we conclude that  $\sigma(L(T_u(w_1))) \cap \sigma(L(T_u(w_2))) = \emptyset$ . □

The following result shows that no further edit step can be performed at vertices that have been newly introduced by a former augmentation step or have already undergone an augmentation.

**Lemma 4.13.** Let  $(T, \sigma)$  be a leaf-colored tree,  $u \in V^0(T)$ ,  $(T_u, \sigma)$  the tree obtained by augmenting  $T$  at  $u$ , and denote by  $(T_{uw}, \sigma)$  the tree obtained by augmenting  $T_u$  at  $w$ . Then  $T_{uw} = T_u$  for all  $w \in V_{-T} \cup \{u\}$ .

*Proof.* If  $T_u = T$ , then  $V_{-T} = \emptyset$  and thus  $T_{uu} = T_u = T$ . If  $T_u \neq T$ , then the definition of the augmentation step at  $u$  implies that either  $\mathcal{C}_{T_u}(u)$  is connected or all connected components of  $\mathcal{C}_{T_u}(u)$  are singletons. In either case Lemma 4.12 ensured that augmentation at  $u$  leaves  $T_u$  unchanged, i.e.,  $T_{uu} = T_u$ . By construction,  $\mathcal{C}_{T_u}(w)$  is connected for  $w \in V_{-T} \setminus \{u\}$  and thus, we have  $T_{uw} = T_u$ . □

We now show that the application of all possible non-trivial augmentation steps in some tree  $(T, \sigma)$  finally leads to a unique tree  $(\mathcal{A}(T), \sigma)$ . It can be computed according to Algorithm 1.

**Lemma 4.14.** For every leaf-colored tree  $(T, \sigma)$  there is a unique tree  $(\mathcal{A}(T), \sigma)$  obtained from  $(T, \sigma)$  by repeated application of augmentation steps until only trivial augmentation steps remain. The tree  $(\mathcal{A}(T), \sigma)$  is computed by Algorithm 1.

*Proof.* Lemma 4.13 together with Observation 4.11 implies that (i) every vertex  $u$  in  $T$  can be non-trivially augmented at most once, (ii) the newly introduced vertices cannot be non-trivially augmented at all, and (iii) augmentation of two distinct inner vertices of  $T$  yields the same result irrespective of the order of the augmentation steps. Thus,  $(\mathcal{A}(T), \sigma)$  is unique. The correctness of Algorithm 1 now follows immediately. □

**Lemma 4.15.** Alg. 1 with input  $T = (V, E)$  and  $\sigma$  runs in  $O(|V|^2|\mathcal{S}|)$  time and  $O(|V|^2)$  space, where  $\mathcal{S} = \sigma(L(T))$  is the set of species under consideration.

*Proof.* Assigning the color set  $L(T(u))$  to each  $u$  requires  $O(|V||\mathcal{S}|)$  time, where  $|\mathcal{S}| < |V|$ . The total effort to construct all  $\mathcal{C}_T(u)$  is bounded by  $O(|V|^2|\mathcal{S}|)$ , corresponding to comparing the color sets of all pairs of vertices of  $T$ . The total size of all color-set intersection graphs is  $O(|V|^2)$ . Computation of the connected components is linear in the size of the graph, which also bounds the editing effort for each  $u$ , implying the claim. □

We close this section by showing that augmentation does not affect the underlying BMG and thus, the unique tree obtained by Alg. 1 still explains the same BMG.

---

**Algorithm 1:** Augmented tree

---

**Data:** Leaf-colored phylogenetic tree  $(T, \sigma)$   
**Result:** Augmented tree  $(\mathcal{A}(T), \sigma)$

```
1 foreach  $u \in V^0(T)$  in pre-order do
2   Compute  $\mathfrak{C}_T(u)$ .
3    $\mathcal{C} \leftarrow$  set of connected components of  $\mathfrak{C}_T(u)$ 
4   if  $|\mathcal{C}| > 1$  then
5     foreach  $C \in \mathcal{C}$  such that  $|C| > 1$  do
6       Introduce a vertex  $w$  and the edge  $uw$ .
7       foreach  $v_i \in C$  do
8         Remove the edge  $uv_i$ .
9         Add the edge  $wv_i$ .
10      end
11    end
12 end
```

---

**Proposition 4.16.** *For every leaf-colored tree  $(T, \sigma)$  holds  $\vec{G}(T, \sigma) = \vec{G}(\mathcal{A}(T), \sigma)$ .*

*Proof.* Let  $u \in V^0(T)$  and  $T_u$  be the tree after augmenting  $T$  at vertex  $u$ . Put  $A := \{uw \mid w \in V_{-T}\}$  and note that all edges of  $T_u$  in  $A$  are inner edges. Now consider  $e \in A$ . Since  $w \in V_{-T}$ , an edit step was performed to obtain  $w$  and thus,  $|\mathcal{C}| > 1$  in  $\mathfrak{C}_T(u)$ . Lemma 4.12 and  $|\mathcal{C}| > 1$  imply that for any  $v' \in \text{child}_{T_u}(u)$  with  $v' \neq w$  we have  $\sigma(L(T_u(v'))) \cap \sigma(L(T_u(w))) = \emptyset$ . Thus, Cor. 2.11 implies that the edge  $uw$  is redundant in  $(T_u, \sigma)$  w.r.t.  $\vec{G}(T, \sigma)$ .

Denoting by  $T_{u_A}$  the tree obtained from  $T_u$  by contraction of all edges in  $A$ , we obtain  $(T, \sigma) = (T_{u_A}, \sigma)$ . Lemma 2.13 now implies  $\vec{G}(T_u, \sigma) = \vec{G}(T_{u_A}, \sigma) = \vec{G}(T, \sigma)$  for every augmentation step. By Lemma 4.14, we can repeat this argument for every augmentation in the arbitrary order in which  $\vec{G}(\mathcal{A}(T), \sigma)$  is obtained from  $\vec{G}(T, \sigma)$ , and thus  $\vec{G}(\mathcal{A}(T), \sigma) = \vec{G}(T, \sigma)$ .  $\square$

## 4.4 Extremal Labeling of Augmented Trees

While the least resolved tree in general cannot support an event labeling that properly reflects the underlying true history of a gene family, we shall see here that the augmented tree  $(\mathcal{A}(T), \sigma)$  does feature sufficient resolution. To this end, we investigate the extremal event labeling of  $(\mathcal{A}(T), \sigma)$ .

**Lemma 4.17.** *Let  $\hat{t}_{\mathcal{A}(T)}$  be the extremal event labeling of the augmented tree  $(\mathcal{A}(T), \sigma)$  obtained from  $(T, \sigma)$  and let  $u$  be some vertex of  $\mathcal{A}(T)$ . If  $\hat{t}_{\mathcal{A}(T)}(u) = \square$ , then  $\mathfrak{C}_{\mathcal{A}(T)}(u)$  is connected.*

*Proof.* Suppose that  $\hat{t}_{\mathcal{A}(T)}(u) = \square$ . There are two possibilities:

(1)  $u \in V^0(T)$ . If  $\mathfrak{C}_T(u)$  is connected, then  $\mathfrak{C}_{\mathcal{A}(T)}(u) = \mathfrak{C}_T(u)$ . Otherwise, Lemma 4.12 implies that  $\sigma(L(\mathcal{A}(T)(w_1))) \cap \sigma(L(\mathcal{A}(T)(w_2))) = \emptyset$  for all  $w_1, w_2 \in \text{child}_{\mathcal{A}(T)}(u)$ , thus the definition of the extremal event labeling implies  $\hat{t}_{\mathcal{A}(T)}(u) \neq \square$ , a contradiction.

(2)  $u \in V_{-T}$ , i.e.,  $u$  is newly created by augmenting some  $u' \in V^0(T)$ , hence  $\mathfrak{C}_T(u)$  is connected and, by Obs. 4.11 and Lemma 4.13,  $\mathfrak{C}_{\mathcal{A}(T)}(u)$  is connected.  $\square$

**Lemma 4.18.** *Let  $(\vec{G}, \sigma)$  be a BMG and  $(T^*, \sigma)$  its unique least resolved tree. Moreover, let  $\hat{t} := \hat{t}_{\mathcal{A}(T^*)}$  be the extremal event labeling of the augmented tree  $(\mathcal{A}(T^*), \sigma)$ . Then,  $\Theta(\mathcal{A}(T^*), \hat{t}) \subseteq \vec{G}$ .*

*Proof.* Since  $(T^*, \sigma)$  explains  $(\vec{G}, \sigma)$ , we have  $(\vec{G}, \sigma) = \vec{G}(T^*, \sigma)$ . By Prop. 4.16, we have  $\vec{G}(T^*, \sigma) = \vec{G}(\mathcal{A}(T^*), \sigma)$ . Let  $xy$  be an edge in  $\Theta(\mathcal{A}(T^*), \hat{t})$ . By definition,  $\hat{t}(\text{lca}_{\mathcal{A}(T^*)}(u)) = \bullet$  where  $u := \text{lca}_{\mathcal{A}(T^*)}(x, y)$ . By definition of the extremal event labeling,  $\sigma(L(\mathcal{A}(T^*)(v_1))) \cap \sigma(L(\mathcal{A}(T^*)(v_2))) = \emptyset$  for all two distinct vertices  $v_1, v_2 \in \text{child}_{\mathcal{A}(T^*)}(u)$ . The latter is true, in particular, for the two children  $v_x, v_y \in \text{child}_{\mathcal{A}(T^*)}(u)$  with  $x \preceq_{\mathcal{A}(T^*)} v_x$  and  $y \preceq_{\mathcal{A}(T^*)} v_y$ . Therefore,  $\sigma(x) \notin \sigma(L(\mathcal{A}(T^*)(v_y)))$  and  $\sigma(y) \notin \sigma(L(\mathcal{A}(T^*)(v_x)))$ . We conclude that  $x$  and  $y$  are reciprocal best matches in  $\mathcal{A}(T^*)$ . Finally,  $(\vec{G}, \sigma) = \vec{G}(\mathcal{A}(T^*), \sigma)$  implies that  $xy$  is an edge in  $\vec{G}$ .  $\square$

Now we are in the position to prove the main result of this contribution.

**Theorem 4.19.** *Let  $(\vec{G}, \sigma)$  be a BMG,  $(T^*, \sigma)$  its unique least resolved tree, and  $\hat{t} := \hat{t}_{\mathcal{A}(T^*)}$  the extremal event labeling of the augmented tree  $(\mathcal{A}(T^*), \sigma)$ . Then  $(\Theta(\mathcal{A}(T^*), \hat{t}), \sigma) = \text{NH}(\vec{G}, \sigma)$ .*

*Proof.* Let  $(G, \sigma)$  be the symmetric part of  $(\vec{G} = (V, E), \sigma)$ . For simplicity, we write  $G_\Theta := \Theta(\mathcal{A}(T^*), \hat{\tau})$  and  $G_{\text{NH}} := (V, E(\text{NH}(\vec{G}, \sigma)))$ . Recall that, by definition,  $G_{\text{NH}} \subseteq G$  and, by Lemma 4.18,  $G_\Theta \subseteq \vec{G}$ . Finally, as  $G$  contains only edges of  $\vec{G}$ , we have  $G_\Theta \subseteq G$ . Let  $F := E(G) \setminus E(G_{\text{NH}})$  be the set of all edges of  $G$  that are hug-edges, and let  $F' := E(G) \setminus E(G_\Theta)$  be the set of all edges in  $G$  that do not form orthologous pairs. Since  $G_{\text{NH}}, G_\Theta \subseteq G$  it suffices to verify that  $F = F'$  in order to show that  $(G_\Theta, \sigma) = (G_{\text{NH}}, \sigma)$ .

Assume  $e = xy \in F'$ . Hence,  $xy \notin E(G_\Theta)$  and therefore,  $\hat{\tau}(u) = \square$  where  $u := \text{lca}_{\mathcal{A}(T^*)}(x, y)$ . By Lemma 4.17,  $\mathcal{C}_{\mathcal{A}(T^*)}(u)$  has exactly one connected component. This together with Thm. 4.5 implies that  $xy$  is a hug-edge and thus,  $xy \in F$ , and hence  $F' \subseteq F$ .

Assume  $e = xy \in F$  is a hug-edge. Assume, for contradiction, that  $e \notin F'$  and thus,  $\hat{\tau}(u) = \bullet$  where  $u := \text{lca}_{\mathcal{A}(T^*)}(x, y)$ . By definition of the extremal event labeling, it must therefore hold that  $\sigma(L(\mathcal{A}(T^*)(v_1))) \cap \sigma(L(\mathcal{A}(T^*)(v_2))) = \emptyset$  for any two distinct vertices  $v_1, v_2 \in \text{child}_{\mathcal{A}(T^*)}(u)$ . By Prop. 4.16,  $(\mathcal{A}(T^*), \sigma)$  explains  $(\vec{G}, \sigma)$ . This together with Lemma 4.6 implies that there are two distinct vertices  $v_1, v_2 \in \text{child}_{\mathcal{A}(T^*)}(u)$  such that  $\sigma(L(\mathcal{A}(T^*)(v_1))) \cap \sigma(L(\mathcal{A}(T^*)(v_2))) \neq \emptyset$ ; a contradiction. Therefore,  $e \in F'$ , and hence  $F \subseteq F'$ .  $\square$

**Corollary 4.20.** *An edge  $xy$  in a BMG  $(\vec{G}, \sigma)$  is u-fp if and only if  $xy$  is a hug-edge of  $(\vec{G}, \sigma)$ .*

*Proof.* Let  $(\vec{G}, \sigma)$  be a BMG,  $(T^*, \sigma)$  its unique least resolved tree, and  $\hat{\tau} := \hat{\tau}_{\mathcal{A}(T^*)}$  the extremal event labeling of the augmented tree  $(\mathcal{A}(T^*), \sigma)$ . As shown in the proof of Thm. 4.19, every edge  $xy$  of the symmetric part  $G$  that is not a hug-edge satisfies  $xy \in E(G_\Theta)$  and therefore  $\hat{\tau}(u) = \bullet$ , where  $u := \text{lca}_{\mathcal{A}(T^*)}(x, y)$ . Lemma 3.2 implies that  $e$  is not  $(\mathcal{A}(T^*), \sigma)$ -fp and thus, in particular, not  $u$ -fp. That is, all edges in  $(G_\Theta, \sigma) = (G_{\text{NH}}, \sigma)$  are non- $u$ -fp edges. Moreover, Thm. 4.5 implies that all hug-edges in  $E(G) \setminus E(G_{\text{NH}})$  are  $u$ -fp. Since  $(G_{\text{NH}}, \sigma)$  does not contain  $u$ -fp edges, all  $u$ -fp edges must also be hug-edges, which completes the proof.  $\square$

The results imply that the no-hug graph  $\text{NH}(\vec{G}, \sigma)$  is obtained from  $(\vec{G}, \sigma)$  by removing all  $u$ -fp edges. This and the fact that  $\text{NH}(\vec{G}, \sigma) = (\Theta(\mathcal{A}(T^*), \hat{\tau}), \sigma)$  is an orthology graph implies that  $\text{NH}(\vec{G}, \sigma)$  is the best estimate of the orthology relation that we can make for a given BMG  $(\vec{G}, \sigma)$ . By Thm. 2.20,  $\text{NH}(\vec{G}, \sigma)$  must also be a cograph.

We next show that the computation of  $\text{NH}(\vec{G}, \sigma)$  can be achieved in polynomial time. In fact, the effort is dominated by computing the least resolved tree  $(T^*, \sigma)$  for a given BMG.

**Theorem 4.21.** *For a given BMG  $(\vec{G}, \sigma)$ , the set of all u-fp edges can be computed in  $O(|L|^3|\mathcal{S}|)$  time, where  $L = V(\vec{G})$  and  $\mathcal{S} = \sigma(L(T))$  is the set of species under consideration.*

*Proof.* Given a BMG  $(\vec{G}, \sigma)$ , its least resolved tree  $(T^*, \sigma)$  can be computed in  $O(|L|^3|\mathcal{S}|)$  time (cf. Thm. 2.6 and [12, Sect. 5]). The augmented tree  $(\mathcal{A}(T^*), \sigma)$  can be obtained from  $(T^*, \sigma)$  in  $O(|L|^2|\mathcal{S}|)$  time according to Lemma 4.15. The extremal event labeling  $\hat{\tau}$  can be obtained from the connectivity information on the  $\mathcal{C}_{\mathcal{A}(T^*)}(u)$  in linear time. Computing  $(\Theta(\mathcal{A}(T^*), \hat{\tau}), \sigma) = \text{NH}(\vec{G}, \sigma)$  then only requires evaluation of  $\text{lca}_{\mathcal{A}(T^*)}(x, y)$ , which can be achieved in polynomial time in  $O(|L|^2)$  as described in [12, Sect. 5].  $\square$

As argued in [12, Sect. 5], in practical applications the number of genes between different species will be comparable, that is,  $O(\ell) = O(|L|/|\mathcal{S}|)$  with  $\ell = \max_{s \in \mathcal{S}} |L[s]|$ . In this case, the running time to compute  $(T^*, \sigma)$  reduces to  $O(|L|^3/|\mathcal{S}|)$  and we obtain an overall running time to compute the set of all  $u$ -fp edges of  $O(|L|^3/|\mathcal{S}| + |L|^2|\mathcal{S}|)$ . Thm. 4.19 and 4.21 imply that we do not need to find induced quartets and hourglasses explicitly, nor do we need to identify the hourglass chains. Instead, it is more efficient to compute the least resolved tree  $(T^*, \sigma)$ , its augmentations  $\mathcal{A}(T^*, \sigma)$ , and the corresponding extremal event labeling  $\hat{\tau}$ .

## 5 Quartets, Hourglasses, and the Structure of Reciprocal Best Match Graphs

The characterization of  $u$ -fp edges is in a way surprising when compared to previous results on the structure of RBMGs [13, 14], where quartets were a focal point of the investigation. On one hand, Prop. 3.15 provides the expected connection of  $u$ -fp edges with good and ugly quartets, while on the other hand, the  $u$ -fp edges in hourglasses, cf. Prop. 3.20, show that  $u$ -fp edges can be entirely unrelated to quartets and thus induced  $P_4$ s. In this section, we aim to close this gap in our understanding.

### 5.1 Hourglass-free BMGs

We start with a special case for which quartets are sufficient.

**Definition 5.1.** *A BMG  $(\vec{G}, \sigma)$  is hourglass-free if it does not contain an hourglass as an induced subgraph.*

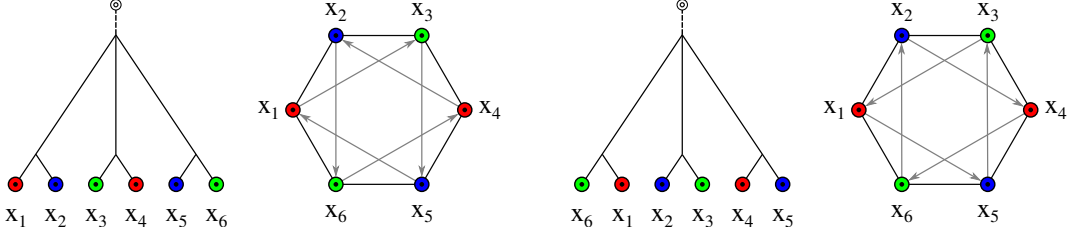


**Figure 9:** Two examples of trees whose BMGs  $\vec{G}(T, \sigma)$  contain a hexagon  $\langle x_1x_2x_3x_4x_5x_6 \rangle$ . There are exactly two distinct possibilities for the placement of the non-symmetric arcs in the subgraph of the BMG induced by the hexagon, see proof of Lemma 5.2.

In particular, an hourglass-free BMG does not contain an hourglass chain either. Geiß et al. [14] found that a certain type of colored 6-cycles is an important characteristic of RBMGs with a “complicated” structure that can only be explained by multifurcating trees. Let us write  $\langle x_1x_2 \dots x_k \rangle$  for an induced cycle  $C_k$  with edges  $x_i x_{i+1}$ ,  $1 \leq i \leq k-1$ , and  $x_k x_1$  in the symmetric part  $G$  of  $\vec{G}$ . We say that  $(\vec{G}, \sigma)$  contains a *hexagon* if the corresponding RBMG  $(G, \sigma)$  contains an induced  $C_6 = \langle x_1x_2 \dots x_6 \rangle$  such that any three consecutive vertices of  $C_6$  have pairwise distinct colors, i.e.,  $\sigma(x_i) = \sigma(x_{i+3})$ ,  $1 \leq i \leq 3$ . A graph  $(\vec{G}, \sigma)$  is *hexagon-free* if it does not contain a hexagon.

**Lemma 5.2.** *If a BMG  $(\vec{G}, \sigma)$  is hourglass-free, then it is hexagon-free.*

*Proof.* By contraposition, suppose that  $(\vec{G}, \sigma)$  contains a hexagon  $\langle x_1x_2 \dots x_6 \rangle$ . Thus,  $P = \langle x_1x_2x_3x_4 \rangle$  is an induced  $P_4$  in  $\vec{G}$  with  $\sigma(x_1) = \sigma(x_4)$ . By [14, Lemma 32]), this  $P_4$  is either a good or a bad quartet. Hence, either the arcs  $(x_1, x_3), (x_4, x_2) \in E(\vec{G})$  and  $(x_3, x_1), (x_2, x_4) \notin E(\vec{G})$ , or  $(x_3, x_1), (x_2, x_4) \in E(\vec{G})$  and  $(x_1, x_3), (x_4, x_2) \notin E(\vec{G})$ , see Fig. 9.

Assume that the arcs  $(x_1, x_3)$  and  $(x_4, x_2)$  exist, i.e.,  $P$  is a good quartet. Now  $P' = \langle x_2x_3x_4x_5 \rangle$  is an induced  $P_4$  in  $\vec{G}$  as well and satisfies  $\sigma(x_2) = \sigma(x_5)$ . Since the arc  $(x_4, x_2)$  exist and by the arguments above,  $P'$  can only be a bad quartet and thus,  $(x_3, x_5) \in E(\vec{G})$  and  $(x_5, x_3) \notin E(\vec{G})$ . Repeating the latter arguments while traversing the induced  $C_6$  implies that  $(x_1, x_3), (x_6, x_4) \in E(\vec{G})$  and  $(x_3, x_1), (x_4, x_6) \notin E(\vec{G})$ . Hence, we obtain the hourglass  $[x_1x_6 \times x_4x_3]$ . Similar arguments imply that there is an hourglass in  $(\vec{G}, \sigma)$  if  $(x_3, x_1), (x_3, x_1) \in E(\vec{G})$  and  $(x_1, x_3), (x_4, x_2) \notin E(\vec{G})$ .  $\square$

Clearly, the converse of Lemma 5.2 is not always satisfied, since, by Obs. 3.18, an hourglass is a BMG without hexagons.

A very useful observation in previous work is the fact that every 3-colored vertex induced subgraph of an RBMG  $(G, \sigma)$  is again an RBMG [14, Thm. 7]. Furthermore, the connected components  $(C, \sigma)$  of every 3-colored vertex induced subgraph of  $(G, \sigma)$  belong to precisely one of the three types [14, Thm. 5]:

**Type (A)**  $(C, \sigma)$  contains a  $K_3$  on three colors but no induced  $P_4$ .

**Type (B)**  $(C, \sigma)$  contains an induced  $P_4$  on three colors whose endpoints have the same color, but no induced cycle  $C_n$  on  $n \geq 5$  vertices.

**Type (C)**  $(C, \sigma)$  contains a hexagon.

The graphs for which all such 3-colored connected components are of Type (A) are exactly the RBMGs that are already cographs, or co-RBMGs for short [14, Thm. 8 and Remark 2]. Together with Lemma 5.2, this classification immediately implies

**Corollary 5.3.** *Let  $(\vec{G}, \sigma)$  be an hourglass-free BMG. Then its symmetric part  $(G, \sigma)$  is either a co-RBMG or it contains an induced  $P_4$  on three colors whose endpoints have the same color, but no induced cycle  $C_n$  on  $n \geq 5$  vertices.*

We already know from Prop. 3.15 and Cor. 4.20 that all *u-fp* edges in an hourglass-free BMG are identified by the good and ugly quartets, which are 3-colored by construction. In hourglass-free BMGs, it is indeed sufficient to consider only the 3-colored  $P_4$ s to identify all *u-fp* edges and thus, to obtain an orthology graph, even though the BMG may also contain 4-colored  $P_4$ s. Since hourglasses can only appear in BMGs that require multifurcations for their explanation (cf. Lemma 3.19), the case of hourglass-free BMGs is the most relevant for practical applications.

Since all *u-fp* edges in an hourglass-free BMG are contained in quartets, it is also easy to identify the ones that are already orthology graphs.

**Corollary 5.4.** *Let  $(\vec{G}, \sigma)$  be an hourglass-free BMG. Then, its symmetric part  $(G, \sigma)$  is a co-RBMG if and only if there are no *u-fp* edges in  $(\vec{G}, \sigma)$ .*

*Proof.* Since  $(G, \sigma)$  is a cograph, it contains no induced  $P_4$ s and thus,  $(\vec{G}, \sigma)$  contains no good or ugly quartets. By Cor. 4.20, all hug-edges are determined by hourglass chains and good or ugly quartets. Since none of them is contained in  $(\vec{G}, \sigma)$ , it also does not contain  $u$ - $fp$  edges. Conversely, suppose that  $(\vec{G}, \sigma)$  contains no  $u$ - $fp$  edges. Then, by Thm. 4.19,  $(G, \sigma) = \mathbb{NH}(\vec{G}, \sigma)$  is an orthology graph and thus, by Thm. 2.20, a cograph.  $\square$

## 5.2 $u$ - $fp$ Edges in Hourglass Chains

The situation is much more complicated in the presence of hourglasses. We start by providing sufficient conditions for  $u$ - $fp$  edges that are identified by hourglass chains.

**Proposition 5.5.** *Let  $\mathfrak{H} = [x_1y_1 \bowtie x'_1y'_1], \dots, [x_ky_k \bowtie x'_ky'_k]$  be an hourglass chain in  $(\vec{G}, \sigma)$ , possibly with a left tail  $z$  or a right tail  $z'$ . Then, an edge in  $\vec{G}$  is  $u$ - $fp$  if it is contained in the set*

$$\begin{aligned} F = & \{x_iy_j \mid 1 \leq i \leq j \leq k\} \cup \{zz'\} \cup \{zy_i, x_iz', zy'_i, x'_iz' \mid 1 \leq i \leq k\} \\ & \cup \{x_ix_{j+1} \mid 1 \leq i < j < k\} \cup \{y_iy_{j+1} \mid 1 \leq i < j < k\} \\ & \cup \{x'_iy'_i, x'_iy_i \mid 2 \leq i \leq k\} \cup \{x_iy'_k, x'_iy'_k \mid 1 \leq i \leq k-1\} \\ & \cup \{x'_1z, x'_1z', y'_kz, y'_kz'\} \end{aligned}$$

*Proof.* Let  $(T, \sigma)$  be an arbitrary tree that explains  $(\vec{G}, \sigma)$ . By analogous arguments as in the proof of Lemma 3.25 and by Lemma 3.24, there is a vertex  $u \in V^0(T)$  with pairwise distinct children  $v_0, v_1, \dots, v_k, v_{k+1}$  such that it holds  $x_1 \in L(T(v_0)), y_k \in L(T(v_{k+1}))$  and, for all  $1 \leq i \leq k$ , we have  $x'_i, y'_i \in L(T(v_i))$ . Since  $x_{i+1} = y'_i$  and  $x'_{i+1} = y_i$  by definition of hourglass chains, it is an easy task to verify that for all edges  $e = ab \in F$  the vertices  $a$  and  $b$  are located below distinct children of  $u$  and thus,  $\text{lca}_T(a, b) = u$  for all such edges. As argued in the proof of Lemma 3.25, we have  $\sigma(L(T(v_0))) \cap \sigma(L(T(v_1))) \neq \emptyset$ . The latter arguments together with Lemma 3.2 imply that every edge in  $F$  is  $u$ - $fp$ .  $\square$

Figs. 6 and 10 furthermore show that hourglass chains identify false-positive edges that are not associated with quartets in the BMG: The BMG in Fig. 6(A) has the  $u$ - $fp$  edge  $xy$ , and the BMG in Fig. 10(B) contains the  $u$ - $fp$  edges  $x_1y_2, x_1z'$  and  $x'_1z'$ . A careful investigation shows that these edges are either not even part of an induced  $P_4$  (such as  $xy$  in Fig. 6 and  $x'_1z'$  in Fig. 10), or at least not identifiable as  $u$ - $fp$  via good, bad or ugly quartets according to Props. 3.11, 3.13 and 3.14, as it is the case for  $x_1y_2$  and  $x_1z'$  in Fig. 10.

This observation limits the use of cograph-editing in the context of orthology detection, at least in the case of gene trees with polytomies: On one hand, Fig. 6 shows that an RBMG  $(G, \sigma)$  can be a cograph and still contain  $u$ - $fp$  edges, on the other hand, 10(C) shows that deletion of the  $u$ - $fp$  edge identified by quartets and thus, induced  $P_4$ s is not sufficient to arrive at a cograph.

## 5.3 Four-colored $P_4$ s

Geiß et al. [14, Thm. 8] establishes that the RBMG  $(G, \sigma)$  is a co-RBMG, i.e., a cograph, if and only if every subgraph induced on three colors is a cograph. Therefore, if  $(G, \sigma)$  contains an induced 4-colored  $P_4$ , it also contains an induced 3-colored  $P_4$ . For hourglass-free BMGs  $(\vec{G}, \sigma)$  it is clear that a 4-colored  $P_4$  always overlaps with a 3-colored  $P_4$ : In this case  $\mathbb{NH}(\vec{G}, \sigma)$  is obtained by deleting middle edges of good quartets and first edges of ugly quartets. Since  $\mathbb{NH}(\vec{G}, \sigma)$  is a cograph, there is no  $P_4$  left, and thus at least one edge of any 4-colored  $P_4$  was among the deleted edges. It is natural to ask whether this is true for BMGs in general. Fig. 11 shows that good and ugly quartets are not sufficient on their own: there are 4-colored  $P_4$ s that do not overlap with the middle edge of a good quartet or the first edge of an ugly quartet. On the other hand, it is clear that at least one of its edges is  $u$ - $fp$ . This does not imply, however, that the  $u$ - $fp$  edges in a 4-colored  $P_4$  are also edges of 3-colored  $P_4$ s.

Still, in the context of cograph-editing approaches it is of interest whether the 3-colored  $P_4$ -s are sufficient. In the following we provide an affirmative answer.

**Lemma 5.6.** *Let  $(\vec{G}, \sigma)$  be a BMG and  $\mathcal{P}$  a 4-colored induced  $P_4$  in the symmetric part of  $(\vec{G}, \sigma)$ . Then at least one of the edges of  $\mathcal{P}$  is either the middle edge of some good quartet or the first edge of a bad or ugly quartet in  $(\vec{G}, \sigma)$ .*

*Proof.* Let  $(T, \sigma)$  be an arbitrary tree that explains  $(\vec{G}, \sigma)$  and suppose that  $\mathcal{P} := \langle abcd \rangle$  is a 4-colored induced  $P_4$  in the symmetric part  $(G, \sigma)$ .

If one of the edges  $ab, bc$ , or  $cd$  of  $\mathcal{P}$  is the middle edge of some good quartet or the first edge of some ugly quartet, then we are done. Hence, we assume in the following that this is not the case and show that at least one of the edges of  $\mathcal{P}$  is the first edge in a bad quartet.

By contraposition of Prop. 3.15, we have  $\mathcal{S}^\cap(a, b) = \emptyset$ ,  $\mathcal{S}^\cap(b, c) = \emptyset$  and  $\mathcal{S}^\cap(c, d) = \emptyset$ . We set  $v := \text{lca}_T(b, c)$  with children  $v_b, v_c \in \text{child}_T(v)$  such that  $b \preceq_T v_b$  and  $c \preceq_T v_c$ , and  $w := \text{lca}_T(a, b)$  with children  $w_a, w_b \in \text{child}_T(w)$  such that  $a \preceq_T w_a$  and  $b \preceq_T w_b$ . Note, that  $v, v_b, w$ , and  $w_b$  are pairwise comparable, since they are all ancestors of  $b$ .

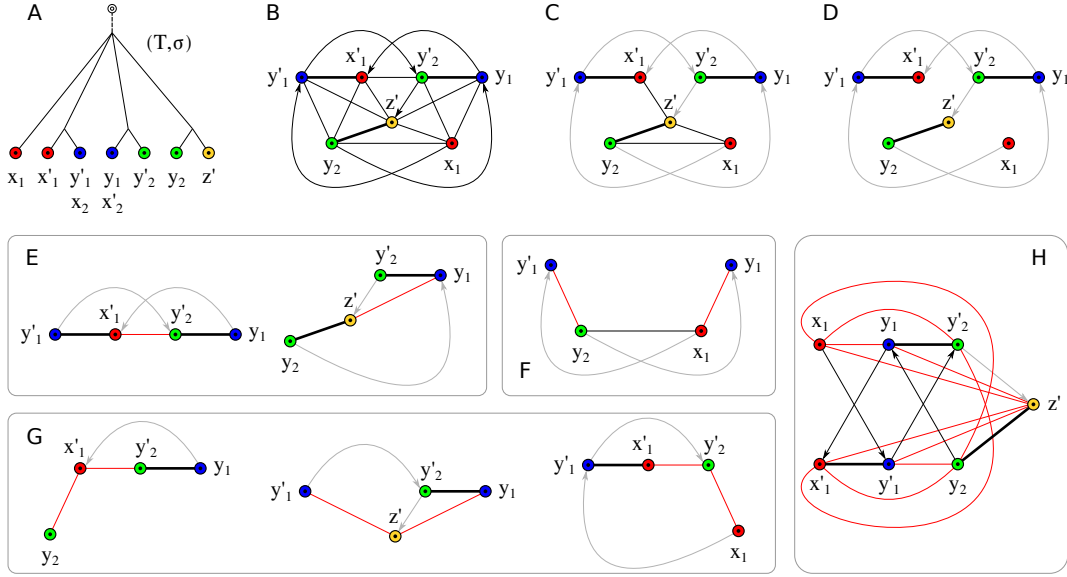


**Figure 10:** The (non-binary) tree  $(T, \sigma)$  in Panel (A) explains the BMG  $(\vec{G}, \sigma)$  in Panel (B), which contains several induced  $P_4$ s and an hourglass chain of length  $k = 2$  with right tail  $z'$ . Edges that are not  $(T, \sigma)$ - $fp$  (and thus not  $u$ - $fp$ ) are shown as thick lines. Thin edges correspond to those that can be identified as  $u$ - $fp$  by the subgraphs in (E–H), where they are highlighted in red. (C) The graph after deletion of all edges that can be identified by good, bad and ugly quartets according to Props. 3.11, 3.13, and 3.14. Note that it contains the induced  $P_4$ s  $\langle y'_1, x'_1, z', y_2 \rangle$  and  $\langle y'_1, x'_1, z', x_1 \rangle$ , which were not induced subgraphs of the original BMG in (B). Its symmetric part  $(H, \sigma)$  differs from  $\mathbb{N}\mathbb{H}(\vec{G}, \sigma)$  (cf. Def. 4.7) since it still contains  $u$ - $fp$  edges. (D) The BMG after deletion of all  $u$ - $fp$  edges. Its symmetric part, comprising the thick edges, is  $\mathbb{N}\mathbb{H}(\vec{G}, \sigma)$ . (E) The two good quartets. (F) The single bad quartet. (G) Examples for ugly quartets that cover the remaining  $u$ - $fp$  edges that are identifiable via quartets. Panel (H) shows the BMG  $(\vec{G}, \sigma)$  in a different layout that highlights the hourglass chain with right tail  $z'$ . All edges that are  $u$ - $fp$  according to Prop. 5.5 are in red. To identify the  $u$ - $fp$  edges in  $(\vec{G}, \sigma)$ , only the subgraphs in Panel (E), (G) and (H) are necessary (cf. Def. 4.4 and Thm. 4.19).

We show that  $w = v$ . Assume, for contradiction, that (i)  $w \prec_T v$  or (ii)  $v \prec_T w$ . In Case (i), we have  $w_a \prec_T w \preceq_T v_b$  and thus,  $\sigma(a) \in \sigma(L(T(v_b)))$ . Hence, as  $\mathcal{S}^\cap(b, c) = \emptyset$ , it must hold that  $\sigma(a) \notin \sigma(L(T(v_c)))$  and  $\sigma(c) \notin \sigma(L(T(v_b)))$ . Lemma 2.4 implies  $ac \in E(G)$ . But then  $\mathcal{P}$  is not an induced  $P_4$ ; a contradiction. In Case (ii), we have  $v_c \preceq_T v \preceq_T w_b$  and thus,  $\sigma(c) \in \sigma(L(T(w_b)))$ . Since  $\mathcal{S}^\cap(a, b) = \emptyset$  we thus have  $\sigma(c) \notin \sigma(L(T(w_a)))$  and  $\sigma(a) \notin \sigma(L(T(w_b)))$ . By Lemma 2.4,  $ac \in E(G)$ ; again a contradiction. Thus  $w = v$ . Analogous arguments can be used to establish  $\text{lca}_T(c, d) = v$ . We therefore have  $v = \text{lca}_T(a, b) = \text{lca}_T(b, c) = \text{lca}_T(c, d)$ . In the following  $v_x$  denotes the child of  $v$  with  $x \preceq_T v_x$  for  $x \in \{a, b, c, d\}$ . Note,  $v_a \neq v_b, v_b \neq v_c$  and  $v_c \neq v_d$ .

We next show that  $v_a, v_b, v_c$ , and  $v_d$  are pairwise distinct. First, assume for contradiction that  $v_a = v_c$ . Together with  $\mathcal{S}^\cap(c, d) = \emptyset$ , this assumption implies that  $\sigma(a) \notin \sigma(L(T(v_d)))$  and  $\sigma(d) \notin \sigma(L(T(v_c)))$ . By Lemma 2.4,  $ad \in E(G)$ , contradicting the assumption that  $\mathcal{P}$  is an induced  $P_4$ . Hence,  $v_a \neq v_c$ . By symmetry of  $\mathcal{P}$ , we can use similar arguments to conclude that  $v_b \neq v_d$ . Finally, assume for contradiction that  $v_a = v_d$ . Then,  $\sigma(d) \in \sigma(L(T(v_a)))$ . Hence,  $\mathcal{S}^\cap(a, b) = \emptyset$  implies that  $\sigma(d) \notin \sigma(L(T(v_b)))$  and  $\sigma(b) \notin \sigma(L(T(v_d)))$ . Again Lemma 2.4 implies  $bd \in E(G)$ ; a contradiction. In summary,  $v_a, v_b, v_c$ , and  $v_d$  must be pairwise distinct.

We claim  $\sigma(c) \in \sigma(L(T(v_a)))$ . Since  $ad \notin E(G)$  and  $\text{lca}_T(a, d) = v$ , Lemma 2.4 implies that  $\sigma(a) \in \sigma(L(T(v_d)))$  or  $\sigma(d) \in \sigma(L(T(v_a)))$ . By symmetry of  $\mathcal{P}$ , we can w.l.o.g. assume that  $\sigma(a) \in \sigma(L(T(v_d)))$  and thus, there is a vertex  $a_d \in L(T(v_d))$  with  $\sigma(a_d) = \sigma(a)$ . In this case,  $\mathcal{S}^\cap(c, d) = \emptyset$  implies that  $\sigma(a) \notin \sigma(L(T(v_c)))$ . This together with  $ac \notin E(G)$  and Lemma 2.4 implies that  $\sigma(c) \in \sigma(L(T(v_a)))$ .

We claim  $\sigma(d) \in \sigma(L(T(v_a)))$ . We assume for contradiction that this is not the case and show that this implies the existence of an ugly quartet  $\langle cdc'd' \rangle$  containing  $cd$  as its first edge, which leads to a contradiction to our initial assumption that none of the edges in  $\mathcal{P}$  is the first, resp., middle edge of an ugly, resp., good quartet. To see this, note that  $\sigma(a), \sigma(c) \in \sigma(L(T(v_a)))$  and Lemma 2.3 imply that there is an edge  $d'c'$  for two vertices  $a', c' \prec_T v_a$  with  $\sigma(a') = \sigma(a)$  and  $\sigma(c') = \sigma(c)$ . Since  $\sigma(a) = \sigma(a')$  and  $\text{lca}_T(a', c') \preceq_T v_a \prec_T v = \text{lca}_T(a', c)$ , we have  $a'c' \notin E(G)$ . Since  $\sigma(a_d) = \sigma(a')$  and  $\text{lca}_T(a_d, d) \preceq_T v_d \prec_T v = \text{lca}_T(a', d)$ , we have  $a'd \notin E(G)$ . Now,  $\mathcal{S}^\cap(c, d)$  implies that  $\sigma(c) \notin \sigma(L(T(v_d)))$ . This and  $\sigma(d) \notin \sigma(L(T(v_a)))$  together with Lemma 2.4 implies that there is an edge  $c'd \in E(G)$ . Thus, we obtain the ugly quartet  $\langle cdc'd' \rangle$  and hence, the desired contradiction. Therefore,  $\sigma(d) \in \sigma(L(T(v_a)))$ . Because of  $\mathcal{S}^\cap(a, b) = \emptyset$  we also have  $\sigma(d) \notin \sigma(L(T(v_b)))$ .



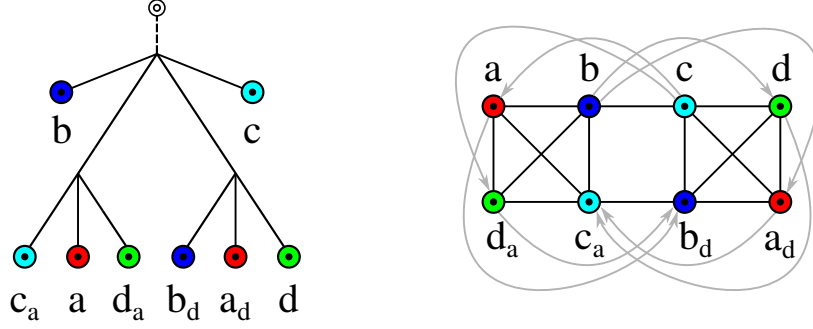


**Figure 11:** The symmetric part of the BMG  $(\vec{G}, \sigma)$  contains the 4-colored induced  $P_4 \langle abcd \rangle$ . None of its edges is the middle edge of a good quartet or the first edge of an ugly quartet. According to Lemma 5.6, there is the bad quartet  $\langle abca_d \rangle$  that contains as first edge the edge  $ab$ .

Since  $\sigma(d) \in \sigma(L(T(v_a)))$ , there is a vertex  $d_a \preceq v_a$  with  $\sigma(d_a) = \sigma(d)$ . Moreover,  $\sigma(b) \notin \sigma(L(T(v_a)))$  and  $\sigma(d) \notin \sigma(L(T(v_b)))$  together with Lemma 2.4 implies that  $bd_a \in E(G)$ . Furthermore,  $\sigma(c) \in \sigma(L(T(v_a)))$  and Lemma 2.4 imply that  $cd_a \notin E(G)$ . Now,  $\mathcal{S}^\cap(c, d) = \emptyset$  implies  $\sigma(d) \notin \sigma(L(T(v_c)))$  and therefore,  $\text{lca}_T(c, d_a) = v \preceq \text{lca}_T(c, d')$  for all  $d' \in L[\sigma(d)]$ . Hence,  $(c, d_a) \in E(\vec{G})$ .

In summary,  $\langle dcbda \rangle$  is an induced  $P_4$  in  $G$ . By [14, Lemma 32], every such induced  $P_4$  forms either a good, bad, or ugly quartet in  $(\vec{G}, \sigma)$  and, since  $(c, d_a) \in E(\vec{G})$ , we can conclude that  $\langle dcbda \rangle$  is a bad quartet with first edge  $cd$ , which completes the proof.  $\square$

**Corollary 5.7.** [14, Thm. 8] *Let  $(G, \sigma)$  be an RBMG. Then,  $(G, \sigma)$  is a cograph if and only if all subgraphs induced by three colors are cographs.*

*Proof.* If  $(G, \sigma)$  is a cograph, then all its induced subgraphs are also cographs [4]. Conversely, if  $(G, \sigma)$  is not a cograph, then it contains at least one induced  $P_4$ . By Lemma 5.6,  $(G, \sigma)$  cannot contain only 4-colored  $P_4$ s and therefore the restriction to at least one combination of three colors contains a  $P_4$  and is thus not a cograph.  $\square$

It is important to recall in this context, however, that the deletion of all *u-fp*-edges identified by quartets does not necessarily lead to a cograph as the example in Fig. 10(C) shows. The quartets alone therefore do not provide a complete algorithm for correcting an RBMG to an orthology graph.

## 6 Simulation Results

We illustrate the potential impact of our mathematical results discussed in the previous sections with the help of simulated data. To this end, we focus on the accuracy of the inferred orthology graph *assuming* that the best matches are accurate. Of course, this is only one of several components in complete orthology detection pipeline, which would also need to consider the genome annotation, pairwise alignments of genes or predicted protein sequences, and the conversion of sequence similarities into best match data. The latter step has been investigated in considerable detail by Stadler et al. [46]. Here, we start from simulated evolutionary scenarios and extract the BMG directly from the ground truth using the simulation library *AsymmeTree* [46].

In brief, *AsymmeTree* generates realistic evolutionary scenarios in four steps. (1) A planted species tree  $S$  is generated using the Innovation Model [25], which models observed phylogenies well. (2) A dating map  $\tau$  assigns time points to all vertices of  $S$  and thus branch lengths to the edges of  $S$ . (3) On  $S$ , we use a variant of the well-known constant-rate birth-death process with a given age [see e.g. 17, 26] to simulate an event-labeled gene tree  $(T, t, \sigma)$  containing duplication and loss events. Speciations are included as additional branching events that generate copies of all genes present at a speciation vertex in all descendant lineages. The simulated gene trees are constrained to have at least one surviving gene in each species to avoid trivial cases. (4) The observable part of the gene tree is extracted by recursively removing leaves that correspond to loss events and suppressing inner vertices with a single child. *AsymmeTree* can also assign rates to edges of  $(T, t, \sigma)$  to convert evolutionary time differences into general additive distances; however, this is not relevant here since the rates do not affect evolutionary relatedness and thus the BMG.

Extending the simulations used in [13, 46], we also consider non-binary gene trees. This is important here since, by Lemma 3.19, hourglasses cannot appear in BMGs that are explained by a binary tree. There is an ongoing discussion to what extent polytomies in phylogenetic trees are biological reality as opposed to an artifact of insufficient

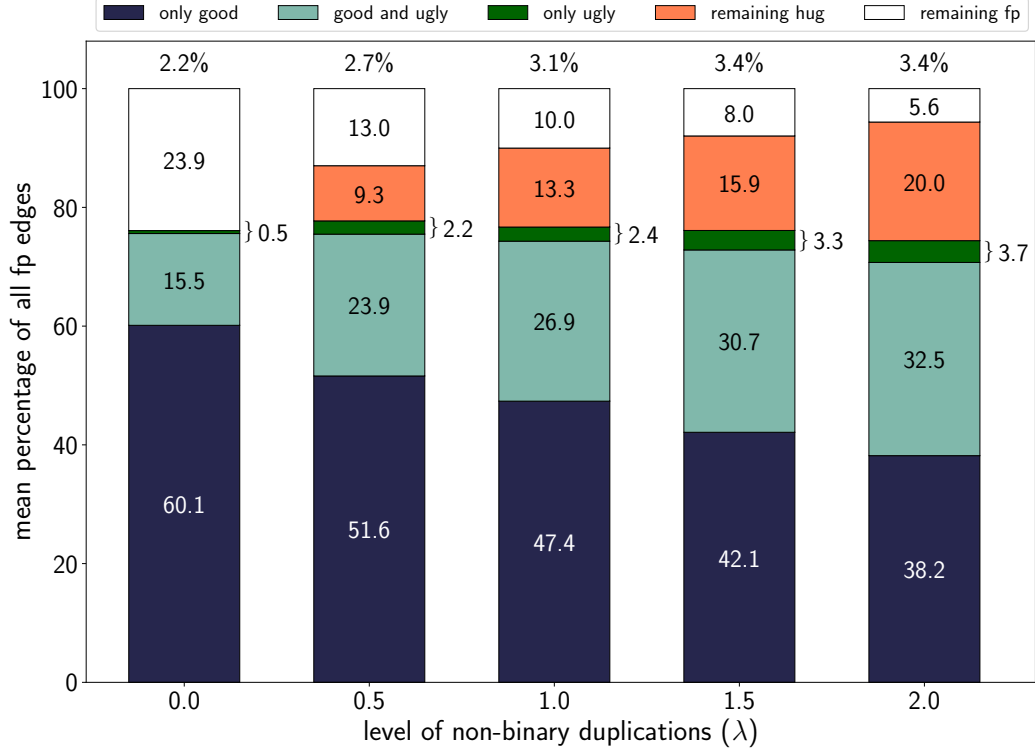


**Figure 12:** Average relative abundance of the different types of hug-edges and undetectable false positives in the BMGs of simulated evolutionary scenarios. We distinguish hug-edges in good and ugly quartets as well as hug-edges appearing only in hourglass chains (orange). In the simulations, the fraction of  $u$ -fp edges that are first edges of bad quartets is too small to be visible and therefore not shown here. The undetectable false positives correspond to complementary gene losses without surviving witnesses of the duplication event. Species trees are binary, while gene trees contain multifurcations. The number of offsprings is modeled as  $2 + k$ , where  $k$  is drawn from a Poisson distribution with parameter  $\lambda$ . For  $\lambda = 0$ , the gene trees are binary. In the experiments, we observed that on average 62.4% of the 25000 simulated BMGs do not contain any false-positive edge (cf. Fig. 13). Those instances are included in the computation of the fraction  $|\mathfrak{F}|/|E(G)|$  (percentage above the bars). However, for the computation of all other values only scenarios that contain false-positives are considered.

resolution. At the level of species trees, the assumption that cladogenesis occurs by a series of bifurcations [e.g. 5, 33] seems to be prevailing, several authors have argued quite convincingly that there is evidence for a least some *bona fide* multifurcations of species [27, 41, 47]. In the simulation, polytomies in species trees are introduced after the first step by edge contraction with a user-defined probability  $p$ .

The reality of polytomies is less clear for gene trees. One reason is the abundance of tandem duplications. Although the majority of tandem arrays comprises only a pair of genes, larger clusters are not at all rare [38]. Although one may argue that mechanistically they likely arise by stepwise duplications, such arrangements are often subject to gene conversion and non-homologous recombination that keeps the sequences nearly identical for some time before they eventually escape from concerted evolution and diverge functionally [18, 31]. As a consequence, duplications in tandem arrays may not be resolvable unless witnesses of different stages of an ongoing duplication process have survived. To model polytomies in the gene tree, we modify step (3) of the simulation procedure by replacing a simple duplication by the generation of  $2 + k$  offspring genes. The number  $k$  of additional copies is drawn from a Poisson distribution with parameter  $\lambda > 0$ .

The simulated data set of evolutionary scenarios comprises species trees with 10 to 30 species (drawn uniformly). The time difference between the planted root and the leaves of  $S$  is set to unity. The duplication and loss rates in the gene trees are drawn i.i.d. from the uniform distribution on the interval  $[0.5, 1.5)$ . Multifurcating gene trees were produced for  $\lambda = \{0.0, 0.5, 1.0, 1.5, 2.0\}$ . In total, we generated 5000 scenarios for each choice of  $p$  and  $\lambda$ . Since the true scenarios, and thus the true gene tree  $T$ , the true BMG  $\vec{G}$ , and the corresponding RBMG  $G$  are known, we can also determine the set

$$\mathfrak{F} := \{xy \mid xy \in E(G) \text{ and } t(\text{lca}_T(x, y)) = \square\}. \quad (2)$$

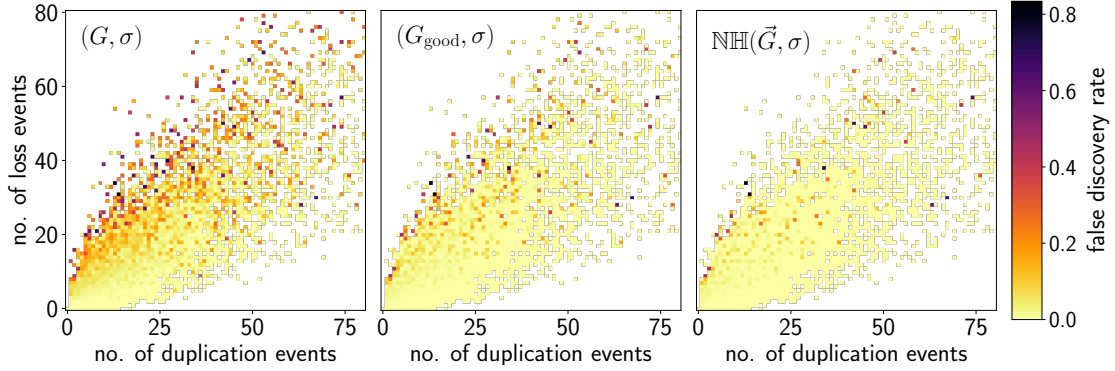


**Figure 13:** False discovery rates computed as proportion of  $fp$  among all edges averaged over all scenarios with given number of duplications and losses. *Left:* RBMGs  $(G, \sigma)$ , i.e.,  $|\mathfrak{F}|/|E(G)|$ . *Middle:* edited RBMG  $(G_{\text{good}}, \sigma)$  with all middle edges of good quartets removed, i.e.,  $|\mathfrak{F} \setminus \mathcal{U}_M|/|E(G_{\text{good}})|$ . *Right:* no-hug graphs  $\text{NH}(\vec{G}, \sigma)$ , i.e.,  $|\mathfrak{F} \setminus \mathcal{U}|/|E(\text{NH})|$ . Scenarios with more than 80 duplication/loss events are not shown.

of false-positive edges. From the BMG, we compute the set  $\mathcal{U}$  of  $u\text{-fp}$  edges as well as the subsets  $\mathcal{U}_M$  and  $\mathcal{U}_U$  of  $u\text{-fp}$  edges that are middle edges of a good or first edges of an ugly quartet, respectively. Note that in general we have  $\mathcal{U}_M \cap \mathcal{U}_U \neq \emptyset$ . We only discuss the results for binary species trees in some detail, since species trees with polytomies yield qualitatively similar results. We observe that the relative abundance of  $u\text{-fp}$  edges in good and ugly quartets increases moderately for larger  $p$ .

First, we note that, consistent with [13, 46], the fraction  $|\mathfrak{F}|/|E(G)|$  of false positive orthology assignments is small in our data set, on the order of 3%. This indicates that, in real-life data, the main source of errors is likely the accurate determination of best matches from sequence data rather than false-positive edges contained in the BMG. Considering the fraction  $|\mathcal{U}|/|\mathfrak{F}|$  of  $u\text{-fp}$  edges in Fig. 12, we find that even in the most adverse case of all gene trees being binary, the BMG identifies more than three quarters of  $\mathfrak{F}$ . It may be surprising at first glance that the problem becomes easier with increasing  $\lambda$  and barely 6% of the false positives escape discovery. A likely explanation is that multifurcations increase the likelihood that an inner vertex has two surviving lineages that serve as witnesses of the event; in addition, multifurcations increase the vertex degree in the BMG, so that in principle more information is available to resolve the tree structure. It is also interesting to note that  $\mathcal{U}_U \setminus \mathcal{U}_M$  is small, i.e., there are few cases of first edges in an ugly quartet that are not also middle edges in a good quartet. The fraction of  $u\text{-fp}$  edges that appear only as first edges of bad quartets is even smaller; only 2-3% of the  $u\text{-fp}$  edges associated with hourglass chains, i.e., less than 0.15% of all  $u\text{-fp}$  edges are of this type. The overwhelming majority of  $u\text{-fp}$  edges associated with quartets thus appear (also) as middle edges of good quartets. This observation provides an explanation for the excellent performance of removing the  $\mathcal{U}_M$ -edges proposed in [13]. In particular in the case of binary trees, which was considered by Geiß et al. [13], there is only a small number of other  $u\text{-fp}$  edges, which are completely covered by  $\mathcal{U}_U$ . Fig. 13 visualizes the appearance of false-positive edges depending on the number of duplication and loss events. Not surprisingly,  $\mathfrak{F}$  is enriched in scenarios with a large number of losses compared to the duplications, and depleted when losses are rare. In fact, in the absence of losses, the RBMG equals the orthology graph, i.e.,  $\mathfrak{F} = \emptyset$  [13, Thm. 4]. Removal of  $\mathcal{U}_M$ , already reduced the false positives considerably.

## 7 Summary and Outlook

We have shown here how all unambiguously false-positive orthology assignments can be identified in polynomial time provided that all best matches are known. In particular, we have provided several characterizations for  $u\text{-fp}$  edges in terms of underlying subgraphs and refinements of trees. Since the best match graph contains only false positives, we have obtained a characterization of *all* unambiguously incorrect orthology assignments. Simulations showed that the majority of false positives comprises middle edges of good quartets, while  $u\text{-fp}$  edges that appear only as first edges of an ugly quartet are rare. Not surprisingly, the hourglass-related  $u\text{-fp}$  edges become important in gene trees with many multifurcations.

The augmented tree  $(\mathcal{A}(T^*), \sigma)$  is the least resolved tree that admits an event labeling such that all inner vertices with child trees that have overlapping colors are designated as duplications while all inner vertices with color-disjoint child trees are designated as speciations. The tree  $(\mathcal{A}(T^*), \sigma)$  therefore does not contain “non-apparent duplications” in the sense of [28], i.e., duplication vertices with species-disjoint subtrees. This is an interesting connection linking the literature concerned with polytomy refinement in given gene trees [3, 28] with Best Match Graphs.

The extremal event labeling  $\hat{t}$  of  $(\mathcal{A}(T^*), \sigma)$  is the one that minimizes the necessary number of duplications on

$(\mathcal{A}(T^*), \sigma)$ . In a conceptual sense, therefore,  $(\mathcal{A}(T^*), \hat{\tau})$  is a “most parsimonious” solution, matching the idea of most parsimonious reconciliations [16, 37]. From a technical point of view, however, the problem we solve here is very different. Instead of considering a given pair of gene tree  $T$  and species tree  $S$ , we ask here about the information contained in the BMG  $(\vec{G}, \sigma)$ , i.e., we only consider the information on the species tree that is already implicitly contained in  $(\vec{G}, \sigma)$ . The construction of the event-labeled gene tree  $(\mathcal{A}(T^*), \hat{\tau})$  in fact *implies* a set  $\mathfrak{S}$  of informative triples, namely those  $\sigma(x)\sigma(y)|\sigma(z)$  with  $\sigma(x)$ ,  $\sigma(y)$ ,  $\sigma(z)$  pairwise distinct and  $\hat{\tau}(\text{lca}_{\mathcal{A}(T^*)}(x, y, z)) = \bullet$ , that are displayed by the species tree  $S$  [19, 24]. Nothing in our theory, however, ensures that  $\mathfrak{S}$  is a consistent set of triples, much less that  $\mathfrak{S}$  is consistent with a given species tree  $S$ .

Since constraints on reconciliation maps deriving from the species phylogeny are fully expressed by informative triples, no such constraint exists in particular for any vertex  $u$  of  $\mathcal{A}(T^*)$  that has only leaves as children. That is, false-positive orthology assignments among the children of  $u$  cannot be identified from the BMG alone because there are no further descendants to witness  $u$  as duplication event. Additional evidence, such as the assumption of a molecular clock or synteny must be used to resolve situations such as the complementary loss shown in Fig. 1.

On the other hand, every gene tree  $T$  can be reconciled with every species tree  $S$  [13, 16, 37] at the expense of reassigning events as duplications. Clearly, if  $\mathcal{A}(T^*)$  is already binary, consistency will require the relabeling of some speciation nodes as duplications. Can one characterize and efficiently compute the minimal relabelings? In the general case, a further refinement of  $\mathcal{A}(T^*)$  may be sufficient. Is a refinement of speciation nodes sufficient, or are there in general speciation nodes in  $(\mathcal{A}(T^*), \hat{\tau})$  that need to be refined into separate speciation and duplication events?

Since orthology graphs are cographs contained in the RBMG  $(G, \sigma)$ , it is of interest to compare the deletion of all *u-fp* edges in  $(G, \sigma)$  with finding a (minimal) edge-deletion set to obtain a cograph. These two problems are clearly distinct: The simplest example is the BMG  $(\vec{G}, \sigma)$  in Fig. 6(A): its symmetric part  $G$  is already a cograph but  $(\vec{G}, \sigma)$  contains the hug-edge  $xy$ , which must be deleted. Despite its practical use [23, 29], this observation relegates cograph-editing [20, 32, 49] to the status of a heuristic approximation for the purpose of orthology detection.

For practical applications, one has to keep in mind that best matches are inferred from sequence similarity data. Despite efforts to convert best (blast) hits into evolutionary best matches in a systematic manner [46], estimated BMGs will contain errors, which in most cases will violate the definition of best match graphs. This begs the question how an empirical estimate of a BMG can be corrected to a closest “correct” BMG that (approximately) fits the data. The analogous RBMG-editing problem is NP-hard [21]. Complexity results for the BMG-editing problem, however, have not become available so far.

Orthology prediction tools intended for large data sets often do not attempt to infer the orthology graph, but instead are content with summarizing the information as *clusters of orthologous groups* (COGs) in an empirically estimated RBMG [39, 48]. Formally, this amounts to editing the BMG to a set of disjoint cliques. The example in Fig. 7 shows that this approach can destroy correct orthology information: the BMG  $(\vec{G}, \sigma)$  does not contain *u-fp* edges and thus, it is the closest orthology graph. However,  $(\vec{G}, \sigma)$  is not the disjoint union of cliques.

## Acknowledgements

We thank Carsten R. Seemann for fruitful discussions and his helpful comments. This work was supported in part by the Austrian Federal Ministries BMK and BMDW and the Province of Upper Austria in the frame of the COMET Programme managed by FFG, and by the German Research Foundation (DFG, grant no. STA 850/49-1).

## References

- [1] Adrian M Altenhoff, Brigitte Boeckmann, Salvador Capella-Gutierrez, Daniel A Dalquen, Todd DeLuca, Kristoffer Forslund, Jaime Huerta-Cepas, Benjamin Linard, Cécile Pereira, Leszek P Prysycz, Fabian Schreiber, Alan Sousa da Silva, Damian Szklarczyk, Clément-Marie Train, Peer Bork, Odile Lecompte, Christian von Mering, Ioannis Xenarios, Kimmen Sjölander, Lars Juhl Jensen, Maria J Martin, Matthieu Muffato, Quest for Orthologs consortium, Toni Gabaldón, Suzanna E Lewis, Paul D Thomas, Erik Sonnhammer, and Christophe Dessimoz. Standardized benchmarking in the quest for orthologs. *Nature Methods*, 13:425–430, 2016.
- [2] Sebastian Böcker and Andreas W. M. Dress. Recovering symbolically dated, rooted trees from symbolic ultrametrics. *Adv. Math.*, 138:105–125, 1998.
- [3] W C Chang and O Eulenstein. Reconciling gene trees with apparent polytomies. In D Z Chen and D T Lee, editors, *Computing and Combinatorics. COCOON 2006*, volume 4112 of *Lect. Notes Comp. Sci.*, pages 235–244, Berlin, Heidelberg, 2006. Springer.
- [4] D G Corneil, H Lerchs, and L S Burlingham. Complement reducible graphs. *Discr. Appl. Math.*, 3:163–174, 1981.

- [5] R. DeSalle, R. Absher, and G. Amato. Speciation and phylogenetic resolution. *Trends Ecol. Evol.*, 9:297–298, 1994.
- [6] Christophe Dessimoz, Brigitte Boeckmann, Alexander C. J. Roth, and Gaston H. Gonnet. Detecting non-orthology in the COGs database and other approaches grouping orthologs using genome-specific best hits. *Nucleic Acids Res*, 34:3309–3316, 2006.
- [7] J-P Doyon, V Ranwez, V Daubin, and V Berry. Models, algorithms and programs for phylogeny reconciliation. *Brief Bioinform.*, 12:392–400, 2011.
- [8] W M Fitch. Distinguishing homologous from analogous proteins. *Syst Zool*, 19:99–113, 1970.
- [9] Toni Gabaldón and Eugene V. Koonin. Functional and evolutionary implications of gene orthology. *Nat Rev Genet.*, 14:360–366, 2013.
- [10] M Y Galperin, D M Kristensen, K S Makarova, Y I Wolf, and E V Koonin. Microbial genome analysis: the COG approach. *Brief Bioinform.*, 20:1063–1070, 2019.
- [11] Michael R Garey and David S Johnson. *Computers and intractability: A Guide to the Theory of NP-completeness*. W. H. Freeman, San Francisco, 1979.
- [12] Manuela Geiß, Edgar Chávez, Marcos González Laffitte, Alitzel López Sánchez, Bärbel M R Stadler, Dulce I. Valdivia, Marc Hellmuth, Maribel Hernández Rosales, and Peter F Stadler. Best match graphs. *J. Math. Biol.*, 78:2015–2057, 2019.
- [13] Manuela Geiß, Marcos E. González Laffitte, Alitzel López Sánchez, Dulce I. Valdivia, Marc Hellmuth, Maribel Hernández Rosales, and Peter F. Stadler. Best match graphs and reconciliation of gene trees with species trees. *J. Math. Biol.*, 80:1459–1495, 2020.
- [14] Manuela Geiß, Peter F. Stadler, and Marc Hellmuth. Reciprocal best match graphs. *J. Math. Biol.*, 80:865–953, 2020.
- [15] Paweł Górecki and Jerzy Tiuryn. DLS-trees: A model of evolutionary scenarios. *Theor. Comp. Sci.*, 359:378–399, 2006.
- [16] R Guigó, I Muchnik, and T F Smith. Reconstruction of ancient molecular phylogeny. *Mol Phylogenet Evol*, 6:189–213, 1996.
- [17] Oskar Hagen and Tanja Stadler. TreeSimGM: Simulating phylogenetic trees under general Bellman-Harris models with lineage-specific shifts of speciation and extinction in R. *Methods Ecol. Evol.*, 9:754–760, 2018.
- [18] Kousuke Hanada, Ayumi Tezuka, Masafumi Nozawa, Yutaka Suzuki, Sumio Sugano, Atsushi J Nagano, Motomi Ito, and Shin-Ichi Morinaga. Functional divergence of duplicate genes several million years after gene duplication in *arabidopsis*. *DNA Research*, 25:327–339, 2018.
- [19] Marc Hellmuth. Biologically feasible gene trees, reconciliation maps and informative triples. *Alg Mol Biol*, 12:23, 2017.
- [20] Marc Hellmuth, Adrian Fritz, Nicolas Wieseke, and Peter F. Stadler. Techniques for the cograph editing problem: Module merge is equivalent to edit  $P_4$ 's. *Art Discr. Appl. Math.*, 3:#P2.01, 2020.
- [21] Marc Hellmuth, Manuela Geiß, and Peter F. Stadler. Complexity of modification problems for reciprocal best match graphs. *Theor. Comp. Sci.*, 809:384–393, 2020.
- [22] Marc Hellmuth, Maribel Hernandez-Rosales, Katharina T. Huber, Vincent Moulton, Peter F. Stadler, and Nicolas Wieseke. Orthology relations, symbolic ultrametrics, and cographs. *J. Math. Biol.*, 66:399–420, 2013.
- [23] Marc Hellmuth, Nicolas Wieseke, Marcus Lechner, Hans-Peter Lenhof, Martin Middendorf, and Peter F. Stadler. Phylogenomics with paralogs. *Proc Natl Acad Sci USA*, 112:2058–2063, 2015.
- [24] Maribel Hernandez-Rosales, Marc Hellmuth, Nick Wieseke, Katharina T. Huber, Vincent Moulton, and Peter F. Stadler. From event-labeled gene trees to species trees. *BMC Bioinformatics*, 13(Suppl. 19):S6, 2012.
- [25] Stephanie Keller-Schmidt and Konstantin Klemm. A model of macroevolution as a branching process based on innovations. *Adv. Complex Syst.*, 15:1250043, 2012.
- [26] David G. Kendall. On the generalized birth-and-death process. *Ann. Math. Statistics*, 19:1–15, 1948.

- [27] R M Kliman, P Andolfatto, J A Coyne, F Depaulis, M Kreitman, A J Berry, J McCarter, J Wakeley, and J Hey. The population genetics of the origin and divergence of the *Drosophila simulans* complex species. *Genetics*, 156:1913–1931, 2000.
- [28] Manuel Lafond, Cedric Chauve, Riccardo Dondi, and Nadia El-Mabrouk. Polytoimy refinement for the correction of dubious duplications in gene trees. *Bioinformatics*, 30:i519–i526, 2014.
- [29] Manuel Lafond, Riccardo Dondi, and Nadia El-Mabrouk. The link between orthology relations and gene trees: A correction perspective. *Algorithms Mol Biol.*, 11:4, 2016.
- [30] Manuel Lafond and Nadia El-Mabrouk. Orthology and paralogy constraints: satisfiability and consistency. *BMC Genomics*, 15:S12, 2014.
- [31] Daiqing Liao. Concerted evolution: Molecular mechanisms and biological implications. *Am. J. Hum. Genet.*, 64:24–30, 1999.
- [32] Yunlong Liu, Jianxin Wang, Jiong Guo, and Jianer Chen. Complexity and parameterized algorithms for cograph editing. *Theor. Comp. Sci.*, 461:45–54, 2012.
- [33] W. Maddison. Reconstructing character evolution on polytomous cladograms. *Cladistics*, 5:365–377, 1989.
- [34] Terry A. McKee and F. R. McMorris. *Topics in Intersection Graph Theory*. Society for Industrial and Applied Mathematics, 1999.
- [35] Bruno T. L. Nichio, Jeroniza Nunes Marchaukoski, and Roberto Tadeu Raittz. New tools in orthology analysis: A brief review of promising perspectives. *Front Genet.*, 8:165, 2017.
- [36] Nikolai Nøjgaard, Manuela Geiß, Daniel Merkle, Peter F. Stadler, Nicolas Wieseke, and Marc Hellmuth. Time-consistent reconciliation maps and forbidden time travel. *Alg. Mol. Biol.*, 13:2, 2018.
- [37] R D M Page and M A Charleston. Reconciled trees and incongruent gene and species trees. *DIMACS Ser Discrete Mathematics and Theor Comput Sci*, 37:57–70, 1997.
- [38] Deng Pan and Liqing Zhang. Tandemly arrayed genes in vertebrate genomes. *Comp Funct Genomics*, 2008:545269, 2008.
- [39] Alexander C J Roth, Gaston H Gonnet, and Christophe Dessimoz. Algorithm of OMA for large-scale orthology inference. *BMC Bioinformatics*, 9:518, 2008.
- [40] L. Y. Rusin, E. Lyubetskaya, K. Y. Gorbunov, and V. Lyubetsky. Reconciliation of gene and species trees. *BioMed Res Int.*, 2014:642089, 2014.
- [41] Erfan Sayyari and Siavash Mirarab. Testing for polytomies in phylogenetic species trees using quartet frequencies. *Genes*, 9:132, 2018.
- [42] C. Semple and M. Steel. *Phylogenetics*, volume 24 of *Oxford Lecture Series in Mathematics and its Applications*. Oxford University Press, Oxford, UK, 2003.
- [43] Charles Semple. Reconstructing minimal rooted trees. *Discr. Appl. Math.*, 127:489–503, 2003.
- [44] João C. Setubal and Peter F. Stadler. Gene phylogenies and orthologous groups. In João C. Setubal, Peter F. Stadler, and Jens Stoye, editors, *Comparative Genomics*, volume 1704, pages 1–28. Springer, Heidelberg, 2018.
- [45] Patricia S. Soria, Kriston L. McGary, and Antonis Rokas. Functional divergence for every paralog. *Mol Biol Evol*, 31:984–992, 2014.
- [46] Peter F Stadler, Manuela Geiß, David Schaller, Alitzel López, Marcos Gonzalez Laffitte, Dulce Valdivia, Marc Hellmuth, and Maribel Hernandez Rosales. From pairs of most similar sequences to phylogenetic best matches. *Alg. Mol. Biol.*, 15:5, 2020.
- [47] K Takahashi, Y Terai, M Nishida, and N Okada. Phylogenetic relationships and ancient incomplete lineage sorting among cichlid fishes in Lake Tanganyika as revealed by analysis of the insertion of retroposons. *Mol Biol Evol*, 18:2057–2066, 2001.
- [48] Roman L. Tatusov, Eugene V. Koonin, and David J. Lipman. A genomic perspective on protein families. *Science*, 278:631–637, 1997.
- [49] Dekel Tsur. Faster algorithms for cograph edge modification problems. *Inf. Processing Let.*, 158:105946, 2020.

- [50] B Vernot, M Stolzer, A Goldman, and D Durand. Reconciliation with non-binary species trees. *J Comput Biol.*, 15:981–1006, 2008.
- [51] Rémi Zallot, Katherine J. Harrison, Bryan Kolaczkowski, and Valérie de Crécy-Lagard. Functional annotations of paralogs: A blessing and a curse. *Life*, 6:39, 2016.